



National Library
of Canada

Acquisitions and
Bibliographic Services Branch

395 Wellington Street
Ottawa, Ontario
K1A 0N4

Bibliothèque nationale
du Canada

Direction des acquisitions et
des services bibliographiques

395, rue Wellington
Ottawa (Ontario)
K1A 0N4

Your file *Votre référence*

Our file *Notre référence*

NOTICE

The quality of this microform is heavily dependent upon the quality of the original thesis submitted for microfilming. Every effort has been made to ensure the highest quality of reproduction possible.

If pages are missing, contact the university which granted the degree.

Some pages may have indistinct print especially if the original pages were typed with a poor typewriter ribbon or if the university sent us an inferior photocopy.

Reproduction in full or in part of this microform is governed by the Canadian Copyright Act, R.S.C. 1970, c. C-30, and subsequent amendments.

AVIS

La qualité de cette microforme dépend grandement de la qualité de la thèse soumise au microfilmage. Nous avons tout fait pour assurer une qualité supérieure de reproduction.

S'il manque des pages, veuillez communiquer avec l'université qui a conféré le grade.

La qualité d'impression de certaines pages peut laisser à désirer, surtout si les pages originales ont été dactylographiées à l'aide d'un ruban usé ou si l'université nous a fait parvenir une photocopie de qualité inférieure.

La reproduction, même partielle, de cette microforme est soumise à la Loi canadienne sur le droit d'auteur, SRC 1970, c. C-30, et ses amendements subséquents.

UNIVERSITY OF ALBERTA

**EFFECT OF FINES AND GRADATION ON THE COLLAPSE SURFACE OF
A LOOSE SATURATED SOIL**

BY



© TIMOTHY DAVID PITMAN

A THESIS
SUBMITTED TO THE FACULTY OF GRADUATE STUDIES AND RESEARCH
IN PARTIAL FULFILMENT OF THE REQUIREMENTS FOR THE DEGREE OF
MASTERS OF SCIENCE

IN

GEOTECHNICAL ENGINEERING

DEPARTMENT OF CIVIL ENGINEERING

EDMONTON, ALBERTA

SPRING, 1993



National Library
of Canada

Acquisitions and
Bibliographic Services Branch

395 Wellington Street
Ottawa, Ontario
K1A 0N4

Bibliothèque nationale
du Canada

Direction des acquisitions et
des services bibliographiques

395, rue Wellington
Ottawa (Ontario)
K1A 0N4

Your file *Votre référence*

Our file *Notre référence*

The author has granted an irrevocable non-exclusive licence allowing the National Library of Canada to reproduce, loan, distribute or sell copies of his/her thesis by any means and in any form or format, making this thesis available to interested persons.

L'auteur a accordé une licence irrévocable et non exclusive permettant à la Bibliothèque nationale du Canada de reproduire, prêter, distribuer ou vendre des copies de sa thèse de quelque manière et sous quelque forme que ce soit pour mettre des exemplaires de cette thèse à la disposition des personnes intéressées.

The author retains ownership of the copyright in his/her thesis. Neither the thesis nor substantial extracts from it may be printed or otherwise reproduced without his/her permission.

L'auteur conserve la propriété du droit d'auteur qui protège sa thèse. Ni la thèse ni des extraits substantiels de celle-ci ne doivent être imprimés ou autrement reproduits sans son autorisation.

ISBN 0-315-82138-8

Canada

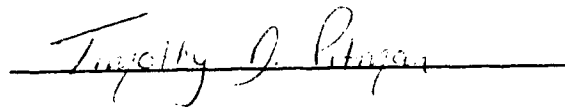
UNIVERSITY OF ALBERTA

RELEASE FORM

NAME OF AUTHOR : **Timothy David Pitman**
TITLE OF THESIS : **Effect of Fines and Gradation on Collapse Surface of
Loose Saturated Sands**
DEGREE : **Masters of Science**
YEAR THIS DEGREE GRANTED : **1993**

PERMISSION IS HEREBY GRANTED TO THE UNIVERSITY OF ALBERTA LIBRARY TO REPRODUCE SINGLE COPIES OF THIS THESIS AND TO LEND OR SELL SUCH COPIES FOR PRIVATE, SCHOLARLY OR SCIENTIFIC RESEARCH PURPOSES ONLY.

THE AUTHOR RESERVES ALL OTHER PUBLICATION AND OTHER RIGHTS IN ASSOCIATION WITH THE COPYRIGHT IN THE THESIS, AND EXCEPT AS HEREINBEFORE PROVIDED NEITHER THE THESIS NOR ANY SUBSTANTIAL PORTION THEREOF MAY BE PRINTED OR OTHERWISE REPRODUCED IN ANY MATERIAL FORM WHATEVER WITHOUT THE AUTHOR'S PRIOR WRITTEN PERMISSION.



Timothy D. Pitman

3365 ROMANS AVE.
HALIFAX, NOVA SCOTIA
CANADA

Date : *6/10/20, 1993*

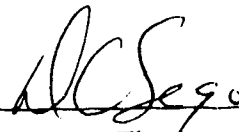
UNIVERSITY OF ALBERTA

FACULTY OF GRADUATE STUDIES AND RESEARCH

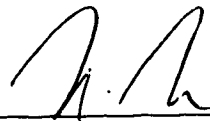
THE UNDERSIGNED CERTIFY THAT THEY HAVE READ, AND RECOMMEND TO THE FACULTY OF GRADUATE STUDIES AND RESEARCH FOR ACCEPTANCE, A THESIS ENTITLED **EFFECT OF FINES AND GRADATION ON THE COLLAPSE SURFACE OF A LOOSE SATURATED SAND** SUBMITTED BY **TIMOTHY DAVID PITMAN** IN PARTIAL FULFILMENT OF THE REQUIREMENTS FOR THE DEGREE OF **MASTERS OF SCIENCE**.



Dr. P.K. Robertson (Thesis supervisor)



Dr. D.C. Segó (Thesis supervisor)



Dr. N.R. Morgenstern



Dr. K. Barron

Date : April 20, 1993

**National Library
of Canada**

Canadian Theses Service

**Bibliothèque nationale
du Canada**

Service des thèses canadiennes

NOTICE

**THE QUALITY OF THIS MICROFICHE
IS HEAVILY DEPENDENT UPON THE
QUALITY OF THE THESIS SUBMITTED
FOR MICROFILMING.**

**UNFORTUNATELY THE COLOURED
ILLUSTRATIONS OF THIS THESIS
CAN ONLY YIELD DIFFERENT TONES
OF GREY.**

AVIS

**LA QUALITE DE CETTE MICROFICHE
DEPEND GRANDEMENT DE LA QUALITE DE LA
THESE SOUMISE AU MICROFILMAGE.**

**MALHEUREUSEMENT, LES DIFFERENTES
ILLUSTRATIONS EN COULEURS DE CETTE
THESE NE PEUVENT DONNER QUE DES
TEINTES DE GRIS.**

DEDICATION

This thesis is dedicated to the memory of my father, David Robert Pitman, who passed away while away at school. You gave me your love and support, and always guided me in the right direction. You may be gone, beyond all grief, pain and sorrow, but I feel your spirit within, guiding me down life's twisting highway. Although I never got to say good-bye, I love you and miss you very much.

ABSTRACT

This thesis focuses on the influence of fines and gradation on the collapse behaviour of loosely prepared sand samples. Loose sand samples, formed by moist tamping and consolidated to the same effective stress level, have been prepared with various percentages of both plastic- and non-plastic-type fines ($<74\mu\text{m}$) and non-plastic sand fines ($>74\mu\text{m}$). These samples have been isotropically consolidated, and subjected to monotonic undrained triaxial compression. Results indicate that increased percentages of fines ($<74\mu\text{m}$) have a pronounced effect on the monotonic undrained behaviour at large strains ($>0.5\%$). This change is represented by increased dilatant behaviour and a shifting of the steady-state line. Variation of non-plastic sand fines, which changes the gradation of the host sand, has shown no effect on the monotonic undrained behaviour. In conjunction with the above results, a shear wave velocity study, using bender element technology, was undertaken. The results and trends of the shear wave velocity study is discussed in this thesis. A discussion is presented on the procedure used to normalize the undrained test results and on how the State Parameter (Ψ) provides insight on liquefaction potential. A supplemental study, involving the Scanning Electron Microscope (SEM), is presented to reinforce the results of the triaxial testing with different fines ($<74\mu\text{m}$) on the monotonic undrained behaviour.

ACKNOWLEDGMENTS

The work described in this thesis was carried out in the Soil Mechanics Laboratory of the Civil Engineering Department at the University of Alberta and was supervised by Dr. P.K. Robertson and Dr. D.C. Sego. The research was supported by Natural Science and Engineering Research Council of Canada, University of Alberta scholarships and faculty support. My deepest appreciation goes out to these bodies for their considerable financial support.

I would like to express my profound gratitude to Dr. P.K. Robertson for his inestimable assistance, guidance and advice during all stages of this thesis. The many helpful discussions with him guided me towards a better understanding of soil behaviour. His kindness and support will always be cherished. I would also like to thank Dr. D.C. Sego for his valuable comments and suggestions. Working with them has been a valuable and pleasant experience.

In particular: I would like to thank Sabanayagam (Sasi) Sasitharan for all his help, encouragement and advice throughout my experimental work. My appreciation for all that you have done will always be remembered and I wish you much success in the your future.

I wish to make special mention to the technical staff that was involved with my thesis. In particular: Steve Gamble for his assistance in the experimental work and George Braybrook for his expertise in the Scanning Electron Microscope work.

It is a pleasure to also acknowledge the help of my fellow students, without whom I would have never been able to carry on. To Warren Miller, thanks for all your help and friendship whilst carrying out your own research and to Catherine Fear whose friendship brought me up when my life was so down. To them and all my fellow students, I wish you a healthy, happy and prosperous future.

My deepest gratitude goes out to my family, which I miss dearly, and to all my friends who have always encouraged and supported me throughout my education.

TABLE OF CONTENTS

	<u>Page</u>
DEDICATION	iv
ABSTRACT	v
ACKNOWLEDGMENTS	vi
TABLE OF CONTENTS	vii
LIST OF FIGURES	x
LIST OF TABLES	xiii
PRINCIPAL NOTATION	xiv
1. INTRODUCTION	1
2. BACKGROUND	
2.1 Historical Definition of Liquefaction	3
2.2 Monotonic Undrained Behaviour	3
2.2.1 Effect of Silts on Monotonic Undrained Behaviour	4
2.2.2 Effect of Anisotropy on Monotonic Undrained Behaviour	5
2.3 Steady-State Concepts	5
2.3.1 Stress Space Behaviour	7
2.3.2 Brittleness Index	9
2.4 Factors Affecting Undrained Monotonic Stress Paths	10
2.5 Steady-State Line	11
2.5.1 State Parameter	12
2.5.2 Difficulties in the Steady-State Approach	13
2.6 Load- versus Strain-Controlled Tests	14
2.7 Shear Wave Velocities	15
FIGURES	16

	Page
3. TESTING PROGRAM	
3.1 Laboratory Testing	22
3.2 Material Tested	22
3.2.1 Test Nomenclature	23
3.3 Testing Program	23
3.4 Triaxial Tests	24
3.4.1 Test Apparatus	24
3.4.2 Sample Preparation	25
3.4.3 Verification of Sample Preparation	29
3.4.4 Problems with Structural Collapse During Sample Saturation	30
3.5 Formulation	30
3.5.1 Shear Wave Velocity	30
3.5.2 Void Ratio	31
3.6 Shear Wave Velocities using Bender Elements	33
3.7 Volume Change During Saturation	35
3.8 Dominating Influence of Fines	36
3.9 Description of Scanning Electron Microscope (SEM) Work Performed	38
TABLES	39
FIGURES	40
4. RESULTS	
4.1 Monotonic Undrained Results	54
4.1.1 Plastic versus Non-Plastic Fines Comparisons	54
4.1.2 Influence of Gradation on Monotonic Undrained Behaviour	57
4.1.3 Normalization of Monotonic Undrained Results	57
4.1.4 Comparison of Test Results	59
4.1.4.1 State Parameter Results	60
4.1.5 Previous Monotonic Undrained Studies	61
4.1.6 Strain Similarities	63
4.1.7 Fines and Gradation Effects on Void Ratio	64

	Page
4.2 Steady-State Line Results	66
4.2.1 Previous Steady-State Studies	67
4.3 SEM Results	68
4.4 Shear Wave Velocity Results	69
TABLES	72
FIGURES	74
5. DISCUSSION	
5.1 Monotonic Undrained Behaviour	101
5.1.1 Behaviour of Critical Stress Ratio (CSR) Line	102
5.2 Steady-State Line Behaviour	102
5.2.1 Coefficient of Uniformity as a Measure of Liquefaction Potential	103
5.3 Discussion of Strain Similarities	104
5.4 Fabric Effects	104
5.4.1 Loose Sands in Nature	106
FIGURE	107
6. SUMMARY and CONCLUSIONS	108
REFERENCES	112

LIST OF FIGURES

Background: (Pages 16-21)

- 2.2.1 Effective Stress Paths for Undrained Triaxial Tests
- 2.3.1 Schematic of Contractive and Dilative Zones
 - 2.3.1.1 Typical Liquefaction Undrained Behaviour
 - 2.3.1.2 State Boundary
 - 2.3.1.3 Idealized Stress Path
 - 2.3.1.3 Strain Differences Prior to Dilation

Testing Program: (Pages 40-53)

- 3.2.1 Grain Size Curves for Ottawa Sand, 70-140 Silica Sand, Crushed Silica Fines and Kaolinite
- 3.2.2 Grain Size Curves for Addition of Various Percentages of Kaolinite to Ottawa Sand
- 3.2.3 Grain Size Curves for Addition of Various Percentages of Crushed Silica Fines to Ottawa Sand
- 3.2.4 Grain Size Curves for Addition of Various Percentages of 70-140 Silica Sand to Ottawa Sand
- 3.4.1.1 Schematic Layout for Freezing Triaxial Samples
- 3.4.1.2 Schematic Layout of the Shear Wave Measuring System
- 3.4.1.3 Photograph of Lab Set-Up
- 3.4.1.4 Photograph of Wykeham-Farrance Loading Press
- 3.4.1.5 Photograph of Volume Change Device
- 3.4.1.6 Photograph of Data Acquisition System
- 3.4.2.1 Photograph of Loading Ram and Base Assemblage
- 3.4.2.2 Photograph of Water and CO₂ Supply
- 3.4.2.3 Photograph of Shear Wave Velocity Apparatus
- 3.4.2.4 Photograph of Laboratory Freezing Set-Up
- 3.6.1 Piezoceramic bender element connections: (a) Series (b) Parallel

- 3.6.2 Bender Element Mounted on Bottom Pedestal
- 3.6.3 Plot of Shear Wave Velocity for Test O10RF350
- 3.9.1 Photograph of Scanning and Sub-Liming Device
- 3.9.2 Photograph of SEM Viewing Device

Results: (Pages 74-100)

- 4.1.1abc Monotonic Undrained Results for Kaolinite
- 4.1.2abc Monotonic Undrained Results for Crushed Silica Sand
- 4.1.3abc Monotonic Undrained Results for 70-140 Silica Sand
- 4.1.1.1 Brittleness Index vs. Percent Material Added for Kaolinite, Crushed Silica Fines, 70-140 Silica Sand and Ham River Sand
- 4.1.3.1abc Consolidation Curves
- 4.1.3.2ab Normalized Plots for Various Percentages of Kaolinite
- 4.1.3.3ab Normalized Plots for Various Percentages of Crushed Silica Fines
- 4.1.3.4ab Normalized Plots for Various Percentages of 70-140 Silica Sand
- 4.1.4.1abc Comparison Plots for 20% Samples
- 4.1.4.2ab Normalized Comparison Plots for 20% Samples
- 4.1.4.1.1 State Parameter Comparison Plot for 20% Samples
- 4.1.4.1.2 State Parameter vs. Percent Material Added
- 4.1.5.1ab Comparison of 20% Crushed Silica Fines enriched Ottawa sand to silt enriched Brenda sand.
- 4.1.5.2ab Comparison of 20% Kaolinite enriched Ottawa sand to Kaolinite enriched Ham River sand
- 4.1.7.1abc Void Ratio vs. Percent Material Added at Various Effective Pressures
- 4.1.7.2 Density Limits as a Function of Grain Shape
- 4.2.1abc Steady-State Line Results
- 4.2.1.1 Steady-State Lines for Sands with Subrounded Grains
- 4.2.1.2 Steady-State Lines for Sands with Subangular Grains
- 4.2.1.3 Steady-State Lines for Sands with Angular Grains
- 4.2.1.4 Steady-State Lines for Kogyuk Sand at Various Silt Percentages
- 4.3.1 SEM Photographs of 20% Kaolinite Samples
- 4.3.2 SEM Photographs of 40% Kaolinite Samples
- 4.3.3 SEM Photographs of 20% Crushed Silica Fines Samples

- 4.3.4 SEM Photographs of 40% Crushed Silica Fines Samples
- 4.4.1 Normalized Shear Wave Velocity vs. Percent Material Added

Discussion: (Page 107)

- 5.1.1 Resistance Ratio vs. Tip Resistance for Silty Sands

LIST OF TABLES

Testing Program: (Page 39)

- 3.2.1 Properties of Materials Used
- 3.2.2 Material Properties for Various Tests
- 3.4.3.1 Density and Void Ratio Variations for Samples a) O20SF
b) O40SF350

Results: (Pages 72-73)

- 4.1.1.1 Undrained Brittleness Indices
- 4.1.4.1 State Parameter Results
- 4.1.6.1 Summary of ϕ Data
- 4.4.1abc Normalized Shear Wave Velocity Results

PRINCIPAL NOTATION

ASTM	American Standards and Testing Methods
A_s	Soil surface area covered by membrane
B	Skempton's parameter
C_u	Coefficient of uniformity
CO_2	Carbon dioxide
CP	Base effective pressure
CP_c	Current effective confining pressure
CPT	Cone penetration test
CSR	Critical effective stress ratio
D	Specimen diameter
D_r	Relative density
e	Void ratio
e_g	Intergranular void ratio
e_{mc}	Membrane corrected void ratio
e_{min}	Minimum void ratio
e_{max}	Maximum void ratio
e_{ss}	Void ratio at steady-state
EP	Effective stress level
F	Flow line
f_c	Fines fraction
UF	Upper flow line
LF	Lower flow line
G	Shear modulus
G_f	Specific gravity of fine particles
G_{max}	Small strain shear modulus
G_s	Specific gravity of granular particles
H_c	Current height of specimen
K	Kaolinite
K_o	Coefficient of lateral earth pressure at rest
L_t	Length of travel
lvdt	Linear voltage displacement transducers

$(N_1)_{60}$	Tip resistance
ρ	Mass density
p_e'	Equivalent effective stress
ϕ_{CSR}	Mobilized friction angle at peak shear stress
ϕ_{PT}	Mobilized friction angle at phase transformation
ϕ_{SS}	Mobilized friction angle at steady-state
ϕ_μ	Constant volume friction angle
RF	70-140 silica sand
RTD	Resistance temperature device
SF	Crushed silica sand
s'	Normal shear stress
t	Shear Stress
t_{peak}	Peak Shear Stress
σ_1	Major principal stress
σ_3	Minor principal stress
σ_d	Deviator Stress
σ_{dp}	Peak Deviator Stress
σ_{dr}	Residual Deviator Stress
δu	Excess pore pressure
ϵ_a	Axial strain
ϵ_m	Unit membrane penetration
ϵ_{PT}	Strain at Phase Transformation
ϵ_v	Volumetric strain
SEM	Scanning electron microscope
SPT	Standard penetration test
Ψ	State parameter
T_t	Travel time
τ/σ'	Resistance ratio
v	Specific Volume
ν	Poisson's ratio
δV	Change in Volume during consolidation
δV_{corr}	Corrected volume change
δV_T	Total volume change
V_{ci}	Volume at the beginning of consolidation

V_p	Compression wave velocity
V_s	Shear wave velocity
V_s'	Normalized shear wave velocity
w	Water content fraction
W_g	Dry weight of specimen

1. INTRODUCTION

Many natural deposits of sands contain some quantity of fines. The fines are usually an assemblage of both plastic- and non-plastic-type particles. The fines can have an important effect on the fabric of the soil including: controlling the shearing mechanism which develops and allowing a possible loose packing in the sand to develop. The undrained behaviour of loose saturated sands has been the focus of considerable engineering research in the past few years. There has been a large effort into the development of sand liquefaction evaluation techniques, including laboratory testing, in situ testing and prediction models.

Most of the fundamental laboratory studies of sand liquefaction behaviour which has been conducted in the past has involved the use of uniformly-graded clean sand, which essentially guaranteed homogeneity and repeatability of tests, as well as direct comparison to other tests. However, most of the natural soils which are encountered in situ contain some quantity of fines and are usually well-graded. To successfully evaluate liquefaction potential, and hence the collapsibility, of in situ sands, it is useful to study the effects of fines content and variation in sand gradation on the behaviour of laboratory sand samples.

There appears to be considerable confusion in the literature about the effects of fines and gradation on liquefaction potential as related to the resistance of sand to cyclic loading. Some researchers (Troncoso, 1990) have found that cyclic strength decreases with increasing fines content, whereas others (Kuerbis and Vaid, 1989) suggest that it can be constant up to 20% fines content. Clearly there was a need for research into the effect of fines, and their associated plasticity and particle size variation on the fabric and hence the liquefaction behaviour of loose sands.

Samples of silty sand and well-graded sands have been tested in the past, but due to different methods employed in sample preparation, laboratory procedures and test evaluations, contradictory conclusions on the effects of fines and gradation on sand behaviour have been reported. The investigation described in this research entails a systematic study of the static monotonic undrained response with the objective of

gaining improved understanding of the effects of fines content and sand gradation on the collapsibility of loose saturated sand samples.

For this research, monotonic undrained triaxial compression tests were carried out on isotropically consolidated loose sand samples. The same preparation method, effective consolidation stress level and laboratory procedure was used for every sample to avoid ambiguity. Undrained triaxial tests on loose samples have been the preferred method for liquefaction studies. There are several reasons for this but arguably the most important is that loose sands can be contractive at large strains during shear and exhibit continuously increasing pore pressures under undrained loading which minimizes the development of nonuniformities within the sample.

The reference to loose in this thesis is defined as soil in a state which is looser than the steady-state, that when sheared undrained will exhibit a post peak loss of resistance, a condition which is necessary for collapse or flow liquefaction. To study the collapse behaviour of loose sand under the influence of varying fines contents and sand gradations, various percentages of both plastic- and non-plastic-type fines ($<74\mu\text{m}$) and non-plastic sand fines ($>74\mu\text{m}$) were added. Subsidiary studies involving shear wave velocity and the Scanning Electron Microscope (SEM) were also carried out in conjunction with the undrained compression tests to help in the development of a rational framework to describe the behaviour of a sand. This behaviour can then be used to represent many naturally occurring sands which are encountered in natural ground conditions.

2. BACKGROUND

2.1 Historical Definition of Liquefaction

Catastrophic flow slides have occurred in a variety of geological materials ranging from clays to gravel. These flow slides are more frequently encountered in saturated deposits of loose sand, sometimes natural but often man-made (Hird and Hassona, 1990). Such slides are the result of collapse or flow liquefaction - the process by which a soil mass suddenly loses a large portion of its shear resistance and flows in a manner resembling a liquid until the shear stresses acting on the mass are as low as the reduced shear resistance (Castro and Poulos, 1977). Collapse liquefaction involves the collapse of a metastable particle configuration and may be triggered by monotonic, cyclic or shock loading. The collapse of a saturated soil structure is so rapid that the excess pore fluid pressure does not have a chance to dissipate.

The concept of collapse liquefaction dates back to Casagrande in 1936 whose pioneering work was accomplished using direct shear tests. Several decades later Castro (1975) came up with the following comprehensive definition of liquefaction: “a phenomena wherein a mass of soil loses a large percentage of its shearing resistance when subjected to undrained monotonic, cyclic or shock loading and flows in a manner resembling a liquid until the shear stresses acting on the mass are as low as the reduced shearing resistance.”

2.2 Monotonic Undrained Behaviour

Over the entire range of states that can be tested on a particular sand, the observed stress-strain behaviour can be characterized by one of three response types, as illustrated in Figure 2.2.1. Types 1 and 2 are both strain softening responses which can lead to collapse liquefaction and partial or limited liquefaction, respectively. A sand which behaves in this manner is said to be contractive.

Type 1 response exhibits a marked strain softening behaviour, i.e., after the peak is reached in the stress-strain diagram, which occurs at a small strain, there is a marked reduction in resistance until the stress stabilizes at an ultimate or residual strength (Alarcon-Guzman et al., 1988). The reduction in strength is usually termed “flow deformation” and the residual strength as “steady-state strength”.

Type 2 response represents a transition stage in which the strength of the specimen decreases to a residual value and then gains strength (strain hardens). Strain hardening coincides with the onset of dilation and as a consequent, reduction in pore-water pressure (Vaid and Chern, 1985). Also characteristic to Type 2 response is an “elbow” in the stress path which separates strain softening from strain hardening and corresponds to the minimum deviator stress. The temporary stage of strain softening can be referred to as partial or limited liquefaction.

Type 3 response represents a path in stress space in which the sand will exhibit a strain hardening behaviour. Sand which behaves in this manner, under undrained loading, is called highly dilative. If the sand is mildly dilative, the effective stress path may show a recognizable turnaround in the stress path, similar to the case of limited liquefaction.

2.2.1 Effect of Silts on Monotonic Undrained Behaviour

Central to this thesis was the addition of fines to a particular sand, so that its effect on the monotonic undrained behaviour could be studied. A previous study by Kuerbis (1989) indicated that as the non-plastic fines content was increased the dilative behaviour increased. It was also suggested that up to approximately 20% fines, the non-plastic fines occupied only the sand skeleton void space and for the most part had little effect upon soil behaviour.

Friction angles obtained from undrained monotonic testing, which will be discussed in subsequent sections, have been found to vary slightly with density and soil fabric, therefore it is expected that it also may vary with silt content (Kuerbis, 1989) Castro (1962) indicated from his test results that the friction angle of a material increases

with decreasing grain size. These findings will be discussed in context with the results of the present study, in later chapters.

2.2.2 Effect of Anisotropy on Monotonic Undrained Behaviour

Associated, but not central to this thesis is the effect of anisotropy on the monotonic undrained behaviour. Considerable evidence of anisotropy has been demonstrated under drained loading (Arthur and Menzies, 1972; Oda, 1981). It is therefore reasonable to assume that undrained response will also be anisotropic (Kuerbis and Vaid, 1989). It was found by Kuerbis and Vaid (1989) that inherent anisotropy was more pronounced in water deposited specimens as compared to moist tamped sands. This would explain why they found directional variation (compression versus extension) in the undrained response.

A number of researchers (Kuerbis and Vaid, 1989; Vaid and Chung, 1989) have found that undrained strengths in compression and extension are different, but the mobilized friction angle is essentially equal. The research of Seed et al. (1988), Been et al. (1991) and Poulos et al. (1988) has shown that sample preparation may affect the behaviour prior to steady-state but true steady-state conditions are not affected. Hence, the friction angles would be similar. The difference in compression and extension implies that the steady-state line, though unique in stress space is not so in void ratio stress space. Kuerbis and Vaid (1989) attribute the differences in undrained steady-state strength solely to the induced pore pressures, which are larger in extension.

2.3 Steady-State Concepts

When loose saturated sands are loaded undrained they may collapse and strain soften to a constant level of effective stress and shear strength (Type 1 response). This condition has been termed steady-state by Castro (1975) and Poulos (1981). Poulos (1981) defined steady-state as a condition of constant effective stress, constant shear stress, constant volume and constant velocity of deformation.

If the sand exhibits Type 1 response, the void ratio and undrained strength (or effective confining pressure) at steady-state are assumed to be uniquely related (Castro et al., 1982). This relationship between void ratio and stress is called the steady-state line. The steady-state line is a boundary which separates initial states of sand into regions of contractive or dilative behaviour at large strains ($>0.5\%$). It is important to understand that sands will always display a contractive response at small strains ($<0.5\%$).

Collapse liquefaction involves large unidirectional undrained shear deformation in which the soil tends toward a steady-state of deformation, expressed in terms of the steady-state line. Figure 2.3.1 schematically illustrates the contractive and dilative zones. If a soil sample is prepared such that its void ratio and normal stress correspond to point A and is then tested undrained (constant volume and void ratio) to point B, contractive behaviour will be observed. What is happening is that since the sand can not change volume, it transfers stress from its grain structure to the pore fluid pressure (usually water). The increase in pore water pressure causes a decrease in effective normal stress until the steady-state is reached at point B.

A soil specimen prepared to condition at point E, to the left of the steady-state line, and tested undrained to point F (steady-state) may show an initial tendency to contract during small strains, but dilation will soon prevail. If the void ratio and normal stress of a soil specimen corresponds to point C, the sample would be in the transition zone. This zone represents a decrease in strength to a residual value over a limited range of strain ($\sim 5\text{-}6\%$), but will gain strength (dilation) with further straining. This response is termed partial or limited liquefaction.

The magnitude of the pore water pressure developed by samples on the contractant side is a function of the distance from the steady-state line. The larger the distance, the higher is the pore water pressure developed during undrained shear. Contractant soils will generate positive pore water pressures and dilative soils will generate negative pore water pressures at large strains. If dilation occurs throughout the sample, the pore pressures will be equally distributed throughout the sample. More commonly, if dilation occurs the pore pressures are usually localized in the area where shear banding occurs (DeMatos, 1988).

A common misunderstanding is that a contractant soil will always be subject to liquefaction. A contractant soil is only susceptible to collapse liquefaction if the driving shear stresses in situ are larger than the undrained steady-state strength (Poulos et al., 1985). Conversely, if the steady-state strength is greater than the driving stress, then collapse liquefaction can not occur because the associated large unidirectional deformations are not possible (Poulos et al., 1985).

2.3.1 Stress Space Behaviour

To properly understand stress space behaviour, an idealized stress path is schematically shown in Figure 2.3.1.1. The terms and labels expressed will be referred to throughout this thesis. Definitions of these terms can be referenced in the principal notation list. The stress space plots use the variables normal stress (s') and shear stress (t) as indices and are defined as:

$$s' = \frac{(\sigma_1' + \sigma_3')}{2} \quad t = \frac{(\sigma_1 - \sigma_3)}{2}$$

The monotonic undrained response of a very loose sand is shown schematically in Figure 2.3.1.1. During monotonic loading the pore water pressure increases and the effective stress path in normal-shear (s' - t) stress space begins to bend to the left. The peak of the effective stress path which corresponds to the peak deviator stress, was defined as the collapse surface by Sladen et al. (1985). After this point the soil strain softens to steady-state. During the collapse process, the pore water pressure continues to increase and levels off after steady-state has been obtained. The effective stress path during collapse usually travels slightly above the straight line path proposed by Sladen et al. (1985). This surface forms part of the critical state boundary (Sasitharan, 1993).

The “collapse surface” concept was first proposed by Sladen et al. (1985). They suggested that for very loose sands there was a surface in void ratio-stress space and that when the undrained effective stress path reached the “collapse surface”, undrained collapse to steady-state occurs. This was a significant contribution to the

study of liquefaction. It defined a triggering condition for strain softening to occur in undrained loading. It is important to distinguish between the "collapse surface", which represents a trigger for liquefaction, and the state boundary, which represents the path a sample follows to steady-state. The "collapse surface" as defined by Sladen *et al.* (1985) is not a state boundary, as the post peak soil state can pass above it. Figure 2.3.1.2 schematically illustrates this point. The "collapse surface" can be imagined as the locus of soil states at which destruction of a metastable soil structure is initiated by some form of undrained loading until a condition of steady-state is reached (Sladen *et al.*, 1985). The position of the "collapse surface", in non-normalized stress space, will shift upwards or downwards, with constant slope with variations in void ratio. The boundary surface, represents the surface along which the stress path travels (Sasitharan, 1993). The "collapse surface" is a straight line approximation of the boundary surface. For very loose sands this straight line approximation can be relatively close to reality.

For soils which behave in a limited liquefaction or in a dilatant manner, a phase transformation line can be defined. The phase transformation line was first defined by Ishihara *et al.* (1975). The line represents the stress state where the pore water pressure decreases in loading and increases in unloading of shear stress under undrained conditions (Gu, 1992). Figure 2.3.1.3 shows an idealized stress path and stress-strain curve for a loose sand with an initial state close to steady-state.

The phase transformation line defines the boundary between contractive and dilative responses, marking the commencement of dilatant behaviour. This line exists both in drained and undrained conditions. For this research the phase transformation line can be deduced by drawing a straight line from the origin in stress space through the "elbows" of various tests. The "elbow" is defined in Figure 2.3.1.3. Once the specimen has strained past the phase transformation, the stress path will move along a line towards the state boundary. The initial stress state of a sample, as compared to the steady-state, will determine the path the sample travels to the state boundary.

Phase transformation can easily be identified when limited liquefaction exists, but it also exists for samples which behave in a dilative manner. It is defined as the point where shear dilation commences and the pore pressure starts to drop (Vaid and Chern,

1985). For highly dilative states, phase transformation is hard to discern and a careful study of the pore pressure response is necessary.

The phase transformation line is unique for a particular sand (Vaid and Chern, 1985). Among the sands tested in this research and other sands tested by Negussey et al. (1988), the phase transformation is dependent upon sand fabric. The use of the term sand fabric in this work encompasses parameters such as gradation, fines content, and sand and fines mineralogy, shapes and compressibility. These parameters effect how the soil skeleton is constructed. A different fabric would therefore represent a different soil skeleton construction.

Many of researchers in the past who have used steady-state concepts have treated the phase transformation state ("elbow") as steady-state. This treatment adds conservatism to stability analyses based on steady-state concepts. This is because the effects of strength gained associated with dilation, after phase transformation, are ignored (Kuerbis, 1989).

Although strength gain due to dilation is important, caution must be exercised. Figure 2.3.1.4 will be used to schematically illustrate the concerns which could arise if the strength gain due to dilation was used. If a sand behaves as in A the strain which occurs before dilation begins is large. In this case, undesirable deformations will occur, overshadowing the strength gain due to dilation. If the sand behaves as in B and the strain to reach the onset of dilation is not large enough to cause significant deformations, then it would be appropriate to consider the strength gain due to dilation when designing using steady-state concepts.

2.3.2 Brittleness Index

Bishop (1967) expressed the reduction in undrained strength of a strain-softening material in terms of a brittleness index, I_B , defined as:

$$I_B = \frac{\sigma_{dp} - \sigma_{dr}}{\sigma_{dp}}$$

where

I_B = brittleness index

σ_{dp} = peak undrained shear strength (kPa)

σ_{dr} = residual undrained shear strength (kPa)

The residual shear strength has been described by others (Kramer and Seed, 1988) as the steady-state shear strength. For the purpose of this thesis the definition of σ_{dp} and σ_{dr} can be found on Figure 2.3.1.3. The brittleness index can range from 0 to 1. The higher the value of brittleness index the larger is the reduction in shear strength that could lead to the progressive development of large deformations after the initiation of collapse liquefaction. On the other hand, the initiation of strain softening in a material with a low brittleness index may not lead to significant deformations.

2.4 Factors Affecting Undrained Monotonic Stress Paths

Research into factors affecting steady-state behaviour has been carried out by various authors. Comparing samples at the same void ratio a number of researchers have found the following to affect the steady-state strength:

- (1) Prestrain history (Finn et al., 1970; Ishihara et al., 1980)
- (2) Membrane penetration (Vaid and Negussey, 1982, 1984)
- (3) Sample preparation method (Kuerbis, 1989; Been et al., 1991)
- (4) Extension versus compression (Vaid et al., 1990; Been et al., 1991)
- (5) Stress path followed (Georgiannou, 1988; Been et al., 1991)
- (6) Initial density and level of anisotropy (Georgiannou, 1988; Been et al., 1991).

The above is only a partial list but covers most of the important points. Even in such a small list there are strong differences in opinions on whether the behaviour at steady-state is unique. To debate the findings of these researchers is beyond the scope of this thesis, but in passing this researcher feels that a lot of the problem lies in distinguishing between the shape of the effective stress path and the actual steady-state strength. For example, a sample can follow two very different stress paths, but

ultimately arrive at the same steady-state strength. Until this is properly understood there will always be confusion when the steady-state concepts are used.

2.5 Steady-State Line

It was Castro (1969) who first suggested that the locus of steady-state strengths forms a unique line in void ratio - logarithm of minor effective stress space. He termed this the F line, where F stood for flow. The F line is also widely referred to as the steady-state line in which conditions of constant void ratio, constant velocity, constant shear strength and constant flow structure prevail at this stage of testing (Poulos, 1981).

It is commonly assumed that the steady-state line is unique and that the characteristics of the flow structure developed during steady-state deformation is dependent on void ratio only and independent of consolidation stress, previous history, initial fabric, etc. Therefore previous practice would use the best-fit line through experimental steady-state data to define the F line. Konrad (1990) was one of the first researchers to explore the possibility that the steady-state line may not be unique for a given soil. He found the experimental scatter of steady-state strengths to have a upper and lower bound, which was termed UF and LF lines respectively.

There are a number of factors, inherent in the measurements during the triaxial test, which can give rise to some scatter of results and hence, a range of data points about the steady-state line. Among these factors could be errors in the measurement of load, pore pressure, volume change prior to undrained shear and errors due to non-uniformity of an individual sample. Castro et al. (1982) credit the observed variations to five principle reasons:

- (1) Variations in grain size distribution among specimens;
- (2) Inaccuracies in the measurement of void ratio;
- (3) Inaccuracies in the measurement of shear stress;
- (4) Inaccuracies in the measurement of effective minor principal stress;
- (5) Strain limitations in the triaxial test.

The influence of several basic aspects related to the nature of soil grains (shape; surface texture; plasticity) and of soil gradation (coarseness-fineness; percentage of fines; coefficient of uniformity) effect the position and the slope of the steady-state line.

When fines are added to a sand the issue of compressibility must be addressed. The compressibility of the soil skeleton depends on the nature of the soil grains and the fines. The water which occupies the pore spaces is considered to be incompressible. The fines which are added can range from incompressible (non-plastic) to highly compressible (plastic). The amount of pore pressure which is generated will be influenced by the percentage of water and fines in the pore spaces and the compressibility of the sand and fines. The more compressible the soil skeleton, the higher will be the pore pressure generation. This in turn influences the behaviour of the soil during undrained shear. DeMatos (1988) found that soil compressibility is influenced by:

- (1) grain-type: soil particles vary from very rounded to very angular, the compressibility increasing with angularity;
- (2) grain surface texture: the rougher the surface texture the lower will be the compressibility;
- (3) size distribution: the more well-graded a soil, the higher the pore pressure generated, and the higher is the soil skeleton compressibility.

2.5.1 State Parameter

A parameter, known as the state parameter, Ψ , was defined by Been and Jefferies (1985). The roots of this parameter lie in critical state soil mechanics, and describes the initial state of a sand relative to the steady-state. The concept can be used regardless of the sand matrix structure and combines the influence of void ratio and stress. The state parameter is defined as the difference between the initial void ratio and the void ratio at steady-state. If the difference is positive, strain softening will occur; negative, dilation occurs. Although the state parameter may not be a universal

parameter for all soils which can be used as a measure of the liquefaction potential, the state parameter would provide a index for comparing soils of similar structures.

The weakness of the state parameter approach lies in that all points are referenced to a unique state, the steady-state line. As was pointed out in section 2.5, the steady-state line may not be unique for all sands, but for one sand with one percentage of fines there is one steady-state line. To establish a reasonably accurate steady-state line at least five triaxial tests are required and this would have to be carried out for each percentage of fines. Hence, a large number of tests would be required. Even with the enormous amount of work required, the state parameter has merit as a parameter which can be used to quantify the initial state and hence, the potential for liquefaction to occur.

2.5.2 Difficulties in Steady-State Approach

The main difficulty associated with the application of the steady-state approach, for design, is the uncertainty associated with determining the in situ void ratio and the corresponding steady-state line. Of interest is the magnitude difference between the void ratio in situ and at steady-state, at the same stress level. The basic problem is that the steady-state line for most sands is very flat and therefore small uncertainties in either the in situ void ratio or the location of the steady-state line can lead to large differences at steady-state (McRoberts and Sladen, 1992).

The accuracy with which sand void ratio can be determined in the field is generally low. It is usually difficult using conventional techniques to obtain an undisturbed sample of sand and be certain that the void ratio has not changed. This problem has been around for a long time and has led some researchers to study the possibility of obtaining in situ density from correlations with in situ tests, such as CPT and SPT and through more exotic ways such as nuclear logging and in situ freezing. The use of shear wave velocities also shows some promise of providing a non-destructive method of estimating the in situ state. The simple fact of the matter is, that whatever one does to get a representative measurement of density, in some way influences the value of the resulting density (McRoberts and Sladen, 1992).

To estimate the state of a sand, with known void ratio and stress level, it is necessary to determine the location of the steady-state line. This introduces further potential problems. The inclination of steady-state line is affected by fines content (Sladen et al., 1985) and fabric (Kuerbis, 1989; Vaid and Chern, 1985) and to a lesser extent by gradation (Poulos et al., 1988). Sands which are encountered in situ are seldom homogeneous, so there are practical problems as to which steady-state line to adopt and the number of variations of sand gradation for a specific site which must be tested. This requires difficult decisions which may result in large economic penalties. Some guidance in making these decisions, based on the present research, will be presented in a later chapter.

2.6 Load- versus Strain-Controlled Tests

Some of the first steady-state testing was carried out by Castro (1969) using load-controlled triaxial tests. The studies by both Castro et al. (1982) and Sladen et al. (1985), has determined that there is no significant difference between the results of load (stress) -controlled and strain-controlled tests. Contrary to these findings are the results of Hird and Hassona (1990) who found that strain rate has an important influence. They postulated that at higher strain rates a (dynamic) flow structure is developed in the material, and therefore load-controlled testing is a better representation of field conditions. It was found by Hungr and Morgenstern (1984) that the behaviour of sand is largely independent of strain rate.

As stated previously, this review was not intended to debate these differences, only to show the differences in opinions of previous researchers. For this study, strain-rate-controlled tests were carried out. The underlying reason being that for load-controlled tests, the velocity of deformation from peak to steady-state is so rapid that it would be difficult to measure the stress state within the specimen (Sasitharan et al., 1993). Strain-rate-controlled tests allow for more data to be gathered from peak to steady-state, therefore yielding a well defined effective stress path.

2.7 Shear Wave Velocities

Incorporated into this study was the measurement of shear wave velocities. The shear wave velocity is a direct measure of the stiffness of the soil skeleton, it is sensitive to soil structure (fabric), void ratio (density), effective confining stress (Hardin and Drnevich, 1972) and consolidation history (aging). The effect of these parameters on the shear wave velocities obtained in this study will be presented in section 4.4. The evaluation of small strain shear wave velocity, V_s , is important in the design of dynamic foundations, the evaluation of soil improvement or degradation and the evaluation of liquefaction potential.

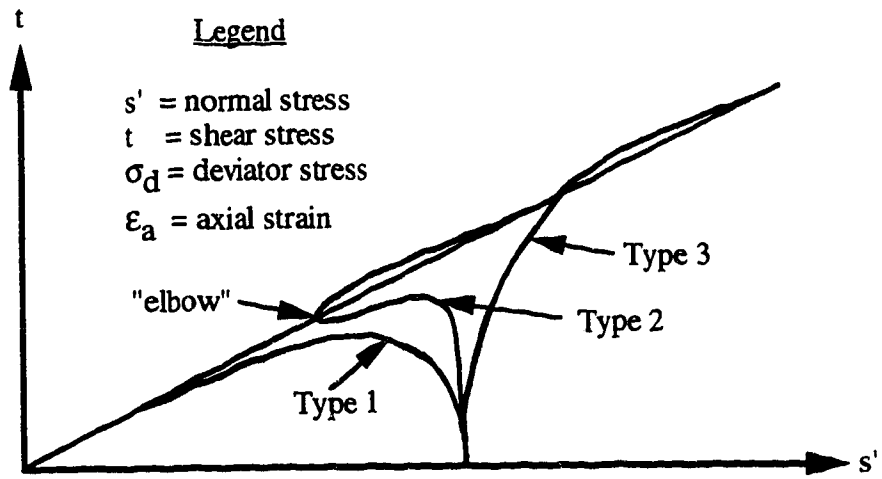
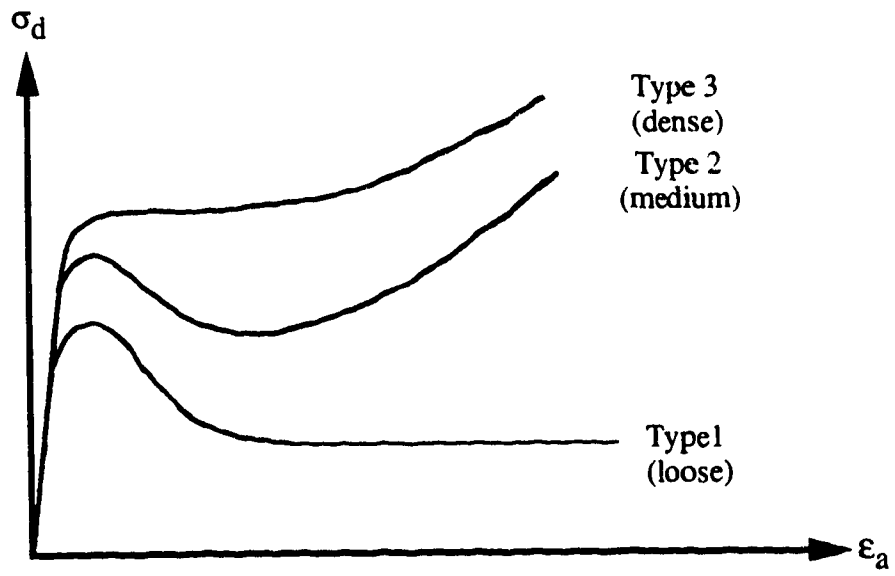


Figure 2.2.1 Effective Stress Paths for Undrained Triaxial Tests

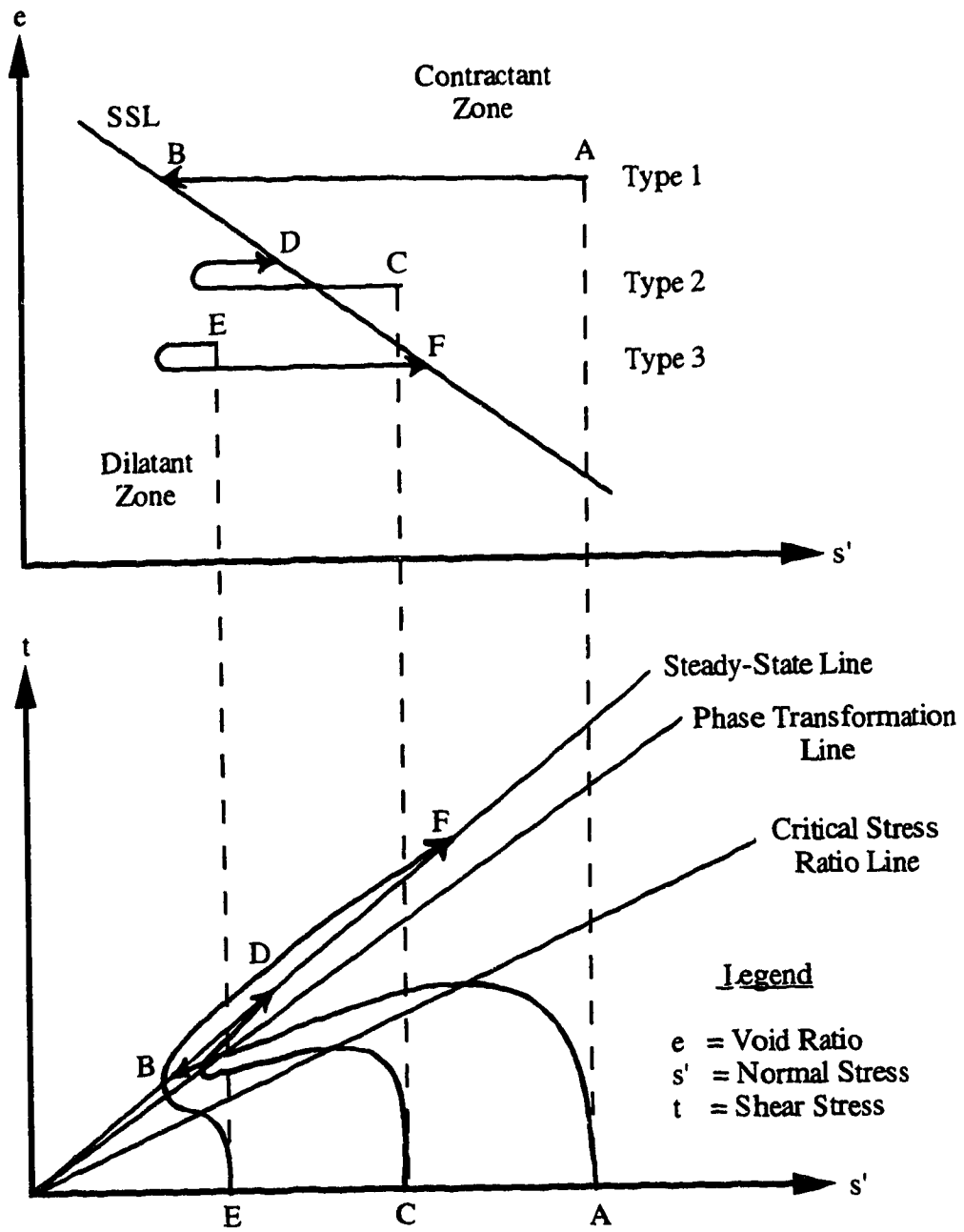


Figure 2.3.1 Schematic of Contractive and Dilative Zones

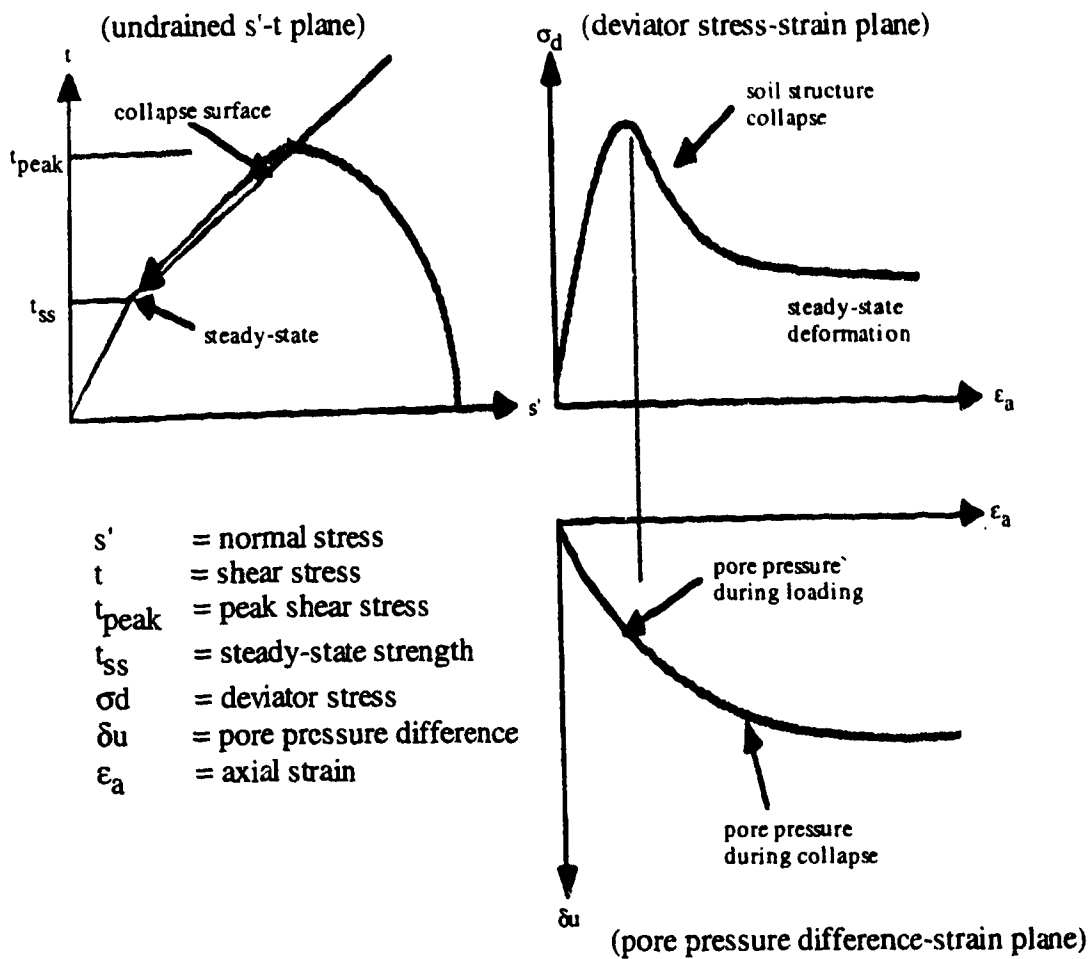


Figure 2.3.1.1 Typical Liquefaction Undrained Behaviour
(after Gu, 1992)

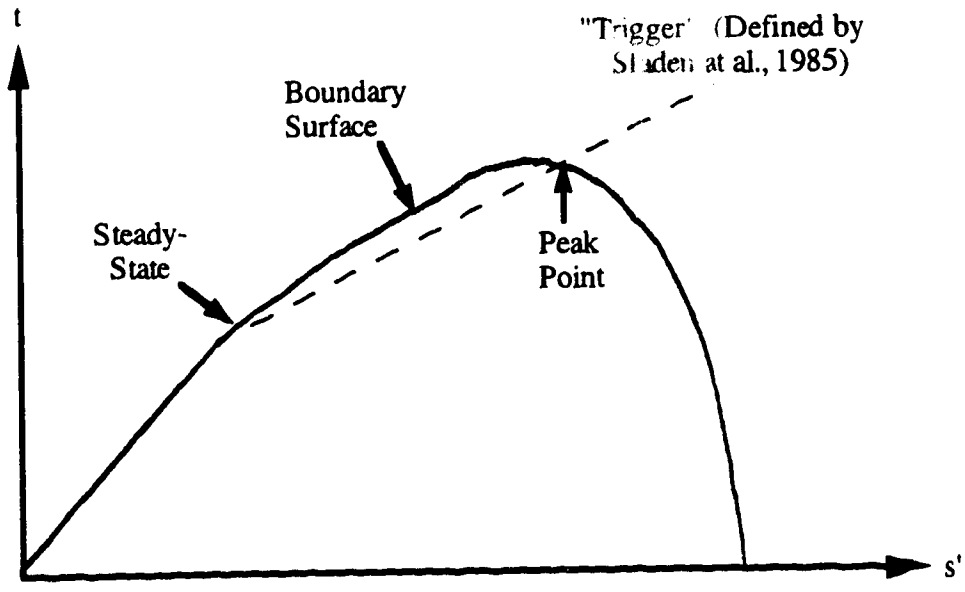


Figure 2.3.1.2 State Boundary

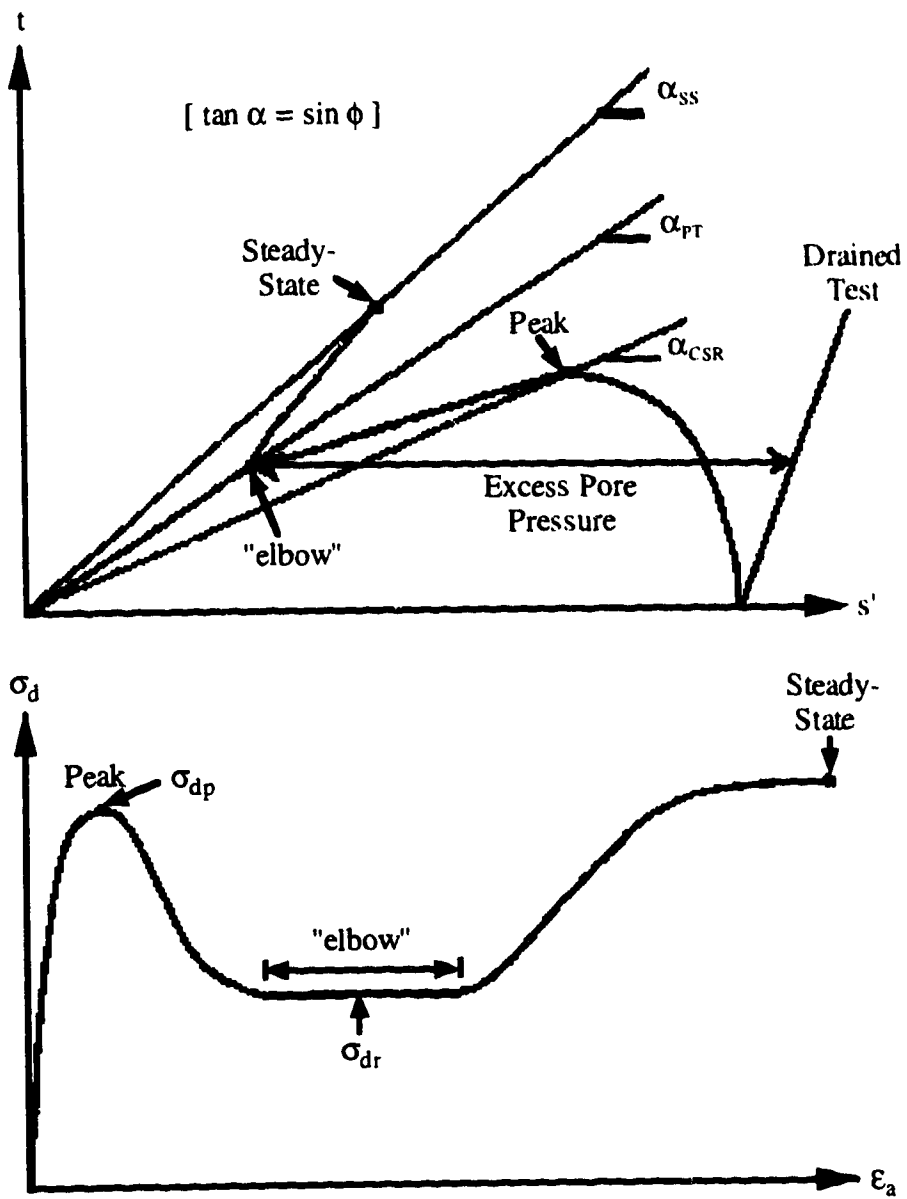


Figure 2.3.1.3 Idealized Stress Path

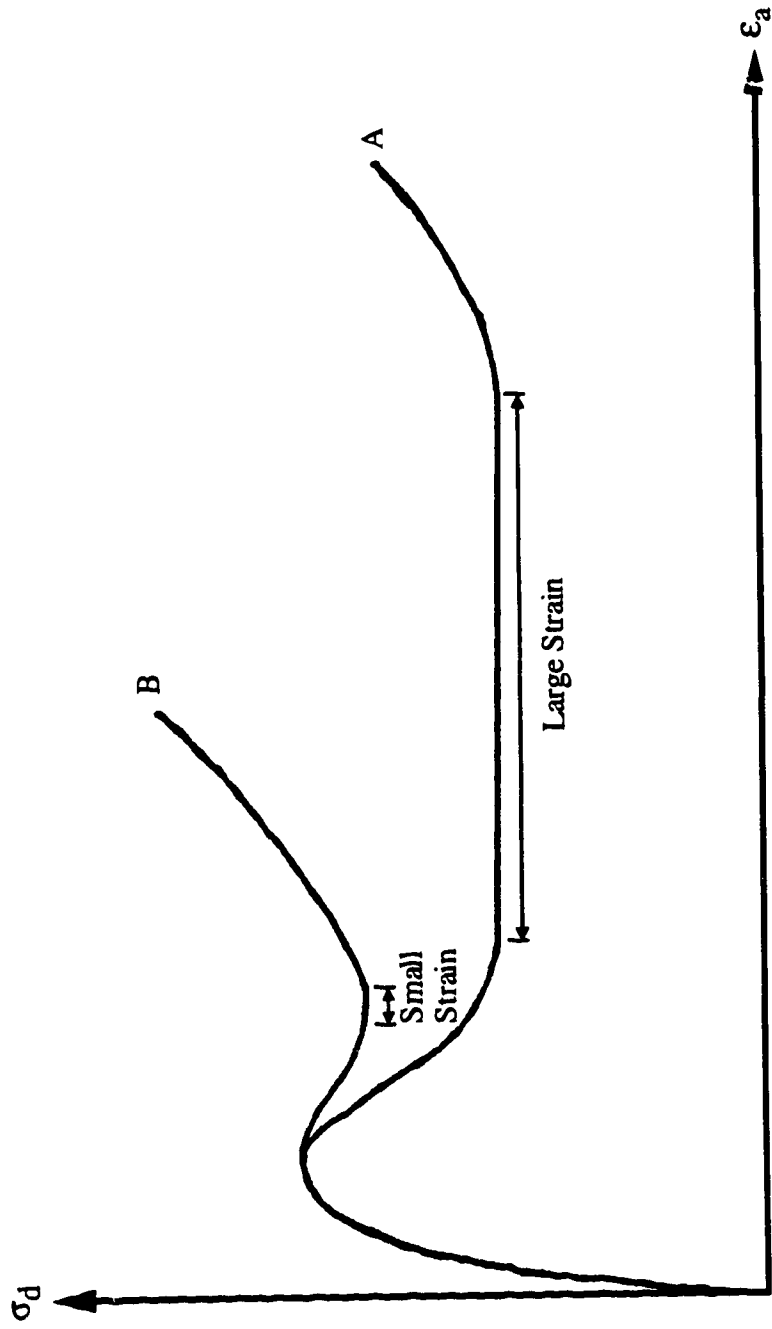


Figure 2.3.1.4 Strain Differences Prior to Dilation

3. TESTING PROGRAM

3.1 Laboratory Testing

A laboratory program was initiated to study the impact of fines, both plastic and non-plastic, and gradation on the monotonic undrained response. Unlike many other studies carried out, this study focuses on two main aspects and keeps other factors, which may or may not influence the results constant. The tests carried out in this research involve the same preparation method, initial effective stress level and test control. By eliminating a number of possible influences a study of the impact of fines and gradation can be undertaken. Although prepared at similar initial void ratios, the void ratios at the initiation of undrained testing were dissimilar. The difference in void ratios occurred during the saturation and consolidation phases and will be explained in later sections.

3.2 Materials Tested

Upon examination of laboratory data presented in the literature (Been and Jefferies, 1985; Hird and Hassona, 1986; Georgiannou, 1988; DeMatos, 1988) there was ambiguity concerning the interpretation of the susceptibility of soils containing fines to liquefaction. Therefore, questions on this aspect still exist. There is no mention in the literature on the comparison of plastic to non-plastic fines and their effect on the undrained response. Still ambiguous is the effect of gradation on liquefaction potential. The results of this study on sand gradation will be compared to the results of DeMatos (1988).

To clarify how the monotonic undrained response of a sand is affected by the addition of fines and varying gradation, a series of three tests were performed. All three sets of tests involve using the same sand and differ by adding different percentages of a plastic type fine, a non-plastic type fine and a non-plastic type sand. The first two sets of tests involve materials of varying coefficient of uniformity ($C_u = \frac{D_{60}}{D_{10}}$) with fines below 74 μm (#200 sieve) size being varied. The last set of tests involves a material of

approximately equal coefficient of uniformity but with no change in the fines below 74 μ m.

For this research, the sand used was a clean, uniform, sub-rounded quartz sand (Ottawa sand, C-109). The plastic-type fines were kaolinite and the non-plastic-type fines were crushed quartz sand. The non-plastic sand used was a clean, sub-rounded quartz sand with gradation between 0.25 to 0.075mm (#70-#140 sieve sizes). The grain size distribution of the four materials are shown in Figure 3.2.1. The physical characteristics for the materials used can be seen in Table 3.2.1.

To study the effect of adding fines and changing gradation, each of the three sets of tests involved adding 10, 20, 30 and 40% of kaolinite, crushed silica fines and 70-140 silica sand to Ottawa sand. The resulting grain size curves can be seen in Figures 3.2.2 to 3.2.4. To help facilitate a better understanding of results in later sections, Table 3.2.2 summarizes how the maximum and minimum void ratios are affected in each material. The ASTM method was used to determine the maximum and minimum void ratios. Although this method is not recommended for fines (<74 μ m) in excess of 12%, others (Kuerbis and Vaid, 1989) have used it successfully up to 30% fines. Before this table can be properly understood a discussion of the nomenclature used in distinguishing tests should be highlighted.

3.2.1 Test Nomenclature

A typical test could be labeled O10K350, O20SF350 or O40RF350. The first letter signifies that Ottawa sand is used and the following two numbers indicates the percentage of either kaolinite (K), crushed silica fines (SF) or 70-140 silica sand (RF) being added. The final three numbers represent the effective stress level at which the samples are consolidated.

3.3 Testing Program

All the samples were prepared by moist tamping, consolidated to the same effective stress level (350kPa) and tested in an isotropic undrained manner using a strain-rate

controlled triaxial apparatus. By keeping these variables constant it was felt a clearer picture of the influence of fines and gradation on the undrained response would be observed.

Built into the triaxial cell were bender elements to facilitate the measurement of shear wave velocities. Although some difficulties arose from the use and subsequent interpretation of the results, the bender elements performed well and provided some insight on how fines and gradation effects the measured shear wave velocities.

3.4 Triaxial Tests

Triaxial tests were conducted using a strain-rate-control technique. For the strain-rate-controlled tests carried out, the strain is controlled by a loading device which strains the sample at a constant rate. To meet the requirement of isotropic conditions weights were added to the triaxial assembly to compensate for the area difference of the loading ram.

3.4.1 Test Apparatus

The triaxial compression test apparatus was made by Wykeham-Farrance and modified so compensating weights could be added.

The major equipment components used in the research were:

- (1) Triaxial cell
- (2) Constant pressure line
- (3) Data acquisition system
- (4) Cell volume change device
- (5) Back pressure change device
- (6) Wykeham-Farrance loading press
- (7) Wave generator, amplifier, oscilloscope and plotter
- (8) Load cell, pore pressure transducers, linear voltage displacement transducers (lvdt's) and pressure gauges.

Figures 3.4.1.1 and 3.4.1.2 are schematic figures to show the triaxial cell assembly for testing, freezing and shear wave velocity measurement. Figure 3.4.1.3 is a photograph of the set-up in the laboratory. To the left hand bottom of this photograph is part of the shear wave velocity measurement devices and to the right is the triaxial cell sitting on the freezing plate in the Wykeham-Farrance loading press. The compensating weights can also be seen added to the top of the loading ram. In the left hand top corner of Figure 3.4.1.3 is a grey cylinder mounted to the wall. A line goes from the bottom port of the grey cylinder to the top port of the triaxial cell and provides the cell pressure.

The Wykeham-Farrance loading press is shown in Figure 3.4.1.4. This screw-type press can provide a constant rate of strain through use of a variable speed gear drive unit. By changing the gear combinations, the rate of strain in the apparatus can be varied. For all the tests carried out the rate used was 0.760mm/min ($\approx 0.66\%/min$).

The cell volume change could be monitored during testing by the device shown in the bottom right hand corner of Figure 3.4.1.5. The device was designed by the University of Alberta laboratory personnel. The unit consists of a cylinder with a moving internal diaphragm inside and a lvdt attached to the outside to track the movement of the diaphragm. As the volume changes in the triaxial cell, the diaphragm is displaced upwards or downwards, depending on the orientation of the valve on the front. By recording the voltage change of the lvdt and calibrating it to the volume change of the cylinder, accurate volume changes in the triaxial cell can be measured.

The electronic data acquisition system, as shown in Figure 3.4.1.6, was used to read the various pressure transducers, load cell and volume change transducers. The electronic data acquisition system consists of a microcomputer and a datalogger board. A switching and control box, with the necessary amplifier for low signal output of the transducers, was attached to the data logger.

3.4.2 Sample Preparation

The soil specimens were approximately 63mm in diameter and varied in height from 110 to 120mm. Of concern was the end restraint effects that might come into play

during testing. From a review of the literature it was found (Georgiannou, 1988) that for height to diameter ratios of 2 to 1, end restraint has little effect. This is only contradicted when samples are strongly dilatant. The higher the dilation, the higher will be the difference between rough and frictionless ends. For this research, height to diameter ratios were around 2 to 1 and only some of the materials behaved in a slightly dilatant manner.

Soil behaviour can be highly dependent on the method of laboratory preparation as was shown in numerous studies (Been et al., 1991; Seed et al., 1988; Kuerbis, 1989; Miura et al., 1982). Two of the more popular methods of soil reconstitution techniques include water pluviation and moist tamping. For the experimental work carried out in this study the latter was used to prepare all samples.

To ensure a strain softening response during undrained shear it is necessary to prepare the samples in a very loose state; ie. the void ratio is larger than the value at steady-state at the same normal effective stress. To achieve such a stress state the samples should be prepared in an unsaturated condition, then saturated and consolidated to the desired effective stress level.

The moist tamping preparation method produces very loose or commonly referred to as bulked, partially saturated samples. Questions arise as to the uniformity of the soil matrix and the sample as a whole. These issues will be addressed in section 3.4.3. The moist tamping method produces samples at high void ratios due to water tension forces acting between the grains. The capillary tension forces control the particle interaction within the soil. This is because capillary tension forces, at low confining stresses, are considerably larger than self-weight forces and thus the particle contacts are essentially random because water tension forces which control the soil structure are independent of direction (Kuerbis, 1989). The magnitude of capillary tensions within a soil varies with grain size (Kuerbis, 1989). Fine grained soils will therefore generate larger capillary tensions and thus be subject to greater bulking and an increased resistance to densification during tamping.

As was observed in this research and by other workers (Sladen et al., 1985) when silty sands are assembled in such a loose state they undergo large strains during saturation.

This is due to the removal of the water tension forces between the grains. It was found that if the soil specimen could be saturated with small induced strains it behaved in a less compressible manner during consolidation and hence, test samples of larger void ratios could be created.

The various samples tested in this study were prepared by combining predetermined amounts of oven-dried Ottawa sand and by adding varying percentages of kaolinite, crushed silica fines and 70-140 silica sand. The combined ingredients were thoroughly mixed to ensure a uniform mixture. An aluminum split mold and small drop hammer was used to form the specimen.

When using moist tamping, it is difficult to ensure an uniform density distribution in reconstituted samples of sand. The challenge therefore is to minimize the density variations. There are a number of procedures which can be followed in order to achieve this. For the work carried out in this research the method by Mulilis et al. (1977) was followed. This method involves placing the sand in a number of layers (four in this case) and with each layer increase the compactive effort (ie. increase the number of drops of the drop hammer). A check on the variation of density within the sample will be presented in section 3.4.3.

Once the specimen was formed in the aluminum split mold, the top loading ram was placed on the top of the sample making sure that the bender elements were aligned properly. A suction of about 10kPa was applied to the base of the sample so that the split mold could be disassembled. Direct measurement of the sample dimensions was then made. These measurements, together with the known weight and specific gravity of the soil particles, were then used to calculate the void ratio prior to saturation of the sample. The remainder of the cell was assembled, filled with oil and placed in the loading press (Figure 3.4.1.4).

A normal confining stress of 40kPa was applied to the sample prior to saturation. During the early stages of the research there were a number of samples which collapsed during the saturation stage. A discussion of the procedural changes made as a result of this will be presented in section 3.4.4.

The saturation of the samples was carried out in a two-step process. To facilitate higher saturation values ($B=1$), carbon dioxide (CO_2) was first percolated through the sample under a low pressure gradient of 5kPa for about 20 minutes. Water was then flushed through the sample. The supply of water is gravity fed from a tank under a pressure head of 1m. Both the water tank and CO_2 tank can be seen in Figure 3.4.2.2.

It is well recognized that there is likely to be a volume change associated with the saturation process, especially in loose collapsible soils. Section 3.7 will discuss the inherent problems in calculating these volume changes.

The second stage of saturation involved back-pressure techniques. The cell pressure and back pressure were increased in the same increments so that a 50kPa excess pressure difference was maintained with respect to back pressure. By monitoring the sample pore pressure and cell pressure, determination of Skempton's B parameter could be made. When the sample reached B values greater than 0.98 it was considered to be saturated and consolidation was allowed to occur.

All samples tested in this research were consolidated to an isotropic ($K_0=1$) effective stress of 350kPa. Consolidation was carried out in four stages, each stage involving an increase in cell pressure of 100kPa. After each stage a measure of shear wave velocity was taken using the apparatus in Figure 3.4.2.3. All the pressure, lvdt, volume and arrival times are transferred into a formatted spread sheet which calculates among other things, the normalized shear wave velocity (V_{s1}) and the membrane corrected void ratio.

After consolidation was completed the drainage valve was closed and the specimen was sheared undrained at a constant strain rate of 0.760mm/min ($\approx 0.66\%/min$). The magnitude of axial load, axial deformation and sample pore pressures were recorded by the data acquisition system (Figure 3.4.1.6) at intervals of 30 seconds. Most samples were tested to a axial strain of 20% with shear wave measurements taken at test completion and for some samples at 5% axial strain. For samples that were frozen to facilitate SEM work and density checks, the tests were stopped at an axial strain of 15%.

The set-up used for samples that were to be frozen (non-plastic fines) is shown in Figure 3.4.2.4 and schematically in Figure 3.4.1.1. As shown in Figure 3.4.2.4, the loading press and triaxial cell apparatus was placed in a freezer unit to help speed up the freezing operation. Liquid nitrogen was passed through a freezing plate in the base of the triaxial cell. With this type of arrangement the sample freezes from the bottom towards the top. A Resistance Temperature Device (RTD) is incorporated into the top of the triaxial cell and indirectly measures the temperature at the top of the sample. When the top of the sample reached 0°C (RTD reading of 100mV) the sample was considered to be frozen. The cell was then disassembled, the sample removed and placed in the cold storage room for later use.

For samples which contained plastic fines the samples were carefully removed and waxed. Volume checks, using the waxed specimens were carried out to check the values recorded by the data acquisition system. The samples were saved for later use in SEM work.

3.4.3 Verification of Sample Preparation

A verification of both fines and density variations was carried out for this research. To check the fines variation sieve analysis were performed on samples taken from the top, middle and bottom of two samples used in different tests. The variation of fines less than 0.149mm (#100 sieve size), as compared to the gradation curves in Figures 3.2.2 to 3.2.4, was 1%. The small variation in fines is a result of the low rate at which CO₂ and water were passed through the samples. If higher flow rates were used, the upward flow would cause fines to migrate from the bottom of a sample toward the top of the sample. This would result in higher fines content at the top of the sample and hence, a non-uniform sample.

For the two samples which were frozen, density and void ratio variation tests were completed. The results of these tests can be seen in Table 3.4.3.1. The densities and void ratios achieved in the two samples were uniform. The void ratios increased slightly from the bottom to the top of the two samples, but all were close to the

consolidated void ratios tabulated in Table 3.2.2. These results imply that the method of sample preparation provided essentially homogeneous samples.

3.4.4 Problems with Structural Collapse During Sample Saturation

There were a number of samples which failed during the saturation stage. The collapses which occurred were the result of the metastable structure created by the moist tamping preparation technique. In the early stages of testing the normal effective stress level, prior to saturation, was around 12-15kPa. The pressure for flushing water through the sample was created by the head difference between the triaxial cell and the water tank. This pressure was found to be around 10-11kPa. What occurred was that the upward flow of water through the samples was reducing the suctions present, causing the samples to collapse. After discovering the problem the normal effective stress was increased to 40kPa during saturation and no further collapses occurred.

3.5 Formulation

Readings that were recorded by the various transducers and lvdt's were converted from voltage units to their respective units by means of calibration factors. The converted readings were then used to calculate the shear wave velocities, void ratios, axial strains, deviator stress and major and minor principal strains.

3.5.1 Shear Wave Velocity

The formula for shear wave velocity is:

$$V_s = \frac{(H_c - 21.52)}{1000 T_t} \quad [\text{m/s}]$$

where

V_s = shear wave velocity

H_c = current height of specimen [mm]

21.52 = combined height of bender elements protruding into the specimen [mm]

T_t = arrival time [sec].

The formula for normalized shear wave velocity is:

$$V_{s1} = \frac{V_s}{\left(\frac{EP}{100.1}\right)^{0.25}} \quad [\text{m/s}]$$

where

V_{s1} = normalized shear wave velocity (Hardin and Richart, 1963)
(corrected for overburden effects)

EP = current effective stress level (kPa).

3.5.2 Void Ratio

The formula for void ratio used is:

$$e = \frac{G_s (V_{ci} + \Delta V)}{W_g} - 1$$

where

e = sample void ratio

G_s = specific gravity of sand [g/cm³]

V_{ci} = volume at the beginning of consolidation [cm³]

ΔV = change in volume during various stages of back pressure saturation and consolidation [cm³]

W_g = initial dry weight of the specimen [g].

In this study the specimen was covered by a flexible rubber membrane. The volume change which occurs during back pressure saturation and consolidation is a function of

not only of the response to soil deformations but also due to the penetration or withdrawal of the membrane from the interstices around the outside of the specimen (Vaid and Negussey, 1984). Therefore to accurately determine the volumetric deformation of just the soil skeleton, adjustments must be made for membrane penetration.

There has been various attempts by Raju and Sadasivan (1974), Frydman et al. (1973), and Roscoe (1970) to quantify membrane penetration. The method used in this research follows the method presented by Vaid and Negussey (1984). Vaid and Negussey (1984) proposed that the ratio of the total volume change to soil surface area covered by the membrane ($\Delta V_T/A_s$) versus the specimen diameter, D , was a linear relationship for a given sand. In this experiment, the total volume change during consolidation has been measured from an initial state under 50kPa effective confining pressure. The following equation was proposed by Vaid and Negussey (1984):

$$\begin{aligned}\Delta V_{\text{corr}} &= \text{membrane volume correction} + \Delta V \\ &= -0.045 \log \left(\frac{CP}{CP_c} \right) (A_s) + \Delta V\end{aligned}$$

where

- ΔV_{corr} = corrected volume change
- CP = base effective confining pressure (50kPa)
- CP_c = current effective confining pressure
- A_s = soil surface area covered by membrane
= $H (\pi D)$
- H = specimen height
- D = specimen diameter
- ΔV = change in volume during various stages of back pressure saturation and consolidation.

The factor -0.045 is the slope of the unit membrane penetration, ϵ_m versus effective confining pressure for Ottawa sand. If another host sand was to be used a different factor would have to be determined and employed. With the membrane correction, the void ratio formula is:

$$e_{mc} = \frac{G_s (V_{ci} + \Delta V_{corr})}{W_g} - 1$$

3.6 Shear Wave Velocities using Bender Elements

An accurate determination of shear wave velocity in the laboratory was difficult until the development of piezoceramic bender elements (Dyvik and Madshus, 1985). The pioneers in this field of research were Shirley (1978) and Schultheiss (1981).

The bender element is an electro-mechanical transducer which is capable of converting mechanical energy (lateral movement of the bender element) either to or from electrical energy (Gohl and Finn, 1991). The element itself consists of a sandwich of two piezoceramic plates which are bonded together with conducting surfaces between them and on the outsides. The polarization of the ceramic material in each plate and the electrical connections are such that when a driving voltage is applied to the element, one plate elongates and the other shortens.

There are basically two different types of bender elements: series connected and parallel connected. In a series connection the two ceramic plates are of opposite polarization (both are oppositely charged). The parallel connection is reversed and also includes an additional electrode between the plates which is charged with the other pole (either positive or negative). A schematic of these connections can be seen in Figure 3.6.1.

A series connection is better at converting electrical energy into mechanical energy and therefore is used as the generator of shear waves. On the other hand, the parallel connection is more effective at converting mechanical energy to electrical energy and therefore it is used as a receiver of shear waves in the soil specimen.

To prevent an electrical short of the elements when exposed to moisture, the entire assembly is coated with an epoxy (PF 5-7B marine sealant in this experiment). As well, after the assembly is placed in the top and bottom caps of the triaxial apparatus it is sealed with sealant RTV to prevent moisture and sand grains from entering. More details can be found in Dyvik and Madshus (1985). For more details see Figure 3.6.2.

The shear wave velocity was measured using the apparatus in Figure 3.4.2.3. In clockwise rotation starting from the top left corner is the plotter, oscilloscope, amplifier and the wave generator. A hard copy of each shear wave pattern was plotted out for use in later calculations.

A pulse from the wave form generator provides the electrical energy ($\pm 15\text{V}$, 20Hz) for the driving bender element. Upon receiving this energy the bender element behaves as a fixed end cantilever moving the soil particles in the same direction as the tip. This generates a shear wave which propagates down the sample and is received by the receiver bender element. The resulting electrical signal is collected by an oscilloscope (Philips PM 3365A digital storage oscilloscope) and is amplified to produce a plot such as in Figure 3.6.3 from test O10RF350. The entire schematic set-up was shown in Figure 3.4.1.2.

The shear wave is assumed to propagate from the tip of the transmitting bender element to the tip of the receiving bender element. The length of travel of the shear wave, L_t , is then equal to the consolidated length of soil minus the combined length of the bender elements. The travel time, T_t , of the shear wave through the sample is considered to be the time difference between the rise of the square wave driving signal and the first significant jump in the received wave signal. The shear wave velocity through the soil specimen is thus:

$$V_t = \frac{L_t}{T_t}$$

and the shear modulus (G) is calculated as:

$$G = \rho V_s^2$$

where ρ is the present mass density of the soil.

The tips of the bender elements are embedded in the soil specimen, making sure that they are aligned parallel so that a “clean” signal is received. A “clean” signal is one where the wave signal received is not distorted and there is a clean point where the

wave is first received. If the elements are not aligned parallel, the received signal will be displaced by some phase shift, making the exact travel time difficult to determine. Since the travel times are extremely small, minor errors in determining the consolidated height of the sample can result in large variations in the measured shear wave velocity. The volume change during saturation and consolidation are measured by an electrical transducer and are considered to be extremely accurate. The only source of error can arise from measuring the initial sample height. Although this is done with great accuracy, it is still a potential source of error.

Hardin and Richart (1963) did a number of experiments to determine some of the parameters affecting shear wave velocity. They found that the higher the moisture content in Ottawa sand the lower was the shear wave velocity. From their studies on crushed quartz silt the principal effect of saturation was on the consolidation behaviour of the material, which in turn relates to void ratio changes. As well, they found shear wave velocity to vary linearly with void ratio, independent of grain size, gradation and relative density. From their research, Hardin and Richart (1963) implied that materials with the same void ratio, regardless of the fabric, would have the same shear wave velocity. However, this research has found that fabric plays a very important role in the magnitude and variation of shear wave velocities. In some instances fabric may play the leading role, with void ratio having a minor role. This will be discussed in section 4.4.

3.7 Volume Change During Saturation

As previously mentioned it is difficult to determine the volume change that a sample undergoes during saturation. The tests performed by Sladen and Handsford (1987) and the tests conducted in this research have found that the potential for volume change increases as the percentage of fines is increased.

Determining the volume of the sample at the beginning of consolidation, V_c , and hence, the initial void ratio, is a difficult task when working with kaolinite, a plastic-type fines. When working with crushed silica fines, a non-plastic-type fines, the volume change which is measured during water saturation is small, in the order of 3%. Therefore, the volume calculated from the initial sample dimensions has changed very little and can be

used to calculate V_c along with the assumption that there is isotropic volume change occurring ($\epsilon_v = 3 \epsilon_a$).

When plastic-type fines are added, the volume change during saturation can be as high as 11%. This volume change was subtracted from the initial volume, which is calculated from the initial sample dimensions, and used as the volume prior to back pressure saturation (V_b). The volume change which occurred during back pressure saturation, along with V_b , and the isotropic volume change assumption, was used to calculate V_c . The value of V_c calculated in this manner was found to be in gross error. An alternative approach was to use the initial sample dimensions and the total height change to calculate V_c . The total height change is considered to be the combination of the height change during water saturation and during back pressure saturation. Using this height change, along with the isotropic volume change assumption, V_c was calculated.

To verify the calculation of V_c , various kaolinite enriched samples were retrieved after undrained loading and tests were performed to calculate the actual volume of the sample. This volume was usually about 5% smaller than V_c calculated above. This difference is accounted for by the volume change which occurred during sample retrieval.

3.8 Dominating Influence of Fines

Whether or not the fines or coarse fraction will tend to dominate the behaviour of a soil can be anticipated to some extent in terms of the percentage of fines in the soil. Water is strongly attracted to plastic-type fines and results in plasticity; whereas the non-plastic-type fines have little affinity for water and do not develop significant plasticity (Mitchell, 1976).

It is possible from an observational point of view to estimate the quantity of fines needed to prevent direct contact between granular particles. This will be presented in section 4.1.6. From a theoretical point of view the above task is extremely difficult.

It is visualized that each sample consists of a skeleton structure formed by the sand grains with the voids filled with fines and water. The underlying assumption when deriving the relations below is that the quantity of fines is insufficient to separate any sand grains.

The conventional definition of void ratio, e , is misleading because one e value can have several different fines contents. To cope with this problem intergranular void ratio, e_g , was formulated. The drawback of e_g is that it is inadequate in characterizing sands with different types of fines and it gives no indication of the distribution of fines within the soil. A full discussion of this with relation to the SEM results will be presented in section 4.3.

For sake of completion the equations for e and e_g are presented below:

$$e = \frac{w G_s G_f}{(1 - f_c) G_f + f_c G_s}$$

$$e_g = \frac{G_s (w G_f + f_c)}{G_f (1 - f_c)}$$

$$(1 + e) = (1 - f_c) (1 + e_g)$$

where

e = void ratio

e_g = intergranular void ratio

w = water content

G_s = specific gravity of granular particles

G_f = specific gravity of fine particles

f_c = fines fraction.

3.9 Description of Scanning Electron Microscope (SEM) Work Performed

To better understand what was taking place at the intergranular level, SEM work was performed. The results in section 4.3 will be used to explain the difference in behaviour at different percentages of fines, for both plastic- and non-plastic-type fines. A total of four sets of tests were performed. Two sets of tests involve kaolinite at 20 and 40% fines contents and the other two sets of tests involve crushed silica fines at 20 and 40% fines contents.

The procedure for preparing the samples varied for the kaolinite and crushed silica fines. Kaolinite samples could not be frozen prior to testing. This is because the 1-D freezing used in this research would cause significant frost heaving and distortion in the sample (Dávila, 1992). The crushed silica samples were frozen prior to SEM testing and sectioned into 5mm slices.

For the kaolinite samples a suction needle-like device was used to probe the sample for a specimen. After obtaining the specimen it is quickly dipped in liquid nitrogen. This flash freezing technique does not allow the specimen to change volume or distort. Once the sample is frozen the procedure for the two types of fines was similar.

From each specimen a piece was broken off and mounted in a viewing chamber. This sample was then loaded in the device shown in Figure 3.9.1. The samples were then sheared, to show a clear picture of grain orientation and any ice, from the freezing procedure, was sublimed off. The samples were then coated with a thin spray of gold. When electrons are bounced off the sample during testing, the gold absorbs electrons in varying amounts, which gives contrasts and hence, an image can be seen on the device in Figure 3.9.2. The image can then be viewed at different magnifications and polaroid pictures taken for later detailed examination and to provide a permanent record.

Material	G_s	e_{min}	e_{max}	C_u
Ottawa Sand	2.67	0.82	0.50	1.69
Kaolinite	2.60		---	very high
Crushed Silica Flume	2.65	---	---	8.24
70-140 Silica Sand	2.64	---	---	2.05

Table 3.2.1 Properties of Materials Used

Test	C_u	e_{min}	e_{max}	$e_{max}-e_{min}$	e_c
O10K350	10.3	0.343	0.671	0.33	0.42
O20K350	354.5	0.223	0.667	0.44	0.16
O30K350	750.0	0.215	0.770	0.55	0.22
O40K350	1033.3	0.275	0.815	0.54	0.56
O10SF350	5.9	0.393	0.913	0.52	0.78
O20SF350	32.5	0.410	1.114	0.70	0.67
O30SF350	43.9	0.578	1.470	0.89	0.74
O40SF350	62.0	0.762	1.890	1.13	0.77
O10RF350	2.33	0.439	0.701	0.26	0.83
O20RF350	2.70	0.403	0.696	0.29	0.79
O30RF350	2.71	0.413	0.658	0.25	0.79
O40RF350	2.72	0.415	0.681	0.27	0.84

Table 3.2.2 Material Properties for Various Tests

Slice	Thickness (mm)	Diameter (mm)	Weight (g)	Volume (cm ³)	Density (g/cm ³)	Void Ratio e
1 (Bottom)	12.45	65.35	80.2	41.76	1.921	0.67
2	10.37	68.09	72.4	37.76	1.917	0.67
3	11.71	66.88	80.3	41.14	1.952	0.68
4 (Top)	17.25	64.21	107.8	55.86	1.930	0.68

Slice	Thickness (mm)	Diameter (mm)	Weight (g)	Volume (cm ³)	Density (g/cm ³)	Void Ratio e
1 (Bottom)	11.03	61.87	67.7	33.16	2.042	0.75
2	10.26	62.49	64.7	31.47	2.056	0.76
3	10.16	62.97	64.1	31.64	2.025	0.77
4 (Top)	16.60	58.89	88.1	43.58	2.022	0.77

Table 3.4.3.1 Density and Void Ratio Variations for Samples a) O20SF350
b) O40SF350

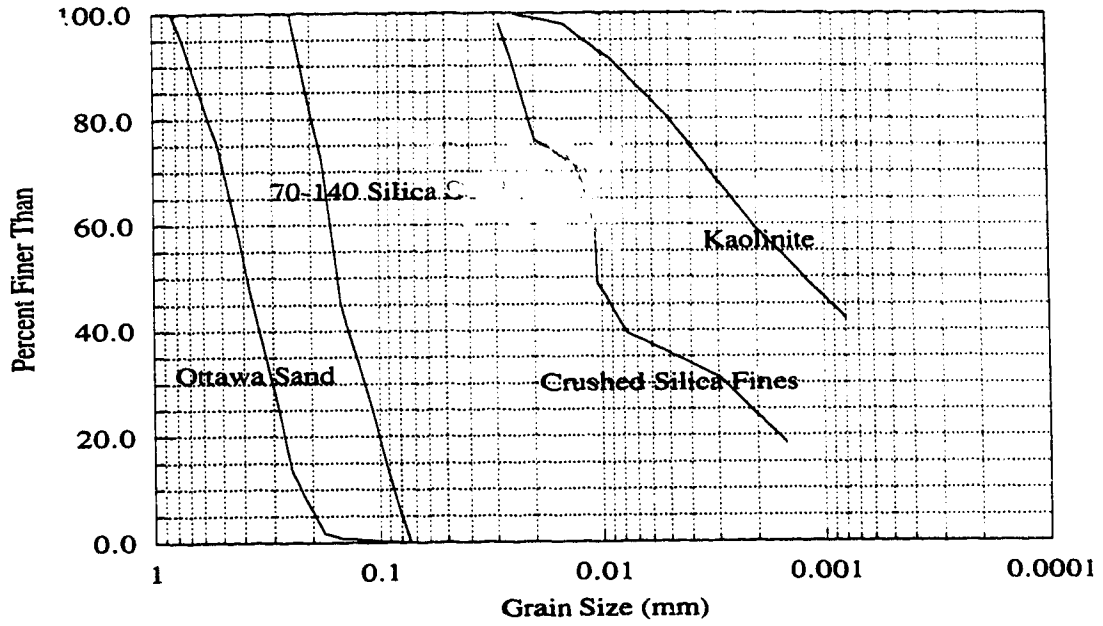


Figure 3.2.1 Grainsize Curves for Ottawa Sand, 70-140 Silica Sand, Crushed Silica Fines and Kaolinite

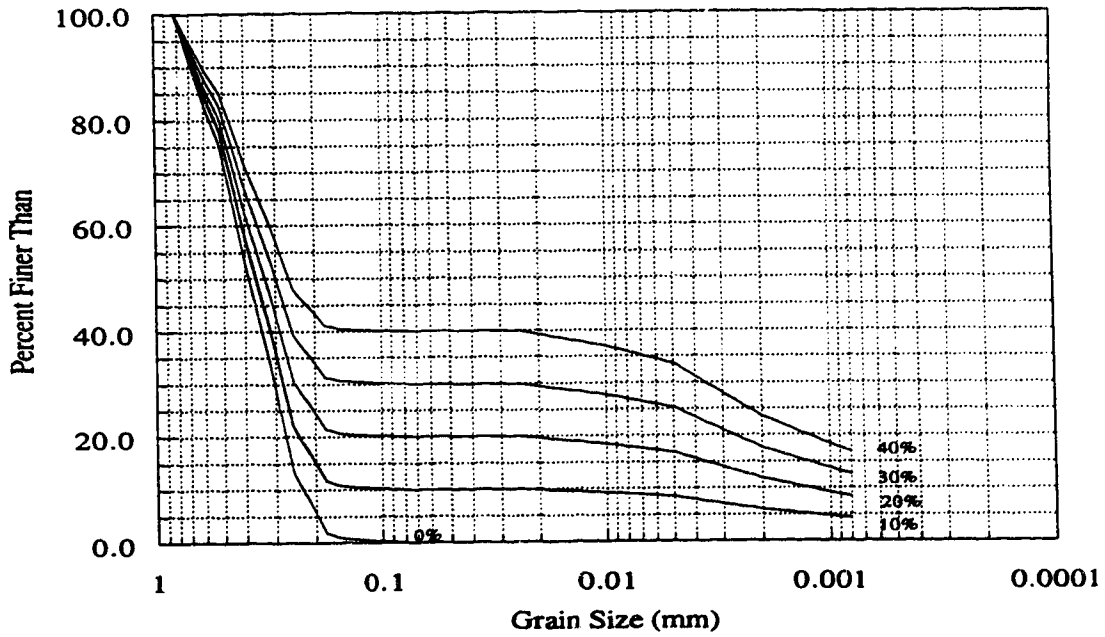


Figure 3.2.2 Grainsize Curve for Addition of Various Percentages of Kaolinite to Ottawa Sand

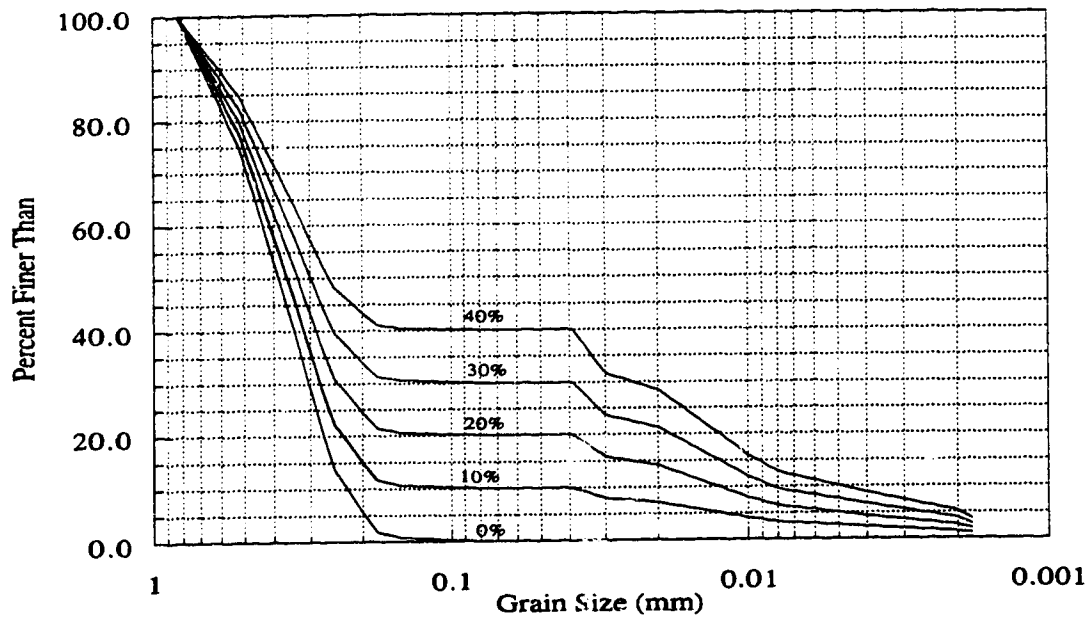


Figure 3.2.3 Grainsize Curve for Addition of Various Percentages of Crushed Silica Fines to Ottawa Sand

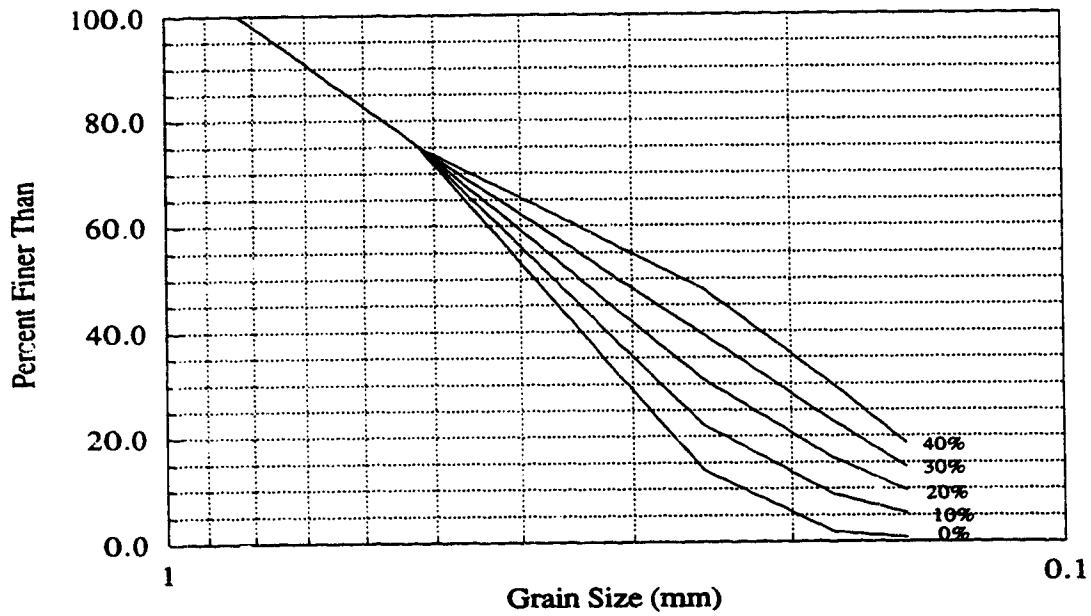


Figure 3.2.4 Grainsize Curve for Addition of Various Percentages of 70-140 Silica Sand to Ottawa Sand

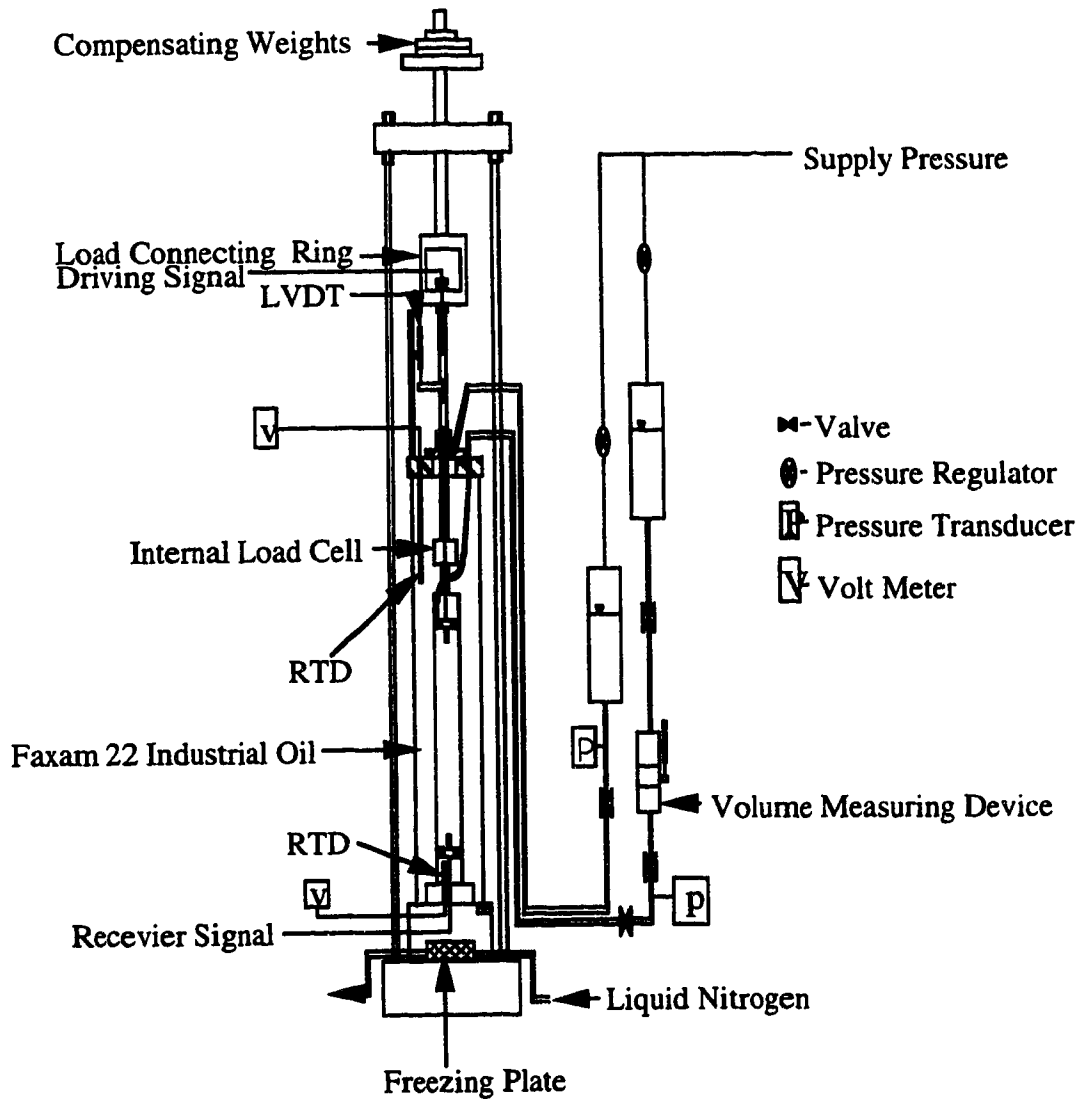


Figure 3.4.1.1 Schematic Layout for Triaxial Cell and Freezing Plate
(after Sasitharan et al., 1992)

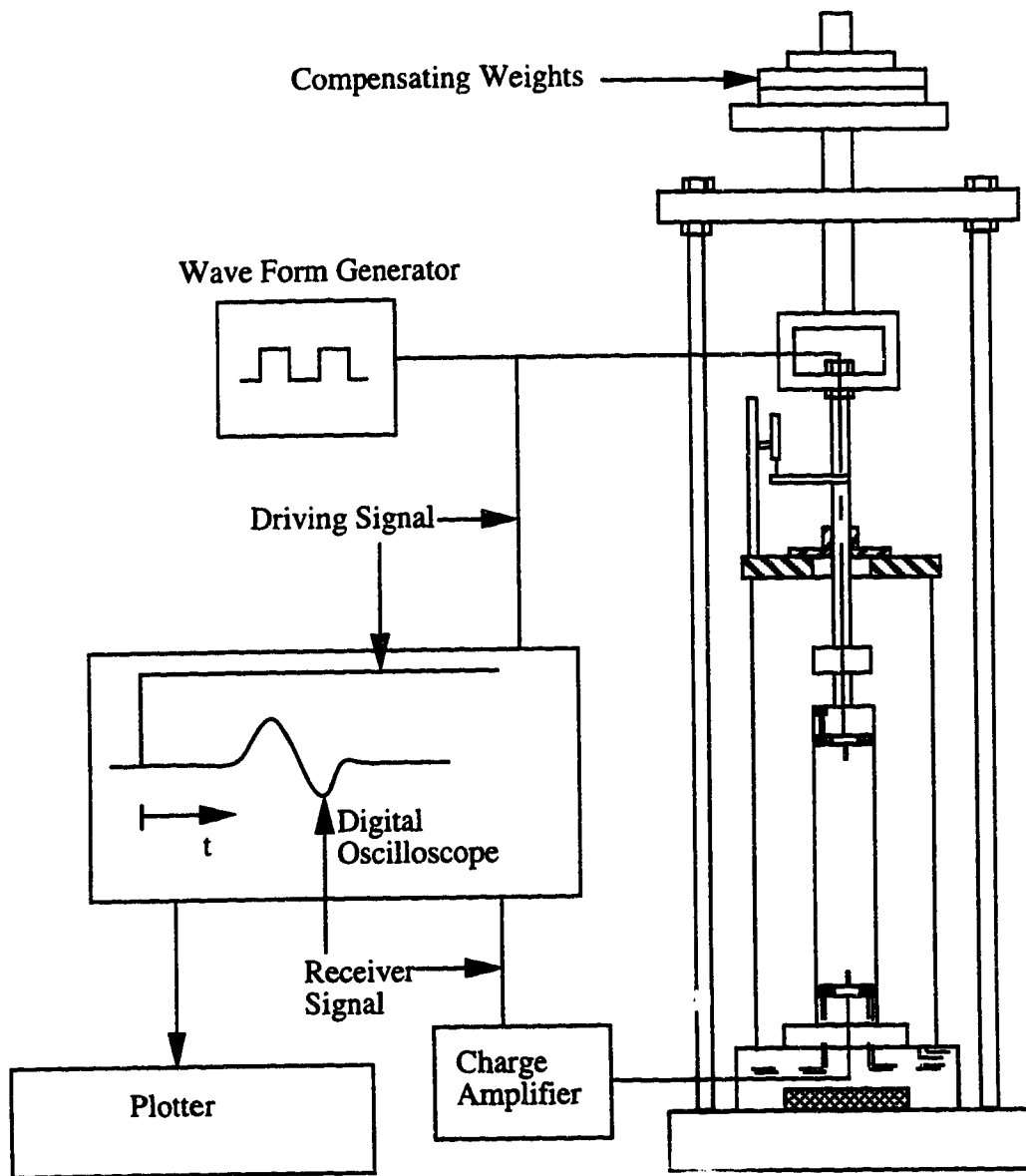


Figure 3.4.1.2 Schematic Layout of the Shear Wave Measuring System
(after Sasitharan et al., 1992)

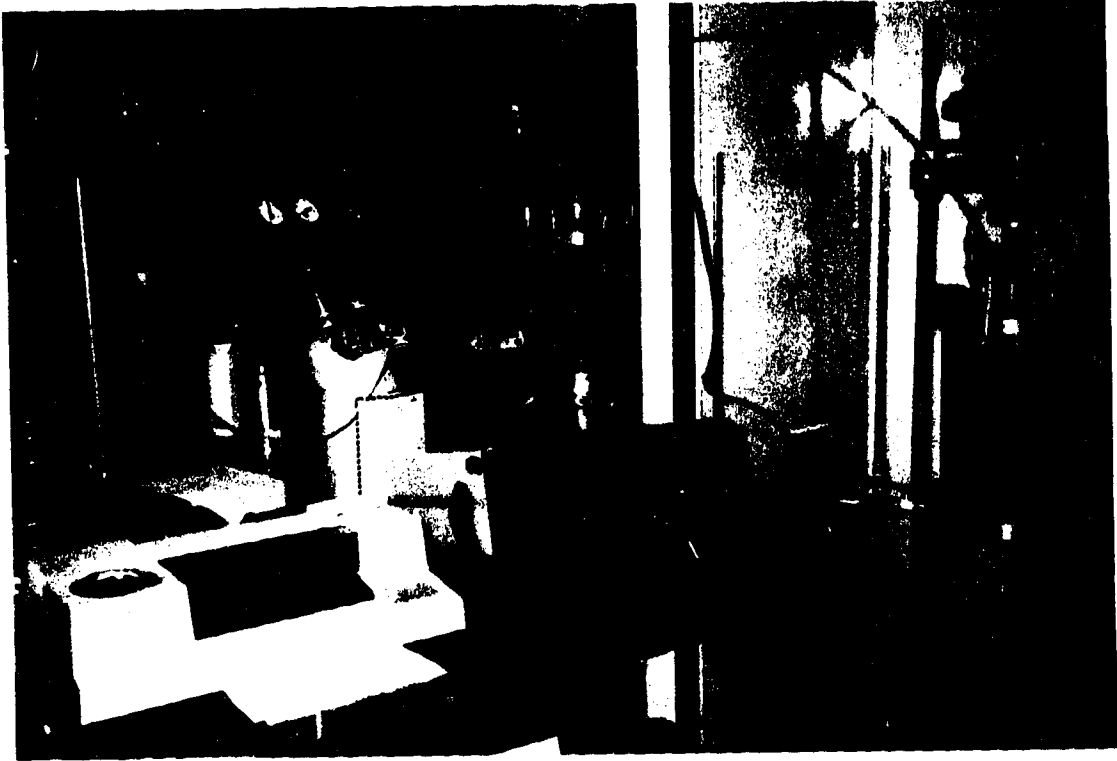


Figure 3.4.1.3 Photograph of Laboratory Set-Up

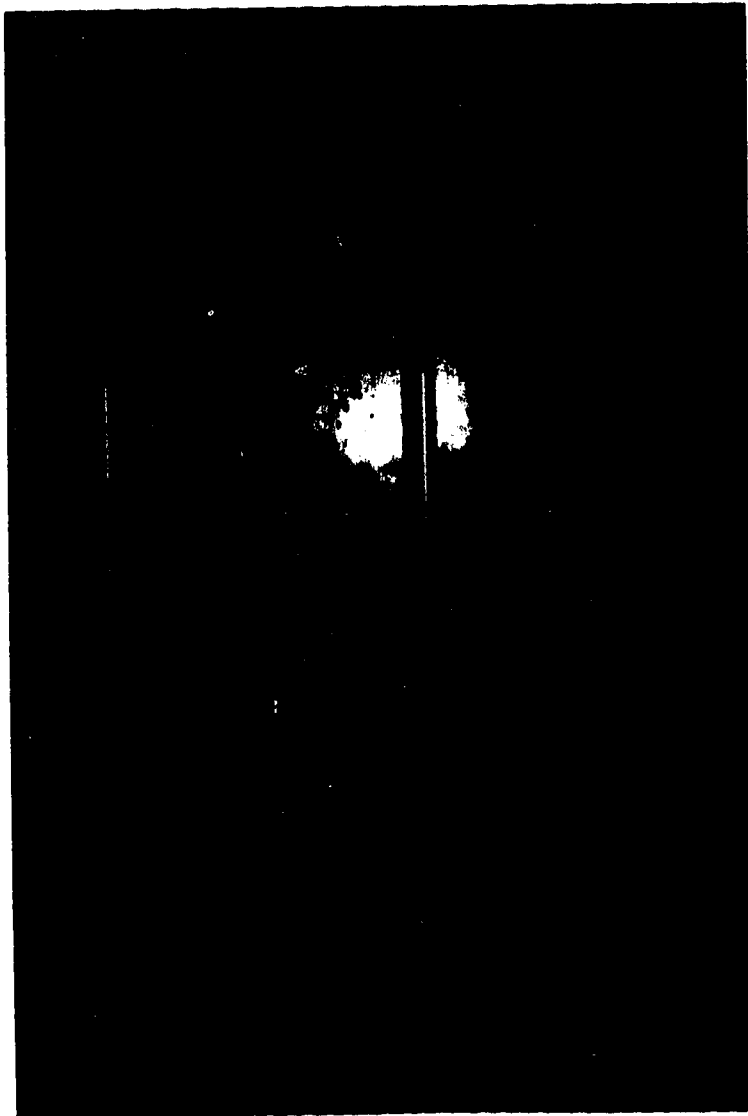


Figure 3.4.1.4 Photograph of Wykeham-Farrance Loading Press

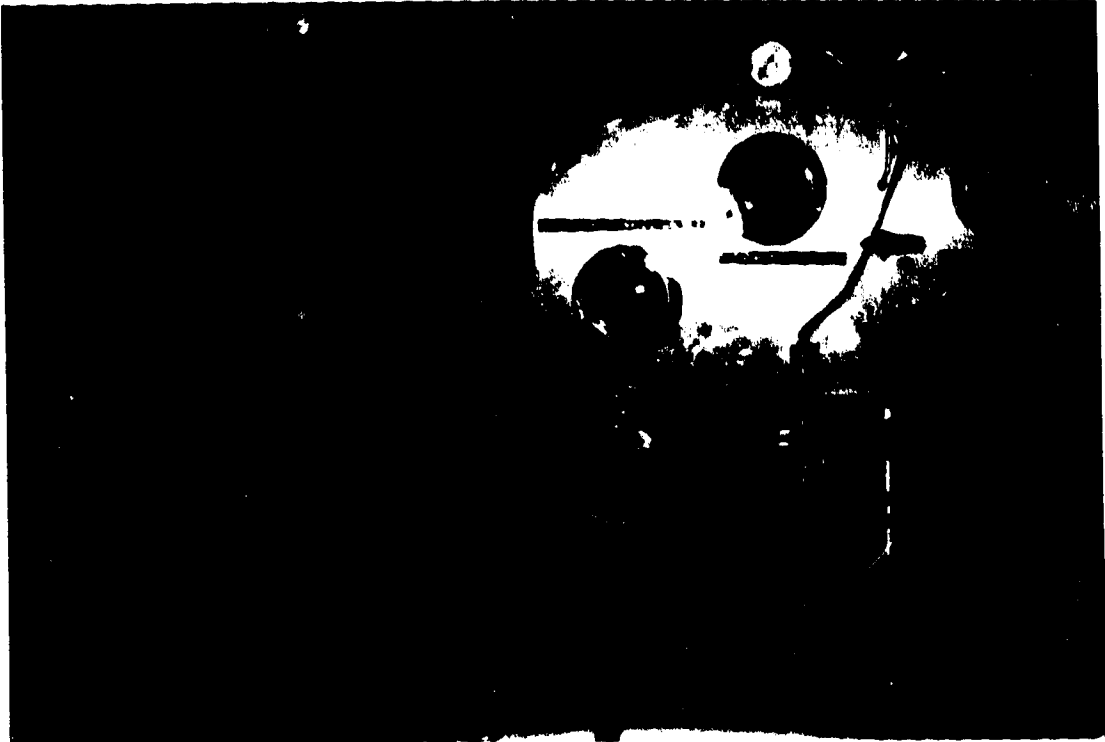


Figure 3.4.1.5 Photograph of Volume Change Device



Figure 3.4.1.6 Photograph of Data Acquisition System

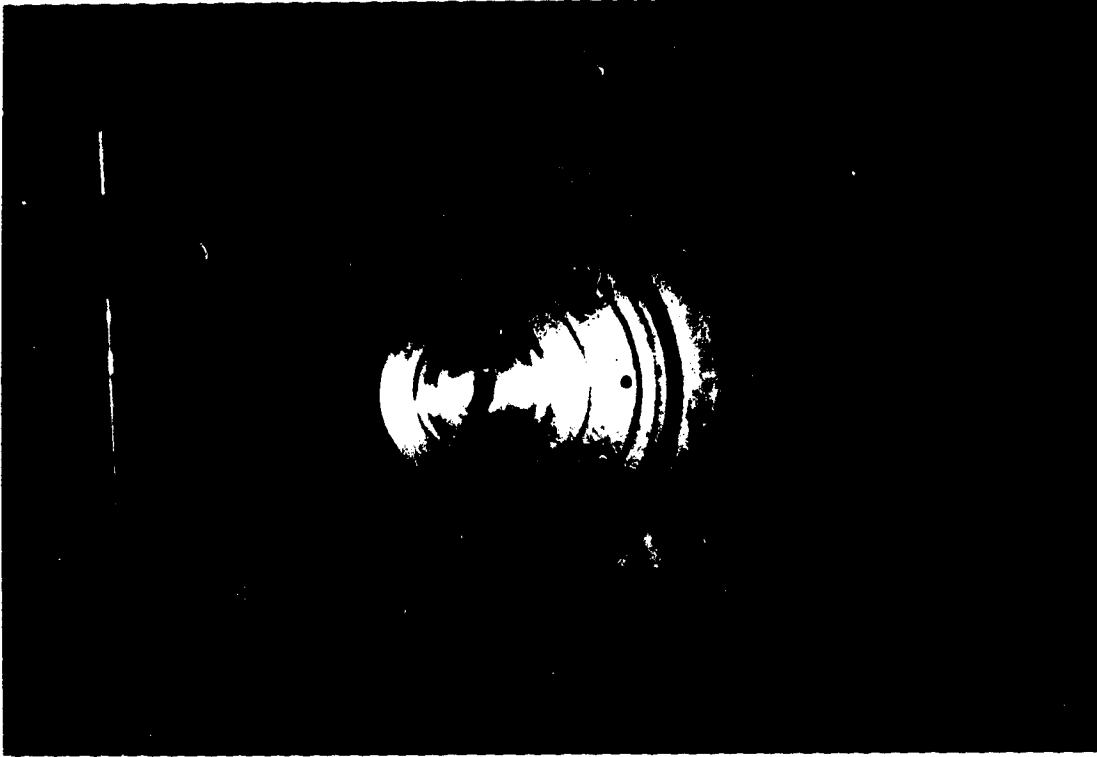


Figure 3.4.2.1 Photograph of Loading Ram and Base Assemblage



Figure 3.4.2.2 Photograph of Water and CO₂ Supply

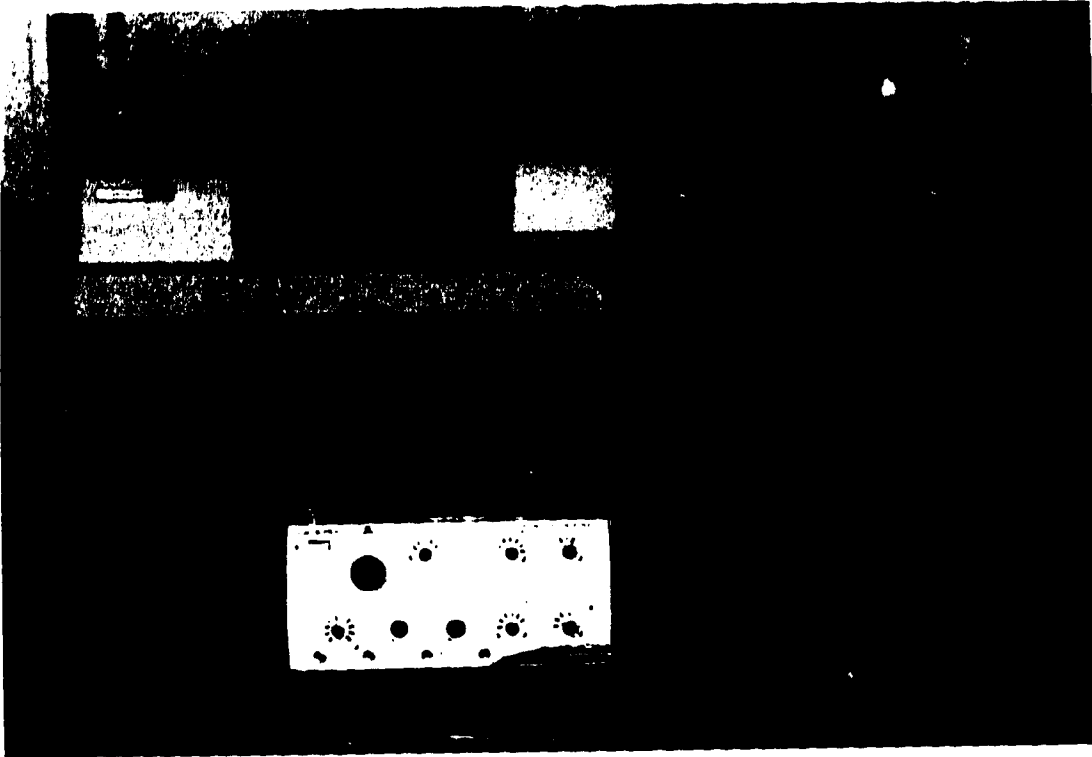


Figure 3.4.2.3 Photograph of Shear Wave Velocity Apparatus

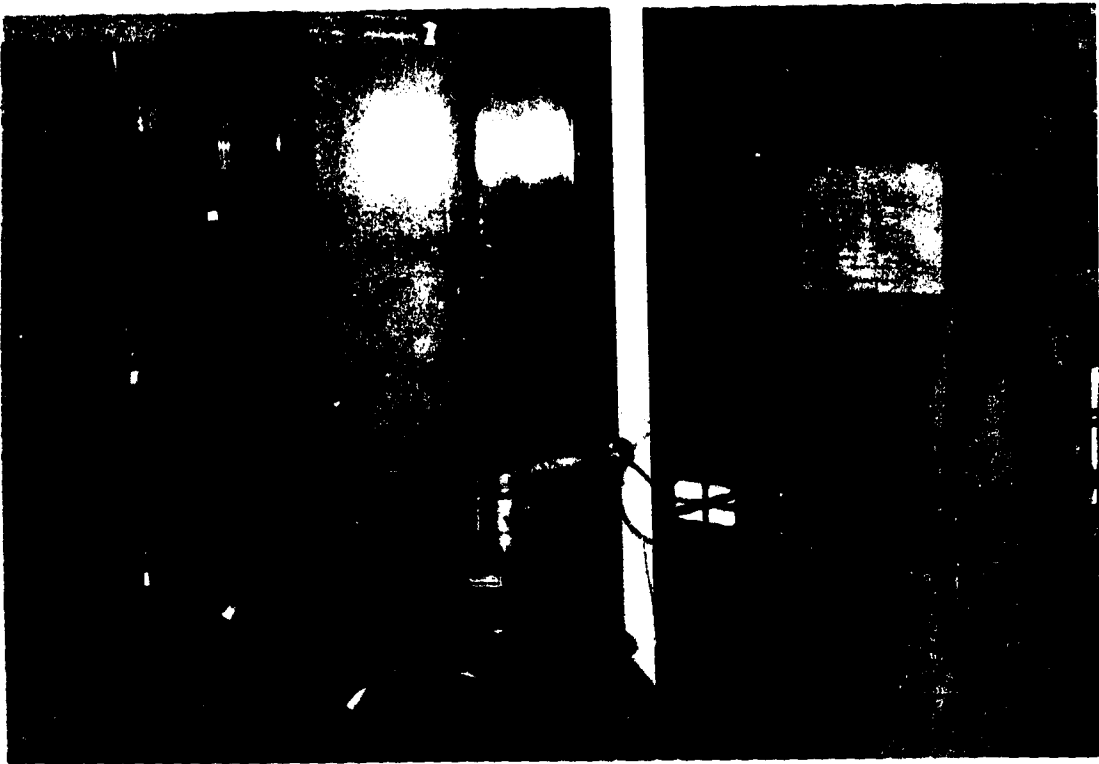


Figure 3.4.2.4 Photograph of Laboratory Freezing Set-Up

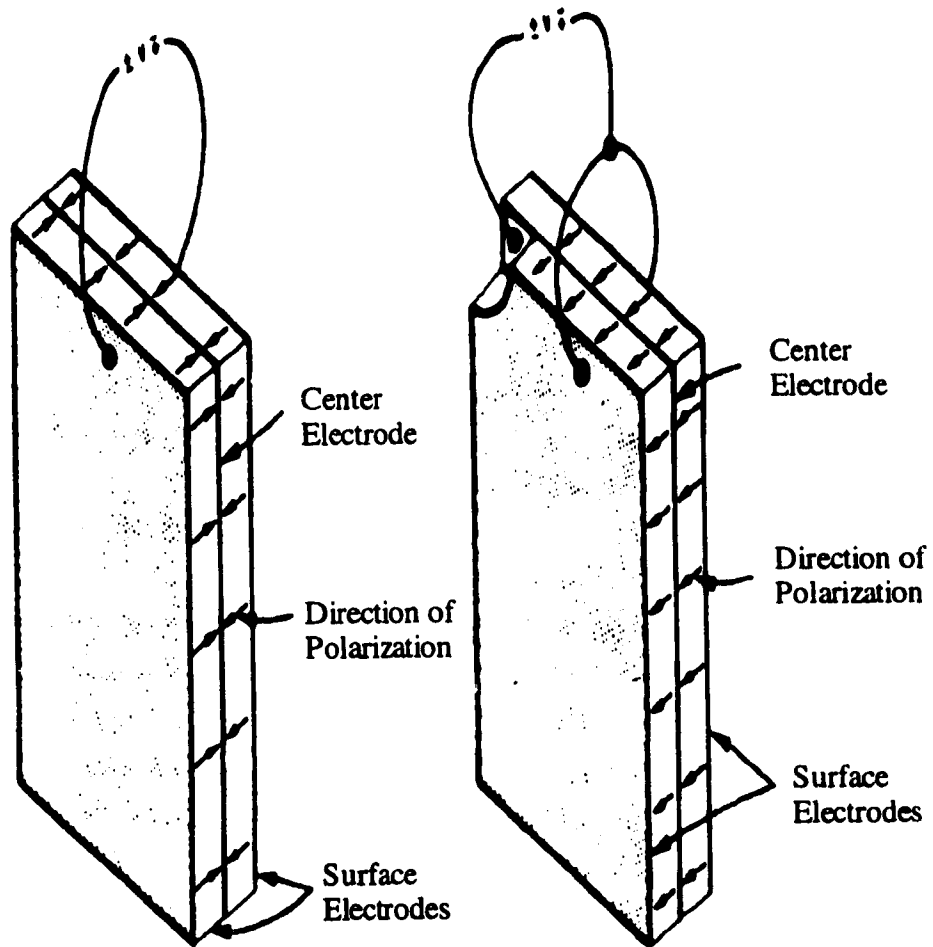


Figure 3.6.1 Piezoceramic Bender Element Connections: (a) Series (b) Parallel (after Dyvik and Madshus, 1985)

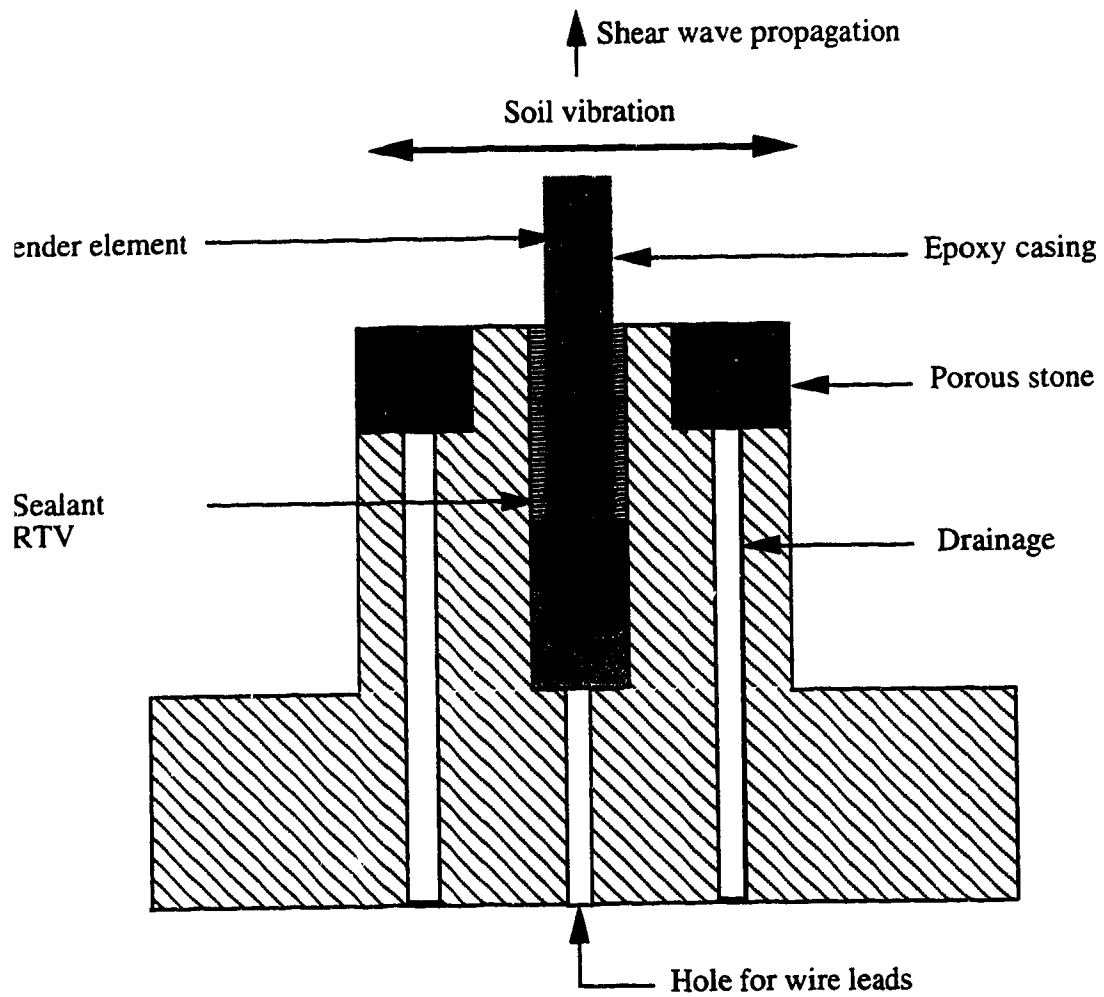


Figure 3.6.2 Bender Element Mounted on Bottom Pedestal
(after Sasitharan et al., 1992)

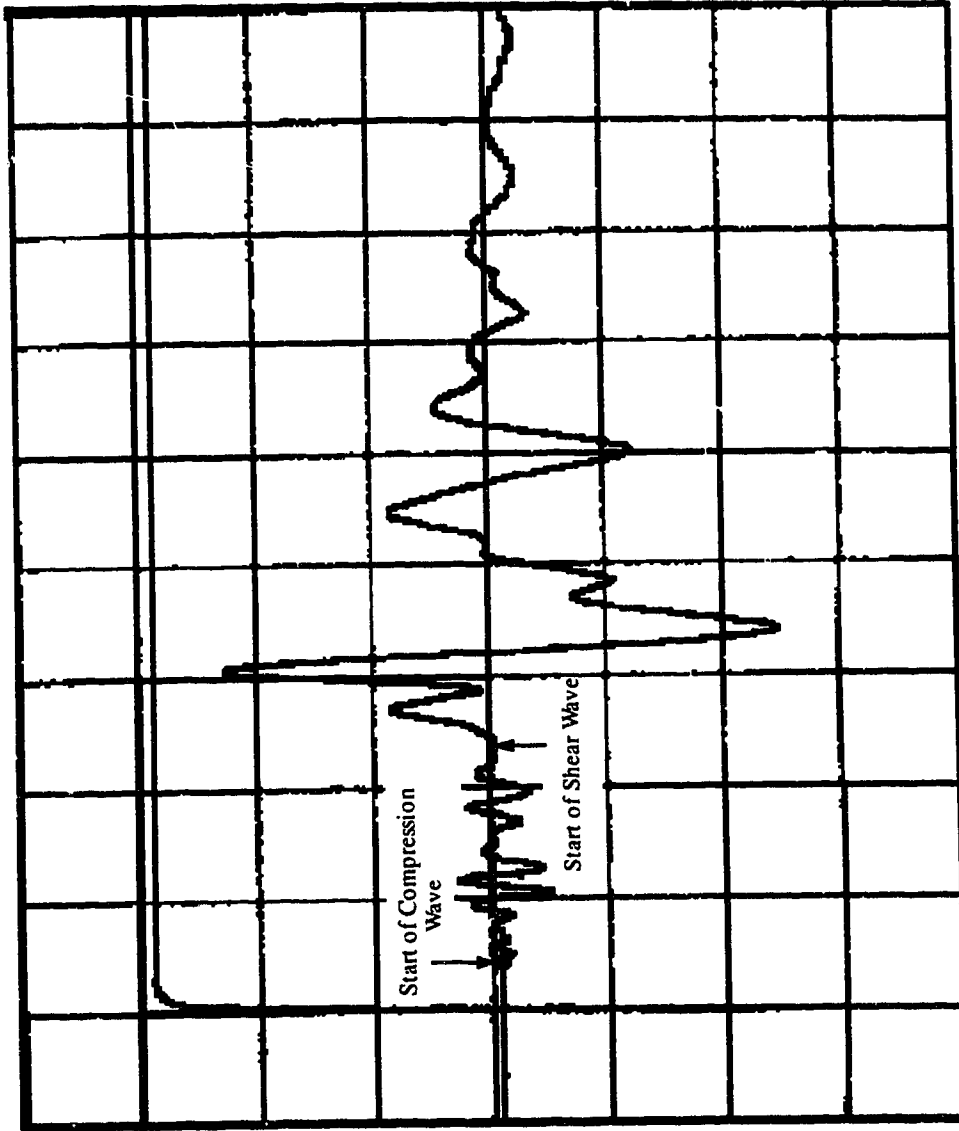


Figure 3.6.3 Plot of Shear Wave Velocity for Test O10RF350

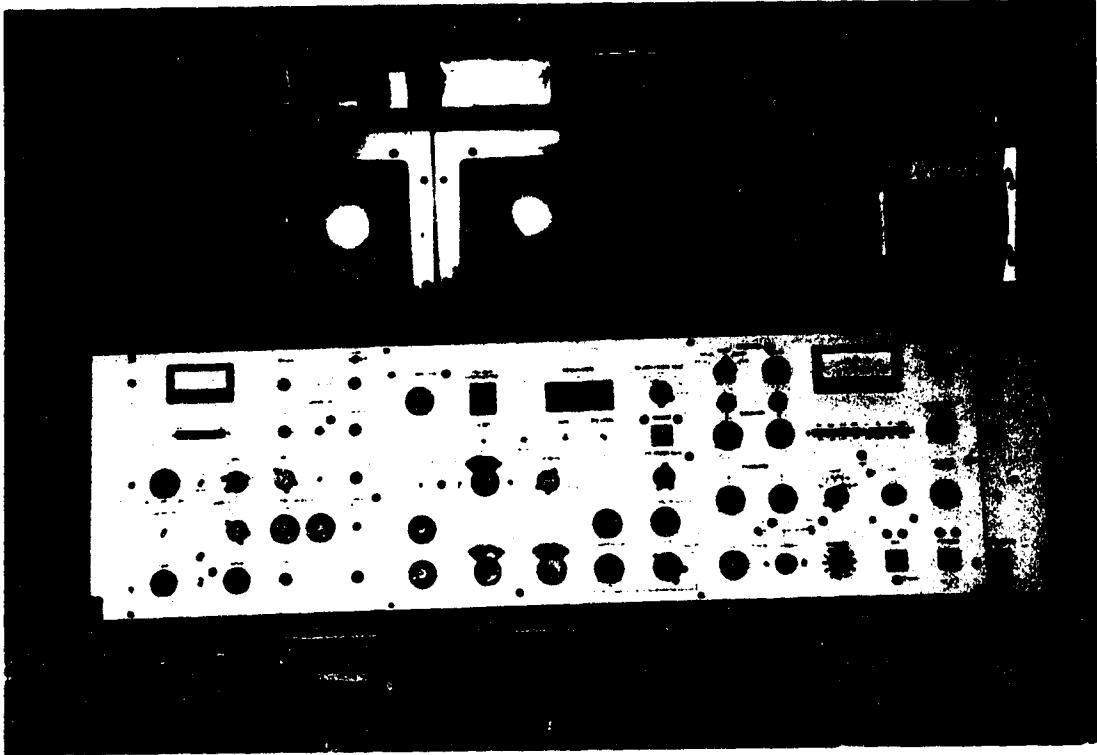


Figure 3.9.1 Photograph of Scanning and Sub-Liming Device

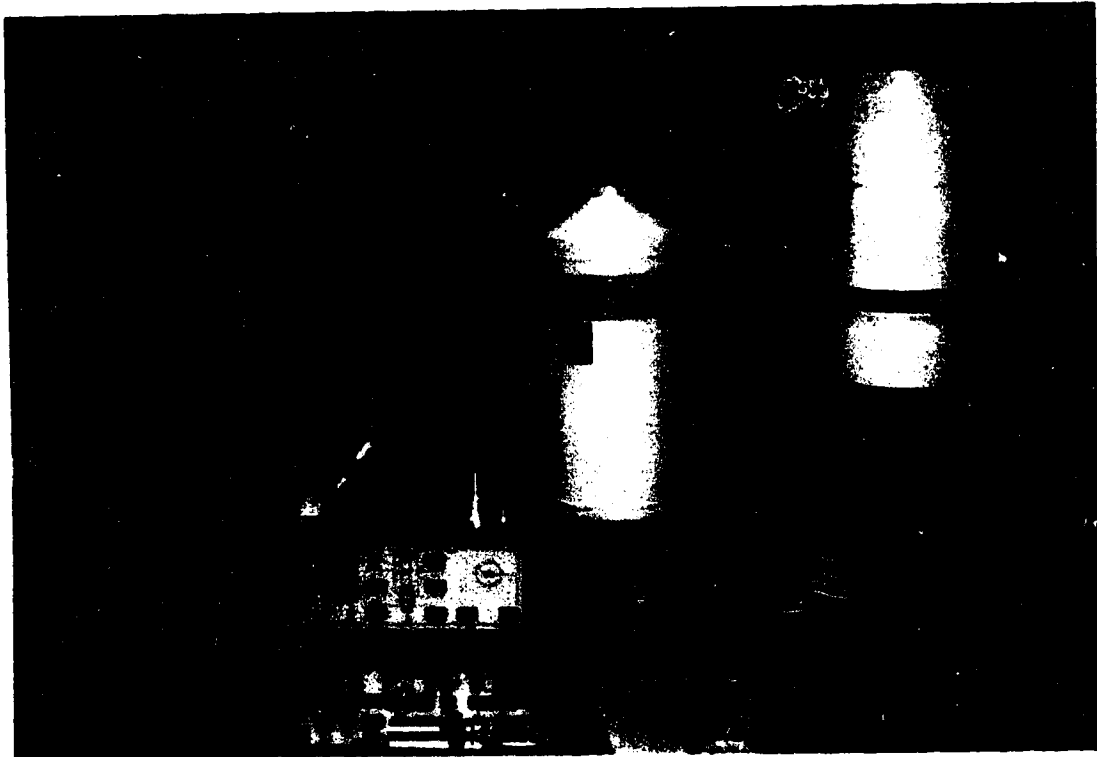


Figure 3.9.2 Photograph of SEM Viewing Device

4. RESULTS

4.1 Monotonic Undrained Test Results

A total of 26 tests were performed in the current research. Tests performed by Sasitharan (unpublished) were also used to establish undrained response and the position of the steady-state line in void ratio-stress space for clean Ottawa sand. The stress space plots use the variables normal stress (s') and shear stress (t) as indices and are defined as:

$$s' = \frac{(\sigma_1' + \sigma_3')}{2} \quad t = \frac{(\sigma_1 - \sigma_3)}{2}$$

The results for kaolinite, crushed silica fines and 70-140 silica sand are presented in Figure 4.1.1 a,b,c to 4.1.3 a,b,c. For each set of tests the results have been presented in the form of stress paths in s' - t space, deviator stress-axial strain and excess pore pressure-axial strain plots. These plots summarize all the tests and are laid out so that a clear picture of the undrained behaviour of samples with various types of fines is established.

Triaxial tests were conducted using a strain-rate-controlled technique. Peak strength was reached at an axial strain of about 0.5% and phase transformation was around 5% axial strain. Maximum obliquity was usually at strains near or a little larger than the 20% to which most of the tests were run. To facilitate larger axial strains, larger triaxial cells would be required.

4.1.1 Plastic versus Non-Plastic Fines Comparisons

As can be seen in Figures 4.1.1 and 4.1.2 a number of similarities exist in the monotonic undrained behaviour. As discussed in section 2.2 and 2.3.1, limited liquefaction results in an “elbow” in the stress path. This “elbow” marks the boundary between contractive and dilative behaviour. From the current research these “elbows”

are clearly defined and show a tendency to climb, marking a reduction in the undrained brittleness, as the fines are increased for both the plastic (kaolinite) and non-plastic (crushed silica) fines.

The undrained brittleness results are tabulated in Table 4.1.1.1 and plotted in Figure 4.1.1.1. When fines ($<74\mu\text{m}$) are varied the brittleness index ranges from 0 (40% fines) to 0.75 (0% fines). When kaolinite and crushed silica fines was added to the Ottawa sand, strain hardening behaviour occurred at 40% fines content. The brittleness index indicates that as the percentage of fines ($<74\mu\text{m}$) is increased the material goes from a brittle to a ductile type behaviour. This means that a material at 0% fines has more potential for large deformations due to strain softening response than a material with 40% fines.

Figures 4.1.1a and 4.1.2a show the stress paths in s' - t space for kaolinite and crushed silica fines. The "elbows" shift upwards as the percentage of fines is increased from 0 to 40%. This has the same meaning as when the brittleness index goes from 0.75 to 0. The ductile behaviour of the kaolinite and crushed silica fines at 40% fines content indicates that the fines ($<74\mu\text{m}$) fraction governs the undrained behaviour of the materials. A fines dominated behaviour behaves as if there was no coarse granular fraction, such as would occur in a clay for example. The percentage of fines is such that there is no contact between the granular particles and all undrained shearing occurs through the fines. Figures 4.1.1b and 4.1.2b for 40% fines content illustrates this behaviour. Note there is no defined peak and that the deviator stress continues to climb, flattening only at large strains. The flattening off represents the stress path is approaching the steady-state condition, which was schematically shown in Figure 2.3.1.3. Further discussion of a fines dominated behaviour will be presented in section 4.3

Figures 4.1.1b and 4.1.2b represent the deviator stress-axial strain plots for kaolinite and crushed silica fines. These figures along with the definition established in section 2.3 were used to calculate the undrained brittleness indices. These figures indicate that the post peak drop decreases with increasing fines percentages (ie. decrease in undrained brittleness). It is interesting to note that after the "elbow" was passed ($\approx 5\%$ axial strain), the deviator stress climbed at different rates for different percentages of

finer. This type of behaviour can be seen in Figure 4.1.1b for the 10 and 20% kaolinite samples and the 20% crushed silica fines sample in Figure 4.1.2b.

The concept of limited liquefaction involves a reduction in pore pressures as the behaviour of the material switches from strain softening to strain hardening. Figures 4.1.1c and 4.1.2c present the excess pore pressures plots for kaolinite and crushed silica fines. For kaolinite fines: 0 and 40% represents zero reduction; 20 and 30% represent a reduction of 5kPa; and 10% represents a reduction of over 60kPa in excess pore pressure. The large reduction in excess pore pressure in the kaolinite sample explains the large rise in deviator stress in Figure 4.1.1b and stress path in Figure 4.1.1a. For the crushed silica fines: 0% represents zero reduction; 10, 20 and 30% represent a reduction of 5kPa; and 40% represents a reduction of 30kPa in excess pore pressure. Again the sample with the largest reduction in excess pore pressure had the greatest climb in deviator stress (Figure 4.1.2b) and in the stress path (Figure 4.1.2a).

A schematic representation of excess pore pressure was shown in Figure 2.3.1.3. For the work in this thesis, a measure of the excess pore pressure was taken as the horizontal distance (constant t) on the stress plot from the total stress path to the “elbows”. From Figures 4.1.1a and 4.1.2a as the percentage of fines increased, the excess pore pressures decrease, a behaviour which is in agreement with the previous studies (Kuerbis, 1989; Georgiannou, 1988) involving limited liquefaction.

It was felt that the undrained behaviour with the addition of plastic and non-plastic type fines would be different. Looking at the maximum-minimum void ratios presented in Table 3.2.1.1 would suggest that at percentages of fines in the range of 20 to 30% samples, samples would behave as purely dilative. The consolidated void ratios at an effective stress level of 350kPa were comparable to the minimum void ratios obtained by ASTM methods. At first glance void ratios as low as 0.223 would intuitively suggest purely dilative behaviour, although a partly contractive behaviour to the phase transformation was observed (Figures 4.1.1 a,b and 4.1.2 a,b).

4.1.2 Influence of Gradation on Monotonic Undrained Behaviour

The monotonic undrained results with varying gradations can be seen in Figure 4.1.3abc. The mixtures of 70-140 silica sand and Ottawa sand resulted in gradations varying from uniform to well-graded, but with no fines ($<74\mu\text{m}$). When the gradation was varied and allowing for experimental scatter, there was very little difference in the undrained response. It is important to note that though gradation varied, there was still 0% fines less than $74\mu\text{m}$ (#200 sieve size) in the samples. The coefficient of uniformity remained relatively constant for the addition of 70-140 silica sand (Table 3.2.1.1). All the samples followed essentially the same stress path, displayed similar post peak drops to phase transformation (represented by similar undrained brittleness indices in Table 4.1.1.1) and strain hardened along the same paths. Because the stress paths (Figure 4.1.3a) were essentially the same, the excess pore pressures were similar. In Figure 4.1.3c all percentages of 70-140 silica sand represented similar excess pore pressure lines, with each percentage displaying no variance in excess pore pressure with increasing strain past phase transformation.

4.1.3 Normalization of Monotonic Undrained Results

To combine all the test results in one unified picture is an extremely difficult task. As was stated earlier there are a number of factors which influence the undrained behaviour of a material, many of which were held constant in the current research. Normalization is usually carried out so that different tests can be more easily compared. There are a variety of different ways to carry out the normalization procedure, most of them relying on an accurate determination of the normal consolidation line. These methods work quite satisfactory for clays, but are difficult to employ for sands. It is difficult to establish the normally consolidated line for sands because it requires tests to be performed at stresses larger than those commonly adopted in soil testing. A second point of difficulty can be seen in Figures 4.1.3.1a,b,c. The figures (Note the different scales on the ordinate axes) show the consolidation curves for the tests done with kaolinite, crushed silica fines and 70-140 silica sand. As can be seen there are multiple consolidation lines. Figures 4.1.3.1a,b indicate there is a transition which occurs at 20% fines content. This transition is associated with the sample matrix. Below a 20%

fines content the samples are considered to have a sand dominated matrix, and above a 20% fines content the samples have a fines dominated matrix. The change in compressibility, due to saturation, associated with the transition from a sand to a fines dominated matrix is reflected in the shifting of the consolidation lines.

Similar findings were found by Georgiannou (1988). The results back up the conclusions by Ishihara et al. (1975) that a unique consolidation line does not exist for sands. Although there may be a number of consolidation lines, there is a tendency for the lines to converge at high stresses levels (Georgiannou, 1988). However for such a convergence to take place, elevated pressures are required and at this stage particle breakage will become a dominant factor.

On the basis of the above observations, it was concluded that multiple compression lines exist for clayey sands and that each line corresponds to a particular initial void ratio. As a consequence of this clayey sands do not obey Rendulic's principle in the range of normal laboratory testing pressures.

Most normalization procedures use the equivalent stress, p_e' , method. This method involves taking the void ratio of a test, projecting it to the normal consolidation line and finding the corresponding stress level. This stress, p_e' , is then used to normalize all points in the test. This method has been shown to work (Georgiannou, 1988), but for the reasons above, it is difficult and inaccurate to apply.

The method of normalization used in the current study has the void ratio playing the dominant role. In two-dimensional stress space (s' - t plot) the shape of the state boundary is unique for a particular void ratio. As one moves to three-dimensional space (e - s' - t) and varies the void ratio, the size of the state boundary changes. A surface connecting all these state boundaries represents a series of unique lines which can be used for normalization. Such a line may be represented by the peak shear stresses, t_{peak} , of different tests.

Both peak shear stress (t_{peak}) and peak deviator stress (σ_{dp}) were used to normalize the results for each test (Figures 4.1.3.2a,b to 4.1.3.4a,b). Figures 4.1.3.2a,b and 4.1.3.3a,b represent the normalized plots for varying fines ($<74\mu\text{m}$). The stress plots

(Figures 4.1.3.2a and 4.1.3.3a) show a clear trend of upwards shifting of the “elbows” (reduction in undrained brittleness). The normalized stress-strain plots (Figures 4.1.3.2b and 4.1.3.3b) clearly show decreasing post peak strain softening with increasing fines contents and up to 30% fines contents, all tests follow the same stress path to peak shear stress. The fines dominated behaviour referred to in section 4.1.1 can be seen in the stress-strain plots for 40% samples. The stress-strain curve for 40% fines is below that for the lower fines content up to the peak shear stress. No strain softening response was observed for samples with 40% fines.

The normalized plots for varying gradations (no fines) can be seen in Figures 4.1.3.4a,b. All the various percentages of 70-140 silica sand for both the stress space and stress-strain plots, exhibit relatively similar paths. Even for the highest percentage of fines (40%) the stress-strain path follows the same path from peak to phase transformation, as with the other percentages of fines.

Although some researchers may argue about the merits of this procedure, it worked extremely well for the tests carried out in this research. A clearer trend of shifting “elbows” for varying gradations can be seen. For all three sets of tests the peak shear stress was at a normal stress, s' , level of 220kPa. The normalized deviator stress-axial strain plots also show a clearer picture of how fines and gradation effects the undrained brittleness.

4.1.4 Comparison of Test Results

To help facilitate a better understanding of the effect of fines ($<74\mu\text{m}$) versus gradation on the collapse surface, comparison plots of the 20% samples were made (Figures 4.1.4.1a,b,c). Figure 4.1.4.1a shows a comparison of the stress paths in s' - t space. The kaolinite and the crushed silica fines samples strain softened to the same normal effective stress level, but reached different peak stress levels. Because of the difference in peak shear stress levels, the deviator stress-axial strain plot (Figure 4.1.4.1b) for the two fines ($<74\mu\text{m}$) samples were different. The kaolinite sample had a higher peak stress value, but the curvature of the deviator stress-axial strain plot for the kaolinite and the crushed silica fines samples was similar, both strain hardening at the same rate.

When gradation was altered by adding 70-140 silica sand, the “elbow” in Figure 4.1.4.1a was lower, the post peak drop in deviator stress (Figure 4.1.4.1b) was followed by a nearly constant value of deviator stress, and the excess pore pressure generated was greater, as compared to the kaolinite and crushed silica fines samples.

The normalized plots (Figures 4.1.4.2a,b) brings together the effects of fines (<74 μm) and gradation of the three types of samples. The figures indicate that the percentage of fines (<74 μm) and not the plasticity of the fines, affects the undrained response of a sand. The higher the percentage of fines the lower is the undrained brittleness. Varying gradation from uniform to well-graded does not have a strong impact on the undrained response of a sand. The normalized plots also show the strength of the normalization procedure used. This can be accounted for by the similarity in small strain (<0.5%) response (Figure 4.1.4.2b). At first glance, the non-normalized results (Figures 4.1.4.1a,b,c) did not show exactly the same behaviour for kaolinite and crushed silica fines, but after normalizing to the peak shear stress, both samples had similar undrained responses. This method deserves more attention during future studies.

4.1.4.1 State Parameter Results

Although the normalization procedure used worked very well in comparing samples at 20% fines content (Figure 4.1.4.2a,b) questions arise when comparing samples at different void ratios. To explain why a 20% kaolinite sample at a void ratio of 0.16 has the same monotonic undrained behaviour as a 20% crushed silica sand sample at a void ratio of 0.67 is difficult. However, the state parameter is a index that may be able to describe why two samples at different void ratios behave in the same undrained manner.

The state parameter (section 2.5.1) is the difference in void ratio *in situ* and the void ratio at steady-state, at the same effective stress level. The *in situ* void ratio for this study is considered to be the consolidated void ratio. For the tests completed in this study only one point on the steady-state line was located for each test. Based on the findings of Verdugo *et al.* (1992) and Sladen *et al.* (1985) the steady-state line can be assumed to be parallel to the consolidated line for a very loose sand, passing through

the point determined for that test. The parallelism of the steady-state line is contradicted by Been and Jefferies (1985), whose results are presented in section 4.2.1. More tests of the same nature as carried out in this study, only at a different effective stress level, would be required to determine the slope of the steady-state line at varying fines contents.

Based on the assumption that the steady-state line is parallel to the consolidated line for that sand, the state parameter was determined for all the tests. Figure 4.1.4.1.1 represents the comparison plot for the 20% samples. Although the consolidated void ratios are vastly different, both kaolinite and crushed silica fines have similar state parameters. A summary of the state parameter results for the tests done in this study are presented in Table 4.1.4.1 and graphically in Figure 4.1.4.1.2. When fines ($<74\mu\text{m}$) are varied, similar state parameters at the same fines content exist, which helps to explain the similarity in the monotonic undrained behaviour. When gradation was varied the state parameter remained essentially constant, which confirms the similarity found in monotonic behaviour and undrained brittleness results.

The difficulty associated with using the state parameter is that it is not a universal parameter. As the state parameter decreases more dilatant behaviour is expected. Table 4.1.4.1 indicates that 10 and 40% kaolinite samples have the same state parameter, hence, should behave in the same undrained manner. The results in Figure 4.1.3.2a,b show that this is not true. However, after a 20% fines content, representing the boundary between a sand versus a fines dominated matrix, the state parameter follows the expected trend. The state parameter at 20% fines content is greater than at 40% fines content. This means that the 40% fines content samples are more dilatant than the 20% fines content samples, which is the case. Although the state parameter is not a universal index, it does help to explain why two samples at different void ratios can behave in the same undrained manner.

4.1.5 Previous Monotonic Undrained Studies

For comparison to the current study, the research of Kuerbis (1989) and Georgiannou (1988) will be reviewed. Kuerbis used Brenda Mine tailings sand, a relatively uniform

angular sand (60% feldspar, 30% quartz and 10% trace minerals) with the addition of a non-plastic-type fines. Georgiannou used Ham River sand, a medium-fine subangular sand (quartz) with the addition of a plastic-type fine (kaolinite).

The results of Kuerbis (1989) (Figures 4.1.5.1a,b) will be discussed first. The method of sample preparation used was water pluviation which results in lower void ratios. For comparison, the results from this study for a 20% crushed silica fines Ottawa sand sample has been shown. At approximately the same fines content (20% crushed silica fines as opposed to 22.3% silt content) the consolidated void ratio for the Brenda sand sample was 0.446 and 0.67 for the Ottawa sand sample. From the stress space plot (Figure 4.1.5.1a) the sample preparation method effects the strain softening manner of the sample prior to phase transformation. The Ottawa sand sample behaves in a more strain softening manner.

The stress-strain comparison plot (Figure 4.1.5.1b) indicates that because the Brenda sand samples strain hardened after reaching peak shear stress, the deviator stress-axial strain plot shows no post peak drops in stress (zero undrained brittleness). This behaviour is comparable to the 40% kaolinite and crushed silica fines samples (Figures 4.1.1b and 4.1.2b). The 20% crushed silica fines sample from this study shows a minor post peak drop in deviator stress.

The $s'-t$ results of Kuerbis(1989) also show a shifting "elbow" as the percentage of fines was increased. Because Brenda sand has angular grains, in comparison to the more rounded Ottawa sand grains, and the difference in the preparation methods, the shifting of the "elbows" is not as dramatic as was observed in the current research, but the trends are similar.

The results of Georgiannou (1988) are presented in Figure 4.1.5.2a,b along with a 20% kaolinite sample, from the current research, for comparison. The work of Georgiannou (1988) involves anisotropically consolidated, water pluviated samples. The void ratios of the samples used was not available in the published materia!. Because of the method of consolidation and sample preparation, the stress paths and stress-strain plots (Figures 4.1.5.2a,b) are relatively different for the Ham River sand and the Ottawa sand. Comparing at 20% fines contents, the Ham River sand samples are more strain

softening and show a strong strain hardening tendency after phase transformation. It is of interest to note that both 20% kaolinite samples reached relatively the same phase transformation point and climbed along similar slopes towards the line of maximum obliquity.

In the stress-strain plot (Figure 4.1.5.2b) the 20% Ham River sand sample has a higher peak stress and larger post peak drop, which is immediately followed by an increase in stress (strain hardening). The undrained brittleness indices, calculated from Figure 4.1.5.2b, are plotted against fines content in Figure 4.1.1.1. The trend of decreasing undrained brittleness with increasing percentages of fines is similar to the current research.

4.1.6 Strain Similarities

There were a number of similarities with the strain levels attained at certain stages in the results from this study, which were in agreement with the findings of numerous researchers (Georgiannou, 1989; DeMatos, 1988; Sladen et al., 1985). Looking at the normalized plots (Figures 4.1.3.2a,b to 4.1.3.4a,b) and the comparison plots (Figures 4.1.4.1a,b,c and 4.1.4.2a,b) there are two distinct types of behaviour; small strain (<0.5%) and large strain (>0.5%) behaviour. For all three sets of tests the small strain behaviour (strain up to peak shear stress or peak deviator stress) was essentially similar. Because of the similarities up to peak shear stress, confidence in the normalization procedure used was gained.

The difference in large strain behaviour can be seen in the normalized plots (Figure 4.1.3.2a,b to 4.1.3.4a,b). When fines (<74 μ m) were varied the post peak drops, representing various undrained brittlenesses, also varied. When the gradation was varied (uniform to well-graded) the monotonic undrained response remained essentially constant, representing the same undrained brittleness.

It is of interest to note the strain at the "elbows" or phase transformation, and the corresponding mobilized friction angle (ϕ_{PT}), mobilized friction angle at peak shear stress (ϕ_{CSR}) and constant volume friction angle at steady-state (ϕ_{SS}). The results have

been tabulated in Table 4.1.6.1. Because of the similarities at small strains it was expected ϕ_{CSR} would be the same for all three sets of tests, and indeed it is ($\approx 15^\circ$).

The strains at phase transformation, ϵ_{PT} , although not tabulated, for all the tests was around 5%. ϵ_{PT} can be determined by reading the shear stress value, t , at phase transformation (the "elbow") from the stress space plots, multiplying by two to arrive at a deviator stress ($\sigma_d = 2t$). From the deviator stress-axial strain plot, ϵ_{PT} can then be read off at the calculated deviator stress level. Although the strains at phase transformation were similar, the corresponding mobilized friction angles (ϕ_{PT}) were influenced by whether fines ($<74\mu\text{m}$) was varied or the gradation varied. The mobilized friction angle was similar ($\approx 25^\circ$) when fines was varied, but when gradation was varied the mobilized friction angle ($\approx 18^\circ$) was decreased to a value closer to ϕ_{CSR} .

It is important to note that the mobilized friction angle at steady-state was about the same for all three sets of tests ($\approx 30^\circ$) and matched the value of clean Ottawa sand. Although the samples did not reach a steady-state condition, they were close, witnessed by the fact that the undrained stress paths reached their maximum mobilized angles. It is therefore of interest to note that fabric controls the large strain ($>0.5\%$) behaviour, but the mobilized friction angle at steady-state is essentially the same.

4.1.7 Fines and Gradation Effects on Void Ratio

As mentioned in section 3.8, it is possible to estimate from an observational point of view the percentage of fines required for separation of granular particles. Figure 4.1.7.1 a,b,c shows the variation of void ratio during consolidation with increasing fines percentages for all three sets of tests. The various lines represent different effective stress levels, from sample preparation to final consolidation. Note that samples were prepared to essentially identical initial void ratios and that the largest changes in void ratio occurred during sample saturation and initial consolidation.

It is of interest to note how the contours at different effective stress levels parallel one another. A dip between 20 and 30% fines ($74\mu\text{m}$) probably indicates the location where grain to grain contact between the sand grains no longer exists. More consolidation

tests would need to be completed to determine the exact percentage of fines required for direct separation to occur.

The contours of void ratio at different effective stress levels for kaolinite (Figure 4.1.7.1a) show a more dramatic change than the contours for crushed silica fines and 70-140 silica sand (Figures 4.1.7.1b,c). This behaviour is expected because the kaolinite is a plastic-type fine, whereas the crushed silica fines and 70-140 silica sand were non-plastic. The plastic-type fines are more compressible (are able to deform around the incompressible Ottawa sand grains) and allow a tighter configuration of the sand-fines mixture, hence, a lower void ratio. The SEM results in section 4.3 will give a clearer picture of this configuration in the kaolinite samples.

Due to similarities in the monotonic undrained results for various percentages of 70-140 silica sand, it is no surprise to find that the contours of void ratio (Figure 4.1.7.1c) are essentially horizontal, representing a similar behaviour at all percentages of fines. As well, the prepared void ratio (e_i) and the consolidated void ratio (e_c) are essentially the same. This signifies that the 70-140 silica sand enriched samples underwent very little volume change during the saturation and consolidation stages. It should be noted that the consolidated void ratio (e_c) is greater than the maximum void ratio (e_{max}) for 70-140 silica sand samples. This may be due to the fabric imparted to the samples during moist preparation or due to the accuracy to which e_{max} can be accurately determined in the laboratory. More research would be required to determine the reason why e_c is greater than e_{max} .

The low void ratios obtained when fines ($<74\mu\text{m}$) are added is consistent with results and research of DeMatos (1988). He found that the fine particles would occupy the void space of the coarser particles and result in a structure characterized by small void ratios. DeMatos (1988) quotes: "Such soils might be thought not to liquefy but they certainly do!" Other examples of liquefaction behaviour cited by DeMatos (1988) include a well graded coal at a void ratio of 0.3 and a well graded gravel at a void ratio of 0.27.

The compressibility of different samples, which was addressed in section 2.5, was interrelated with the packing of soil which is directly related to the max/min void ratios.

An experimental study by Youd (1973) shows that the nature of the grains influences the max/min void ratios. He found that the max/min void ratios limits were controlled primarily by particle shape, particle size range and variations in gradation.

Although Youd was only varying the characteristics of one sand and not the type of fines, he found that as the sand became more angular, both e_{max} and e_{min} increased more dramatically. His results can be seen in Figure 4.1.7.2. There was agreement in the current research which found that the angular fines produced larger e_{max} and e_{min} values (Table 3.2.2). However there was an opposite trend which developed with regard to the relationship between the difference of e_{max} and e_{min} and the coefficient of uniformity, C_u . For the research carried out the $(e_{max} - e_{min})$ increased as C_u increased. Although the C_u increased more dramatically for kaolinite, the $(e_{max} - e_{min})$ increase was more dramatic for the crushed silica fines. For the 70-140 silica sand, C_u remained fairly constant and hence, so did $(e_{max} - e_{min})$.

4.2 Steady-State Line Results

The end points which lie on the constant volume friction angle line and the "elbows" for each set of tests have been plotted along with the steady-state line (Sasitharan, unpublished) for Ottawa sand (0% fines) in Figures 4.2.1a,b,c (Note the different scales on the ordinate axes). Although the samples did not reach a steady-state condition, they were close, due to the fact that the undrained stress paths reached their maximum mobilized friction angles. Since a limited number of tests were performed, all starting from 350kPa, the inclination of a "steady-state" line for each test is not known.

The points which are along the line of maximum obliqueness shift downwards with increasing fines until the percentage of fines is such that grain separation of the host sand occurs. Once grains separation begins the points begin to shift upwards. The higher the compressibility of the fines, the larger is the shifting of the "steady-state" line (ie. kaolinite has the highest compressibility, therefore has the largest shift in the "steady-state" line).

4.2.1 Previous Steady-State Studies

There are a large number of steady-state studies that were carried out by different researchers (such as Been and Jefferies, 1985; Poulos et al., 1985; Konrad, 1990). The work of Poulos et al. (1985) has a direct impact on the current research. Their results for sands with grain types subrounded to angular are presented in Figures 4.2.1.1 to 4.2.1.3.

A number of observations can be made regarding the above figures. For each group of sands the steady-state lines are parallel ranging from a flat slope for subrounded grains to a steep slope for angular grains. A second observation is that as the coefficient of uniformity increases the steady-state line shifts down. This same trend is observed in the current research up to the point of possible grain separation, which was around 20% fines. Except for one test presented by Poulos et al. (1985), all percentages of fines were less than 20%. Only their test 17 had a percentage of fines greater than 20% and the steady-state line became steeper, but showed no significant shift upwards.

Since the tests performed by the above authors were limited to fines below 20% the increasing coefficient of uniformity was suggested as a measure of the liquefaction potential. The use of the term liquefaction potential in the current research describes the ability of a sample to strain soften, leading to collapse liquefaction. It was suggested that the higher the coefficient of uniformity the more pronounced the liquefaction potential. For a given void ratio it is correct that if the steady-state line moves down that potential for liquefaction increases. However, this research has shown that it is not possible to maintain the same void ratio as the fines increases. From this study the coefficient of uniformity was found to increase as the percentage of fines increased which lead to a more dilatant behaviour, hence less potential for collapse liquefaction.

Some interesting results regarding the shifting of the steady-state line was presented by Been and Jefferies (1985). Their results are presented in Figure 4.2.1.4. They added various proportions of Kogyuk fines (non-plastic), up to 10%, to a washed Kogyuk sand (uniform, medium quartzitic sand). It can be noted that the slope of the steady-state line increases with increasing fines. The fine grains are subangular in nature, which explains the increase in steepness of the steady-state line as the percentage of

fines is increased (From comparison of Figures 4.2.1.1 to 4.2.1.3). There was a slight increase in the coefficient of uniformity (1.7 to 2.3) as the steady-state lines shifted downwards again in agreement with Poulos et al. (1985) and the current research.

4.3 SEM Results

Many of the behaviour characteristics of soil, on a microscopic level, have eluded researchers until the development of the Scanning Electron Microscope (SEM). A discussion on the sample preparation and samples tested for microscopic characteristics was presented in section 3.9.

Particle shape is generally defined in terms of surface texture and roundness (Yudhbir and Abedinzadeh, 1991). Surface texture describes the surface features, such as polished, greasy, etc., all of which are too small to affect the overall shape. Roundness refers to the various aspects of the grain surface. Such aspects include sharpness of corners and edges which on a larger scale would be classed as surface texture, but on a smaller scale affect the overall dimensions of the grain. The small scale effect has been captured in the SEM photographs.

The photographs, Figures 4.3.1 to 4.3.4 have been presented in such a fashion that comparisons can be directly made. Figures 4.3.1 and 4.3.2 are photographs of the 20 and 40% kaolinite samples respectively. Figures 4.3.3 to 4.3.4 are photographs of the 20 and 40% crushed silica fines respectively.

The observations that were made were based on two scales: macro-scale ($\geq 200\mu\text{m}$) and micro-scale ($< 200\mu\text{m}$). On a macro-scale the appearance of the two samples with kaolinite and crushed silica fines was similar. At 20% fines both types of samples have some grain-to-grain contacts, whereas at 40% fines the sand grains are essentially floating in the fines matrix. Therefore at 20% fines, the sand grains and fines will act as a composite during undrained loading; at 40% fines, the fines begin to govern the behaviour of the sample during undrained shear.

At the micro-scale the appearance of the two samples is quite different. The void ratios of the kaolinite samples tended to be lower than with the crushed silica fines. This is because the kaolinite fines have a flat elongated shape which can easily fit between the sand grains in a more compact nature. As well, the kaolinite fines are more compressible and therefore fit around and within the asperities of the sand grains. The crushed silica fines, which are composed of angular quartz, are non-compressible and do not fit well within and around the asperities of the sand grains. Therefore the crushed silica fines samples will tend to a higher void ratio than the kaolinite samples, at a similar percentage of fines.

4.4 Shear Wave Velocity Results

A description of the shear wave velocity measurement apparatus was presented in section 3.6. For some of the tests only the compressional wave form was captured. This was because the initial signal representing the compressional wave was amplified, and gave the appearance of the shear wave form. Thinking that the shear wave had been captured, a hard copy was made. Even if the mistake was realized at the next stage of the test, it is impossible to see the original wave form again. To eliminate this problem a data acquisition system, which records the entire wave form digitally, would be useful. If any problems arose during the analysis stage the wave form could be retrieved and viewed again.

Since only the compressional wave form was captured for some tests, and hence, the compressional wave velocity, V_p , could be calculated, the theory of elasticity, shown below, was used to calculate the shear wave velocity (V_s):

$$V_p = V_s \sqrt{\frac{1 - \nu}{0.5 - \nu}}$$

where ν is Poisson's ratio.

The value of Poisson's ratio was estimated from the tests where shear wave velocity was directly measured. The value ranged from 0.485 for kaolinite to 0.495 for crushed

silica fines. The value of Poisson's ratio tended to be constant for each test. Although these values seem high, they are consistent with the results of other researchers who performed tests on mixed soils (Hardin and Drnevich, 1972).

The results of the shear wave study are shown in Tables 4.4.1a,b,c. When fines (<74 μm) were added the shear wave velocities decreased with increasing mean effective stress until the "elbow" was reached, at which point the shear wave velocity increased again. As well, a similar trend to that of Figure 4.1.7.1 was observed. The shear wave velocity tended to be lower for 20 to 30% fines and higher at 10 and 40% fines.

When the gradation was altered by adding 70-140 silica sand a different behaviour was observed. The shear wave velocity tended to increase with increasing mean effective stress and peaked as the stress path approached maximum obliquity. The shear wave velocities at the same stress level was relatively constant, regardless of the percentage of fines, a behaviour which was observed during undrained testing (Figure 4.1.3).

The results when fines (<74 μm) were added (Table 4.4.1a,b,c) indicate that as void ratio decreases shear wave velocity decreases, a trend which opposes the normal trend. Therefore since the shear wave velocity is lower for the 30% fines content sample, as compared to the 10% fines content sample, implies that the void ratio for the 30% fines content sample is higher and therefore the 30% fines content sample has a higher undrained brittleness. However from the monotonic undrained tests, a 30% fines content sample has a lower undrained brittleness compared to a 10% fines content sample. The normal trend of increasing shear wave velocity with decreasing void ratio is displayed by the 70-140 silica sand samples. The reason for the reverse trend when fines are added is not clear. The fabric imparted to the sand when fines are added could be the reason, or the calculation of shear wave velocity using the theory of elasticity for some of the tests could be the reason. The values of shear wave velocity which were calculated using the theory of elasticity have been indicated on Figure 4.4.1. It can be noted that these values fit well within the trends indicated by the values of shear wave velocity which were directly measured.

Based on the monotonic undrained results, similar behaviour occurred when fines ($<74\mu\text{m}$) was added to Ottawa sand and different behaviour was witnessed when gradation of the Ottawa sand varied by adding 70-140 silica sand. In other words, fines ($<74\mu\text{m}$) versus gradation plays an important role in determining shear wave velocity. The results in Tables 4.4.1a,b,c have been normalized for mean normal stress, but the observed trends indicate that fabric influences (such as fines below $74\mu\text{m}$ and gradation variations) affect the shear wave velocity and therefore results should also be normalized for fabric as well.

Brittleness Index

% Material Added	Kaolinite	Crushed Silica Fines	70-140 Silica Sand
0	0.75	0.75	0.75
10	0.36	0.45	0.75
20	0.18	0.27	0.69
30	0.03	0.22	0.71
40	0	0	0.79

Table 4.1.1.1 Undrained Brittleness Indices

State Parameter

% Material Added	Kaolinite	Crushed Silica Fines	70-140 Silica Sand
10	0.008	0.009	0.010
20	0.029	0.030	0.016
30	0.019	0.020	0.014
40	0.008	0.012	0.015

Table 4.1.4.1 State Parameter Results

Fines	ϕ_{CSR} (°)	ϕ_{PT} (°)	ϕ_{SS} (°)
Ottawa Sand (0% fines)	20	29	30
Kaolinite	16	25	31
Crushed Silica Fines	14	24	29
70-140 Silica Sand	15	18	30

Table 4.1.6.1 Summary of ϕ Data

Effective Pressure	0%	10%	20%	30%	40%
50	192.99	204.07	181.17	300.00	262.32
150	188.94	211.58	172.62	235.84	214.41
250	186.16	212.44	170.51	210.05	210.55
350	181.86	197.44	169.88	204.93	206.32
5% Strain	---	---	159.36 (94.77 kPa)	---	214.75 (198.40 kPa)
Test Completion	---	212.99 (227.22 kPa) (20.67%)	160.49 (158.79 kPa) (20.30%)	232.38 (162.01 kPa) (19.90%)	247.40 (217.12 kPa) (21.26%)

Table 4.4.1a Normalized Shear Wave Velocities for Kaolinite

Effective Pressure	0%	10%	20%	30%	40%
50	192.99	183.05	204.62	166.19	193.02
150	188.94	141.87	161.50	125.49	148.16
250	186.16	125.85	141.29	138.37	129.90
350	181.86	115.26	131.12	117.70	118.83
5% Strain	---	180.81 (72.04 kPa)	127.60 (107.41 kPa)	121.94 (107.27 kPa)	184.08 (167.54 kPa)
Test Completion	---	197.38 (92.22 kPa) (20.42%)	128.46 (131.84 kPa) (16.19%)	127.11 (131.51 kPa) (21.26%)	202.96 (226.89 kPa) (15.22%)

Table 4.4.1b Normalized Shear Wave Velocities for Crushed Silica Fines

Effective Pressure	0%	10%	20%	30%	40%
50	192.99	172.07	172.95	167.23	167.77
150	188.94	178.23	163.13	168.95	171.38
250	186.16	174.01	154.61	173.90	175.52
350	181.86	185.01	156.60	184.21	183.16
5% Strain	---	---	---	---	---
Test Completion	---	216.70 (30.78 kPa) (20.76%)	207.02 (57.22 kPa) (16.49%)	215.29 (47.73 kPa) (20.02%)	209.60 (43.71 kPa) (20.20%)

Table 4.4.1c Normalized Shear Wave Velocities for 70-140 Silica Sand

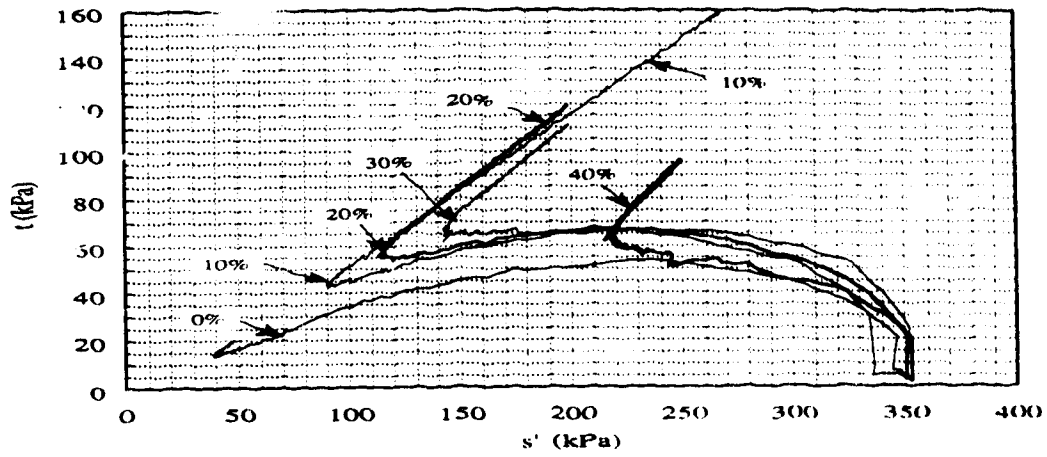


Figure 4.1.1a s-t Plot for Various Percentages of Kaolinite

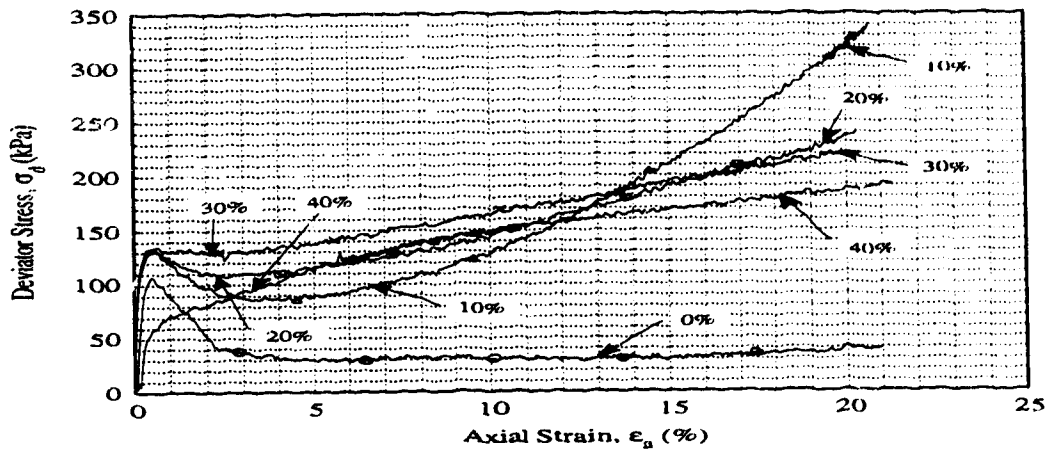


Figure 4.1.1b σ_d vs. ϵ_a for Various Percentages of Kaolinite

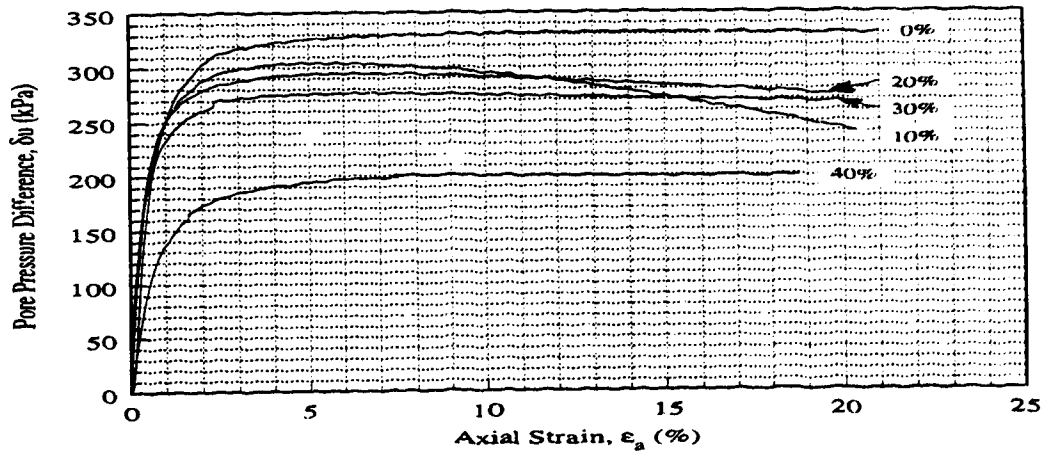


Figure 4.1.1c δu vs. ϵ_a for Various Percentages of Kaolinite

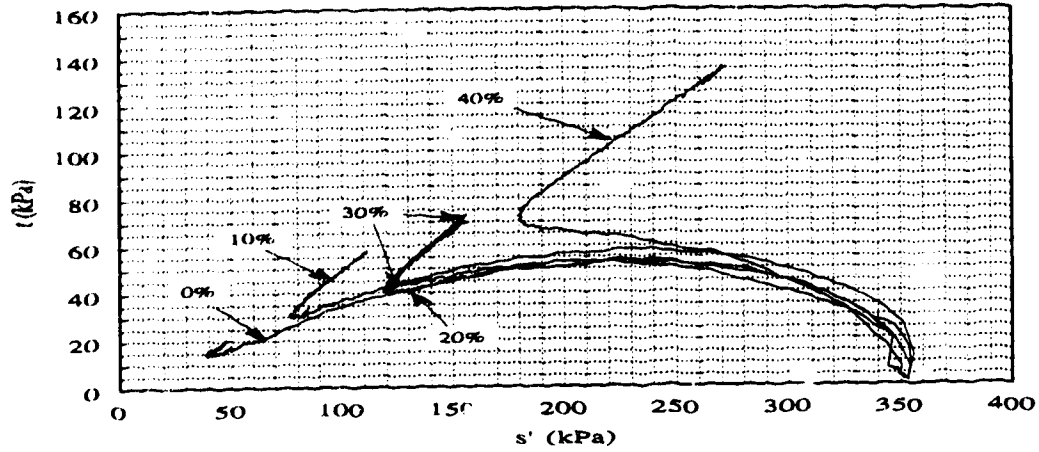


Figure 4.1.2a s-t Plot for Various Percentages of Crushed Silica Fines

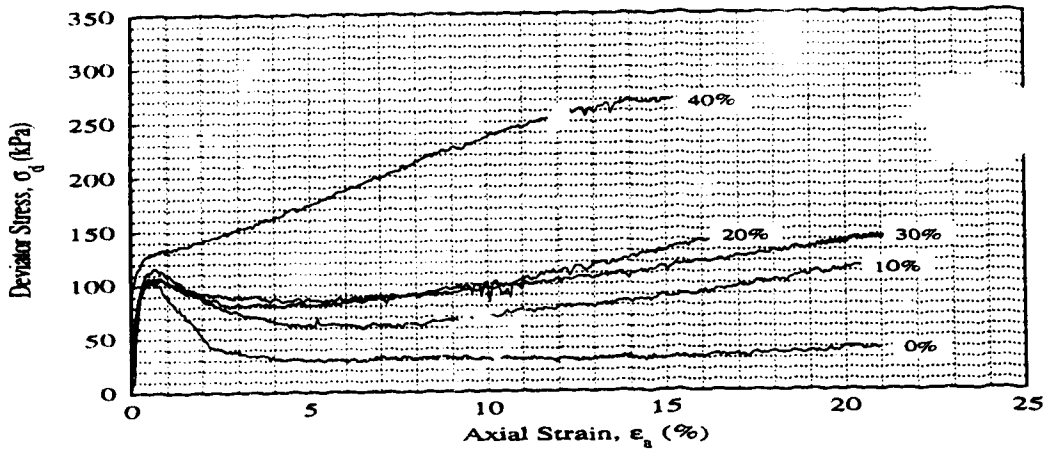


Figure 4.1.2b σ_d vs. ϵ_a for Various Percentages of Crushed Silica Fines

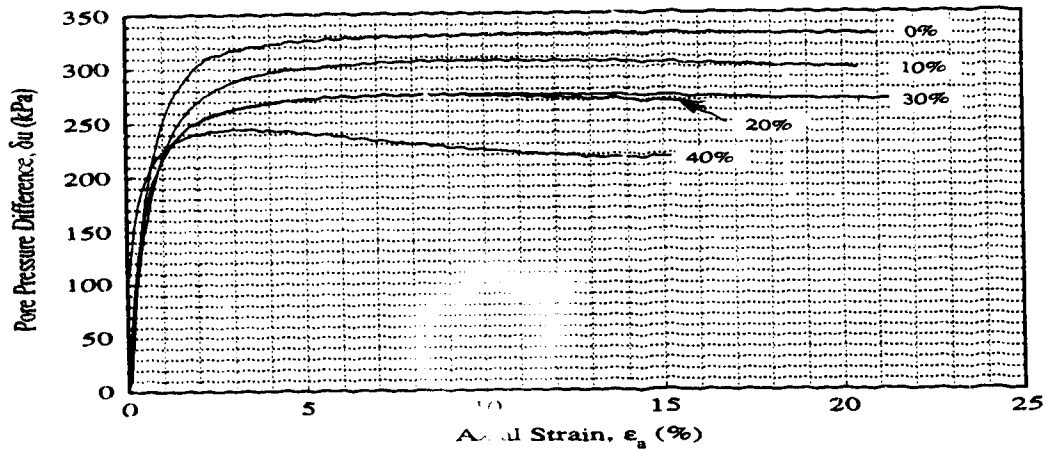


Figure 4.1.2c δu vs. ϵ_a for Various Percentages of Crushed Silica Fines

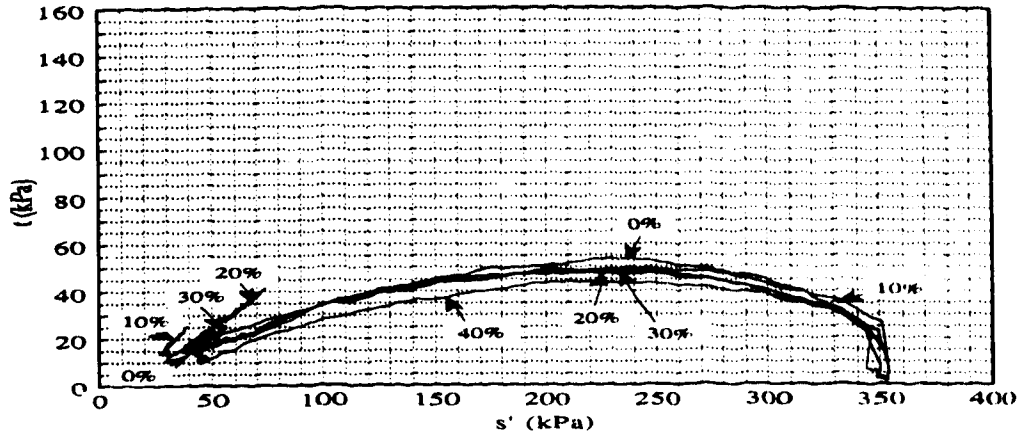


Figure 4.1.3a s-t Plot for Various Percentages of 70-140 Silica Sand

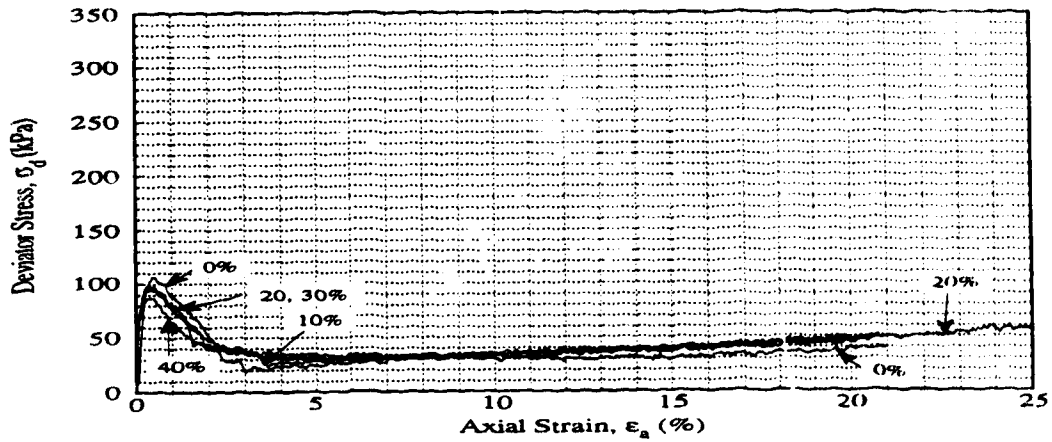


Figure 4.1.3b σ_d vs. ϵ_a for Various Percentages of 70-140 Silica Sand

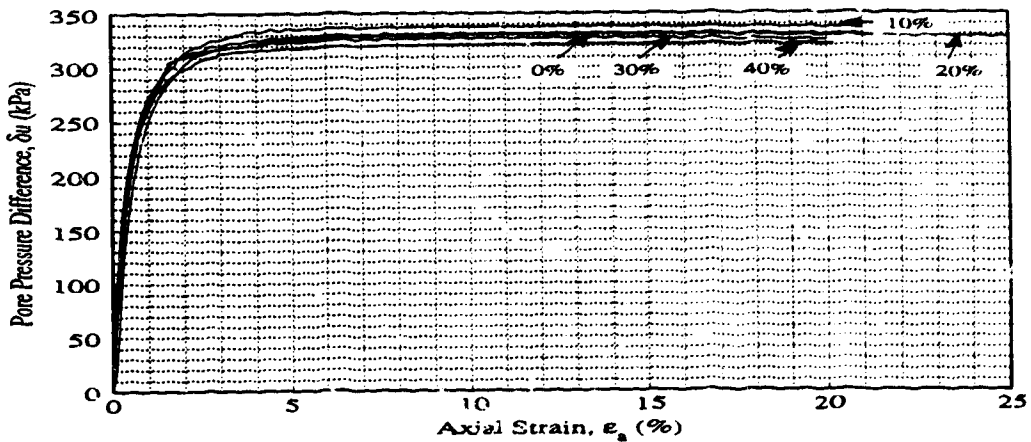


Figure 4.1.3c δu vs. ϵ_a for Various Percentages of 70-140 Silica Sand

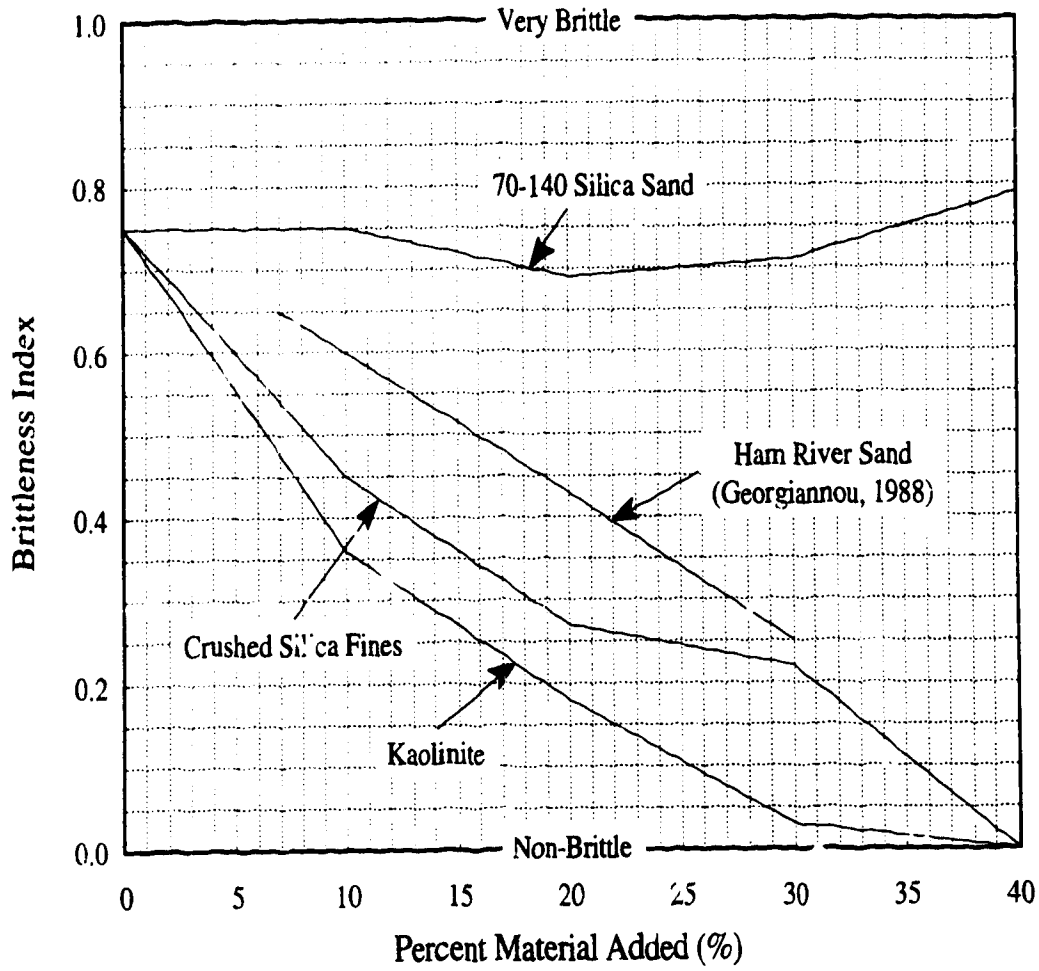


Figure 4.1.1.1 Brittleness Index vs. Percent Material Added for Kaolinite, Crushed Silica Fines, 70-140 Silica Sand and Ham River Sand

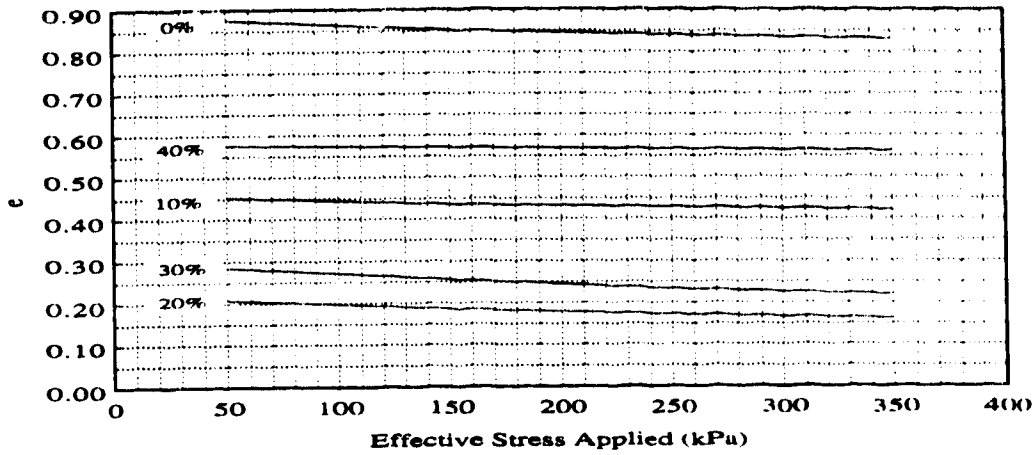


Figure 4.1.3.1a Consolidation Curves for Various Percentages of Kaolinite

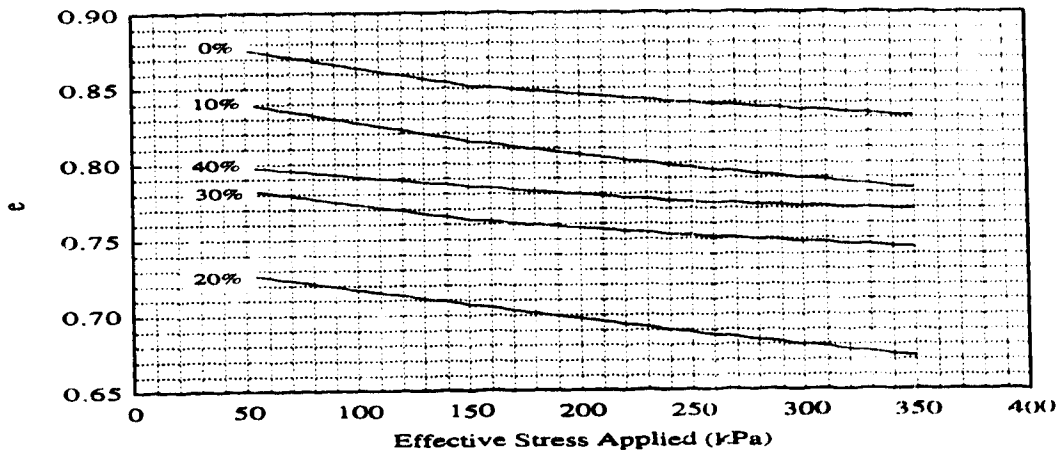


Figure 4.1.3.1b Consolidation Curves for Various Percentages of Crushed Silica Fines

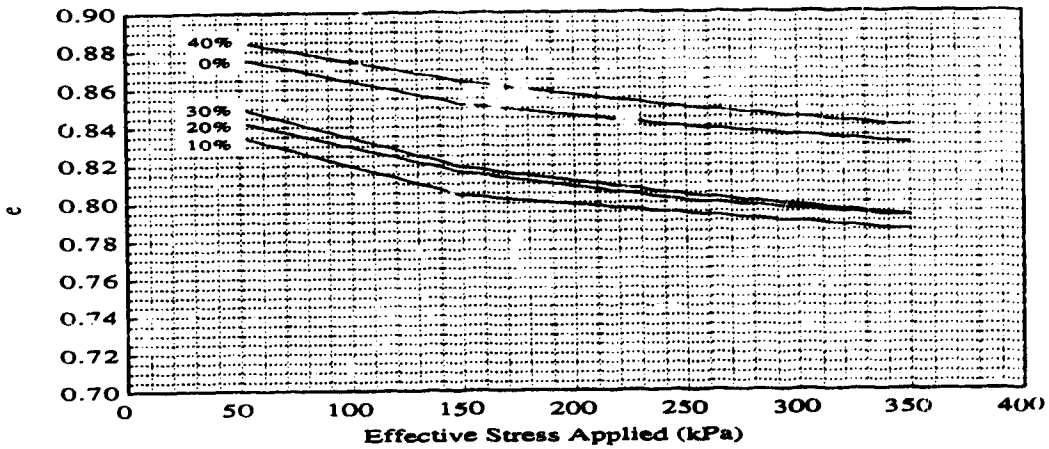


Figure 4.1.3.1c Consolidation Curves for Various Percentages of 70-140 Silica Sand

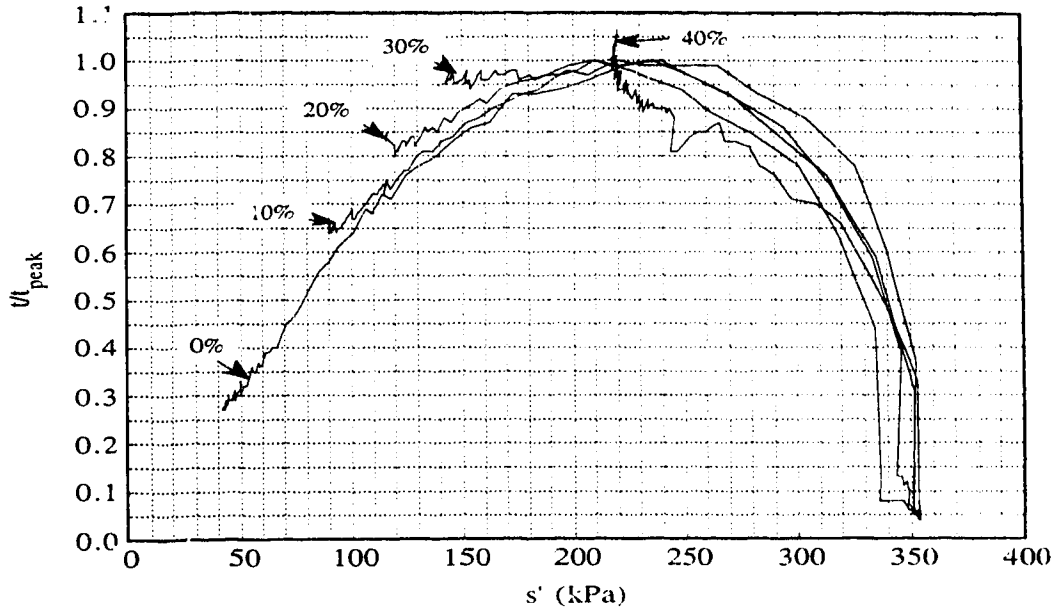


Figure 4.1.3.2a u/t_{peak} vs. s' for Various Percentages of Kaolinite

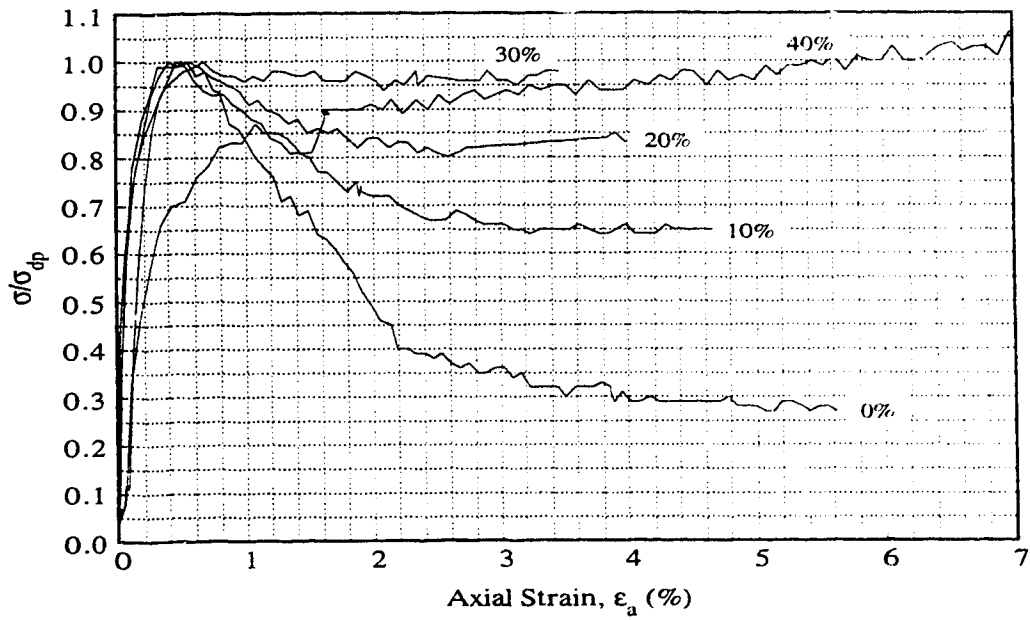


Figure 4.1.3.2b $\sigma/\sigma_{\text{dp}}$ vs. ϵ_a for Various Percentages of Kaolinite

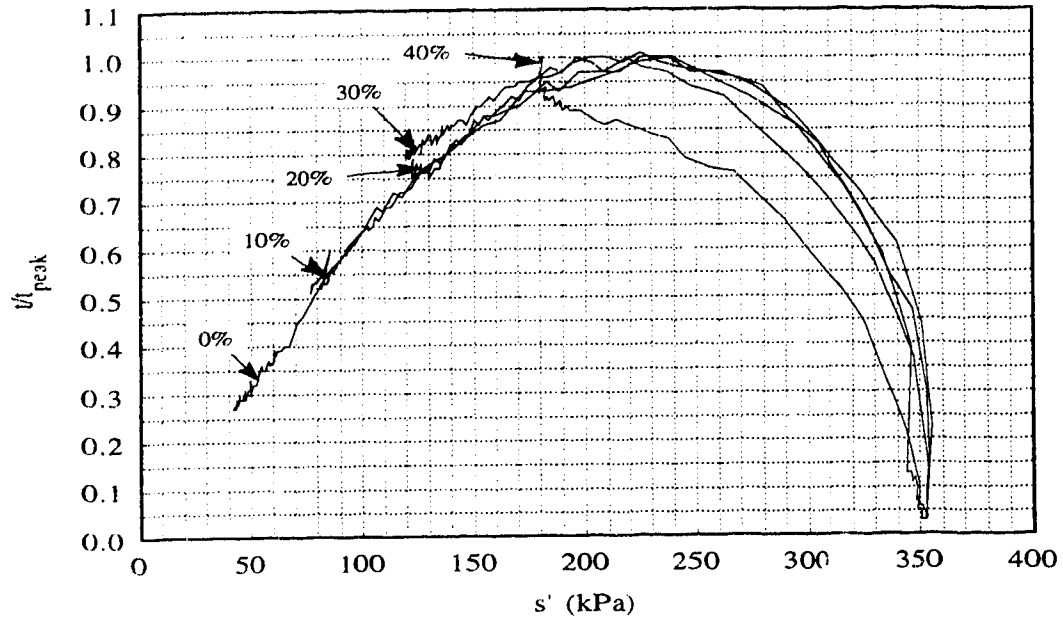


Figure 4.1.3.3a t'/t_{peak} vs. s' for Various Percentages of Crushed Silica Fines

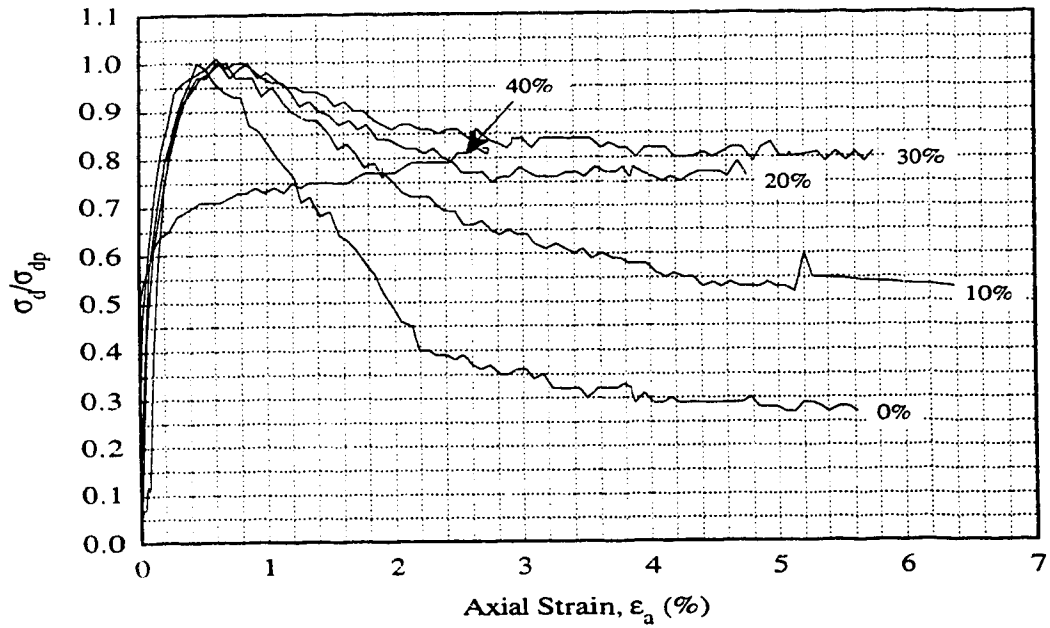


Figure 4.1.3.3b σ_d/σ_{dp} vs. ϵ_a for Various Percentages of Crushed Silica Fines

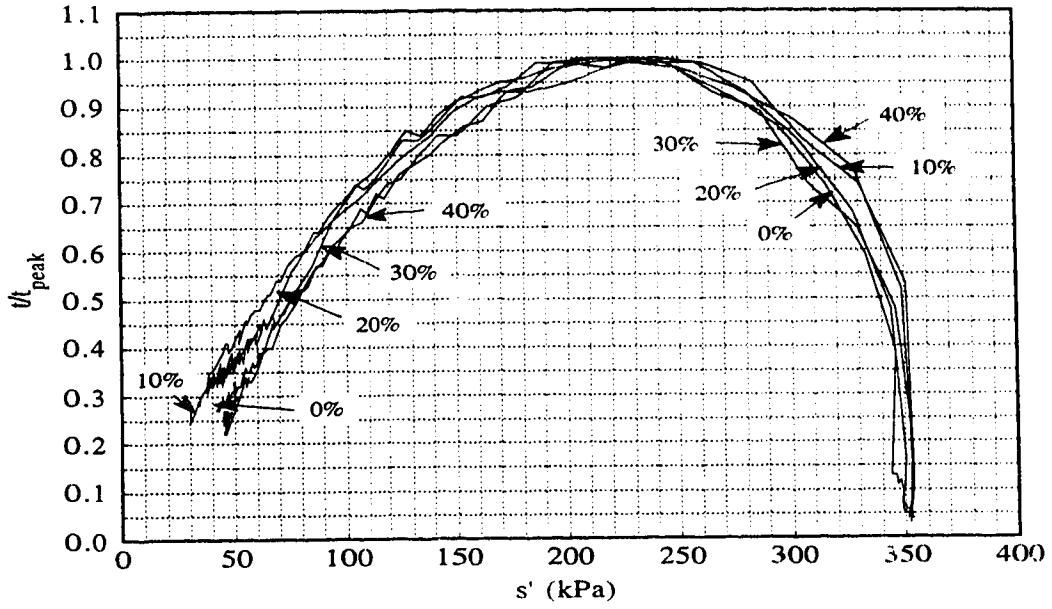


Figure 4.1.3.4a t/t_{peak} vs. s' for Various Percentages of 70-140 Silica Sand

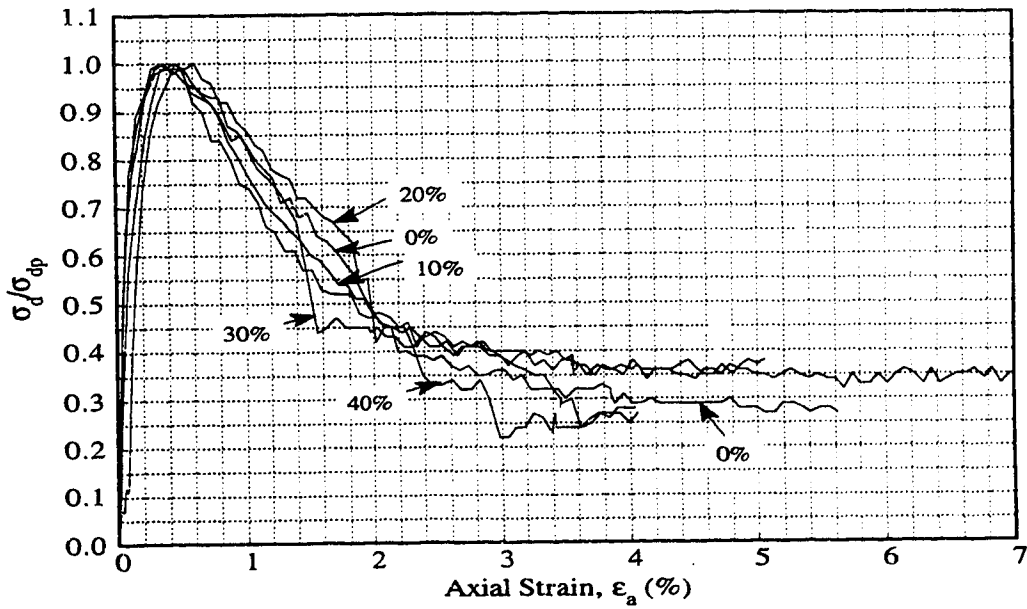


Figure 4.1.3.4b σ_d/σ_{dp} vs. ϵ_a for Various Percentages of 70-140 Silica Sand

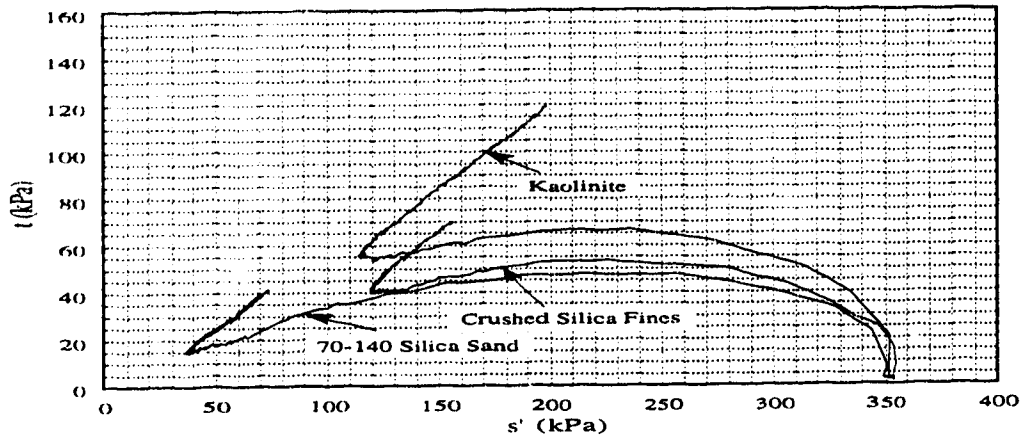


Figure 4.1.4.1a s' - t Comparison Plot of 20% Samples

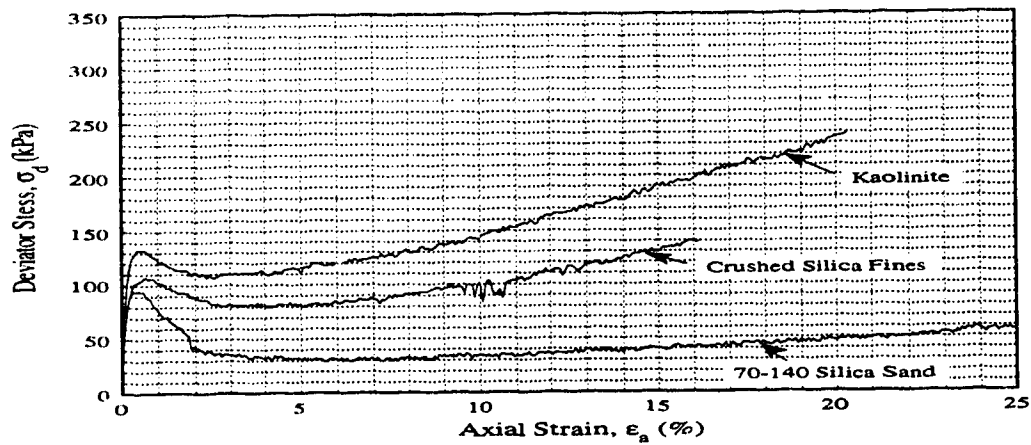


Figure 4.1.4.1b σ_d vs. ϵ_a Comparison Plot of 20% Samples

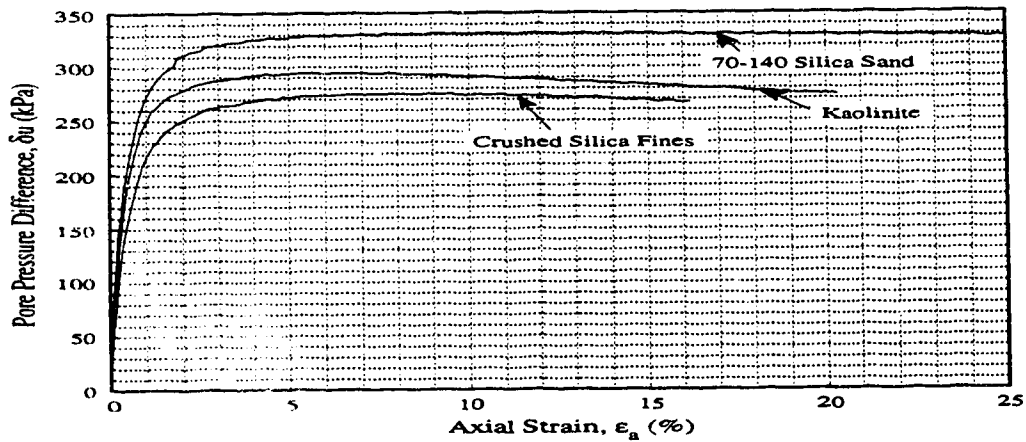


Figure 4.1.4.1c δu vs. ϵ_a Comparison Plot of 20% Samples

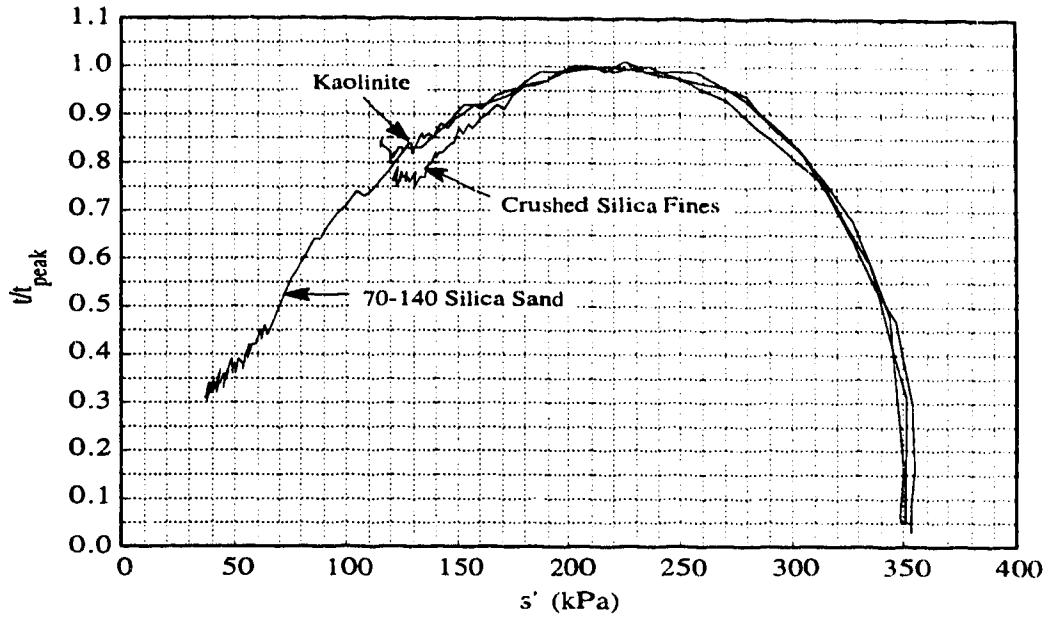


Figure 4.1.4.2a t/t_{peak} vs. s' Normalized Comparison Plot of 20% Samples

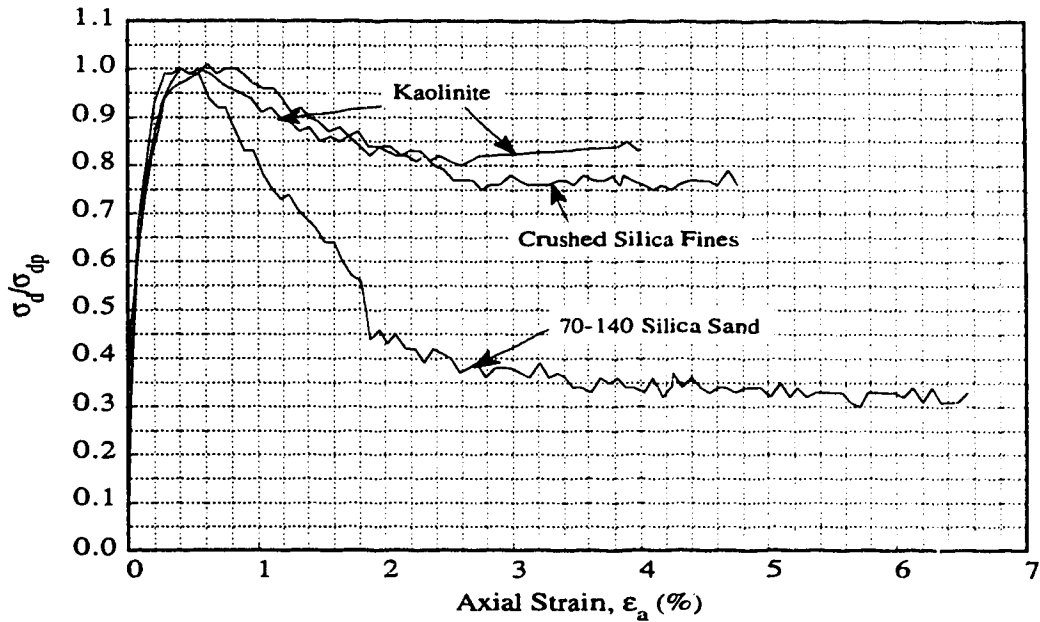


Figure 4.1.4.2b σ_d/σ_{dpeak} vs. ϵ_a Comparison Plot of 20% Samples

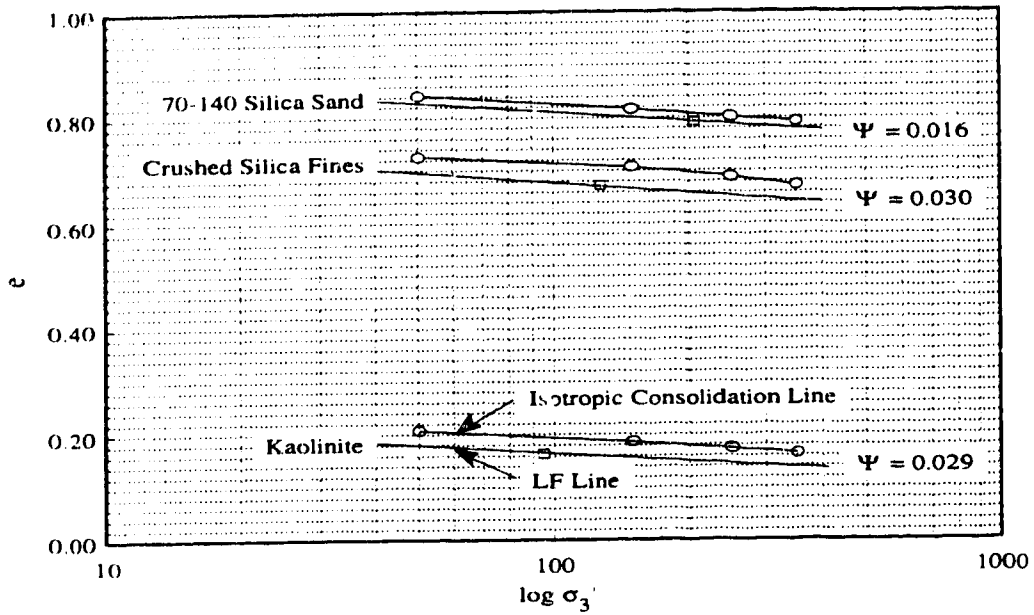


Figure 4.1.4.1.1 State Parameter Comparison Plot for 20% Samples

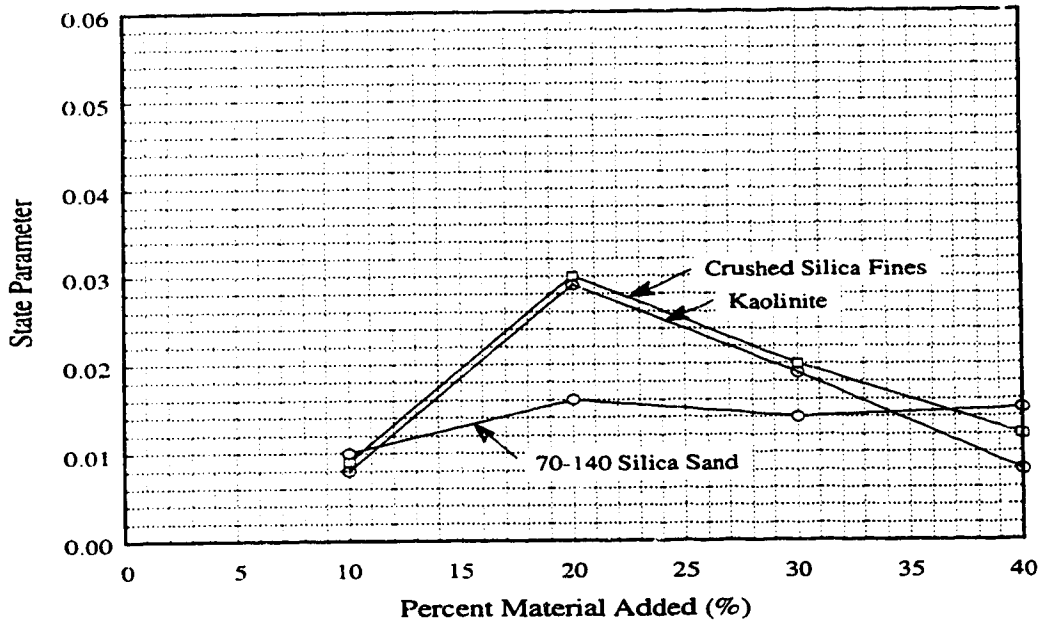


Figure 4.1.4.1.2 State Parameter vs. Percent Material Added

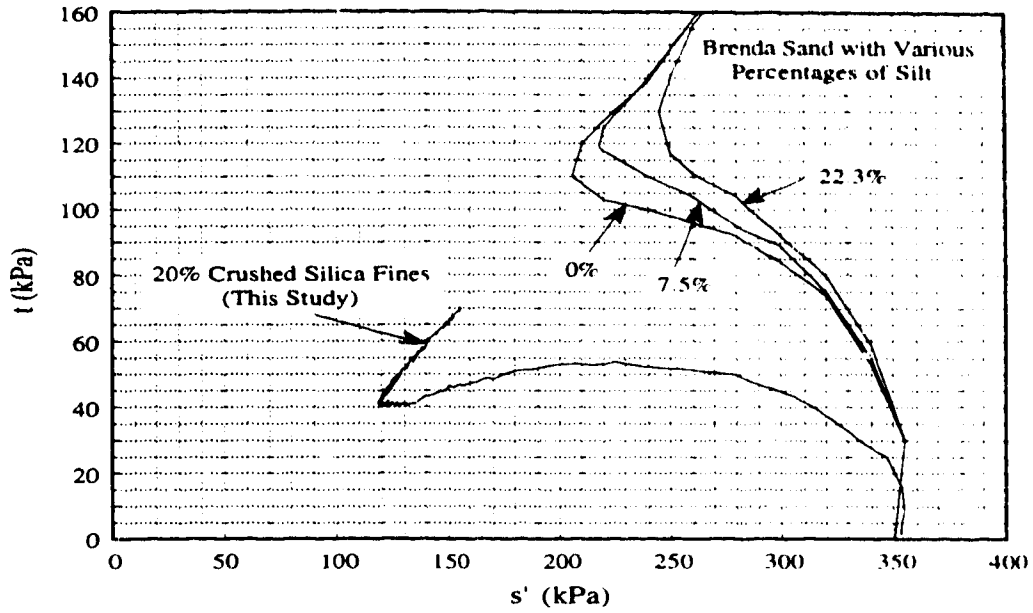


Figure 4.1.5.1 a Comparison of 20% Crushed Silica Fines enriched Ottawa sand to silt enriched Brenda sand (after Kuerbis, 1989)

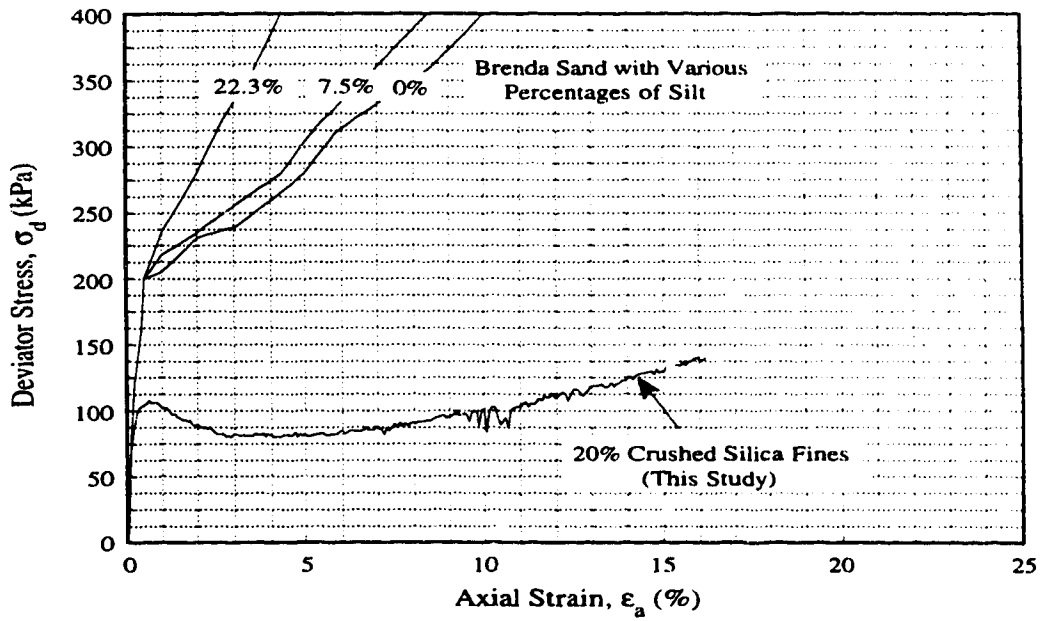


Figure 4.1.5.1b Comparison of 20% Crushed Silica Fines enriched Ottawa sand to silt enriched Brenda sand (after Kuerbis, 1989)

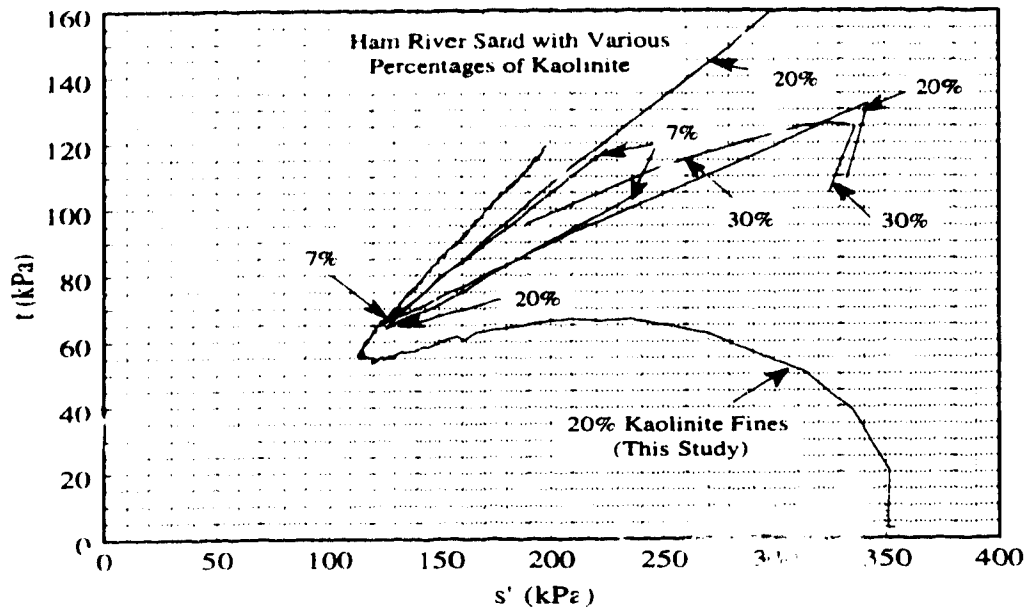


Figure 4.1.5.2a Comparison of 20% Kaolinite enriched Ottawa sand to Kaolinite enriched Ham River sand (after Georgiannou, 1988)

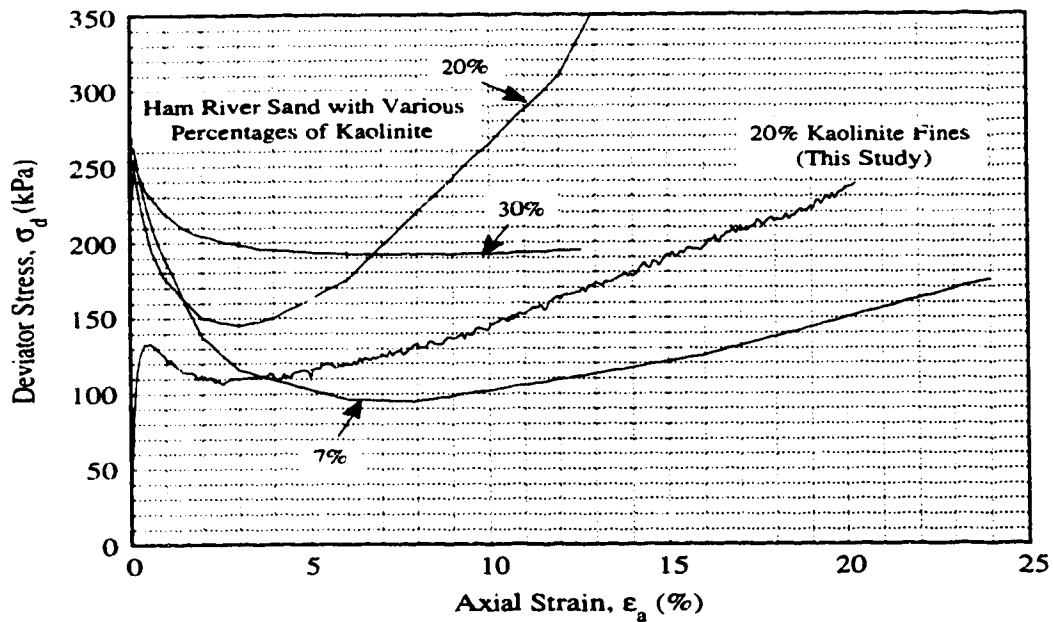


Figure 4.1.5.2b Comparison of 20% Kaolinite enriched Ottawa sand to Kaolinite enriched Ham River sand (after Georgiannou, 1988)

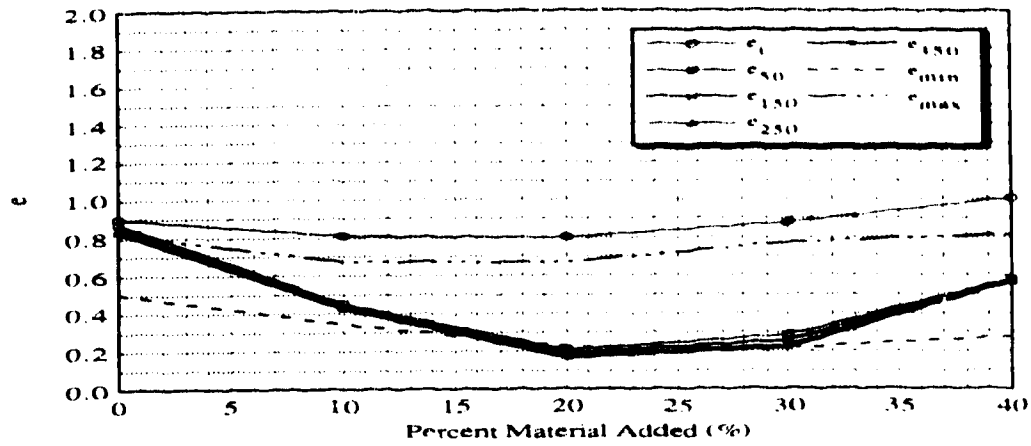


Figure 4.1.7.1a e vs. Percent Material Added at Various Effective Pressures for Kaolinite

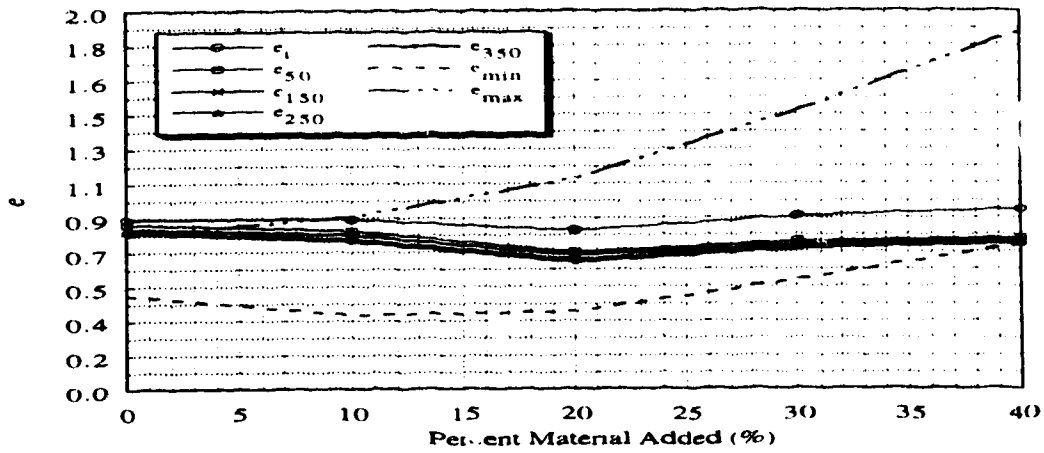


Figure 4.1.7.1b e vs. Percent Material Added at Various Effective Pressures for Crushed Silica Fines

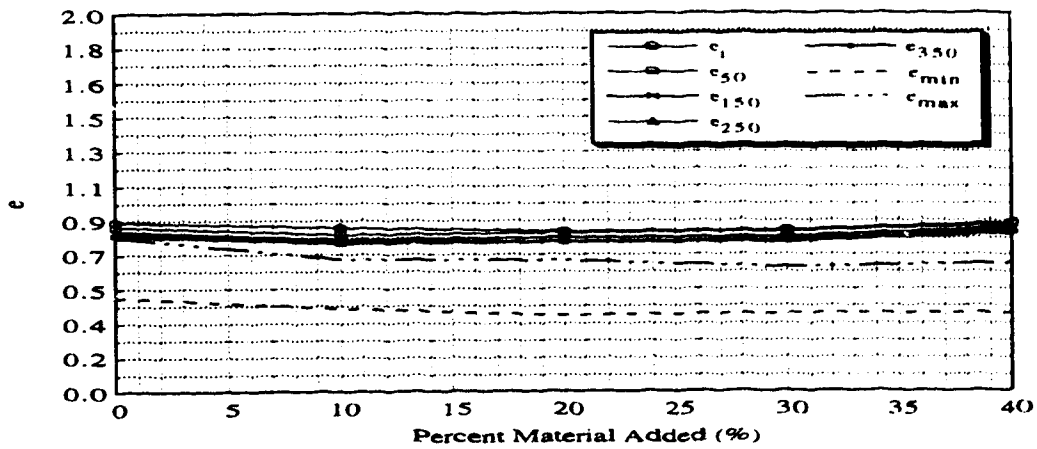


Figure 4.1.7.1c e vs. Percent Material Added at Various Effective Pressures for 70-140 Silica Sand

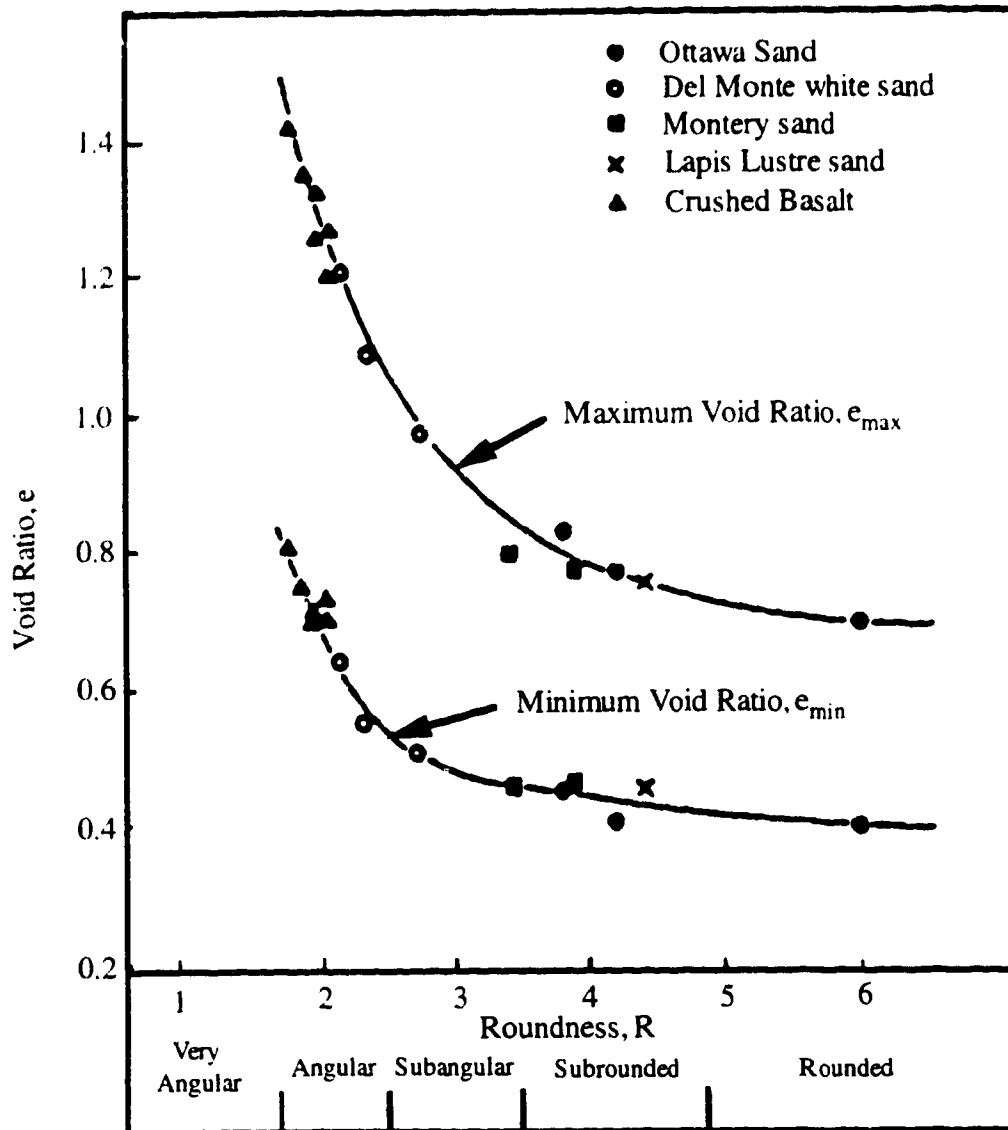


Figure 4.1.7.2 Density Limits as a Function of Grain Shape (after Youd, 1973)

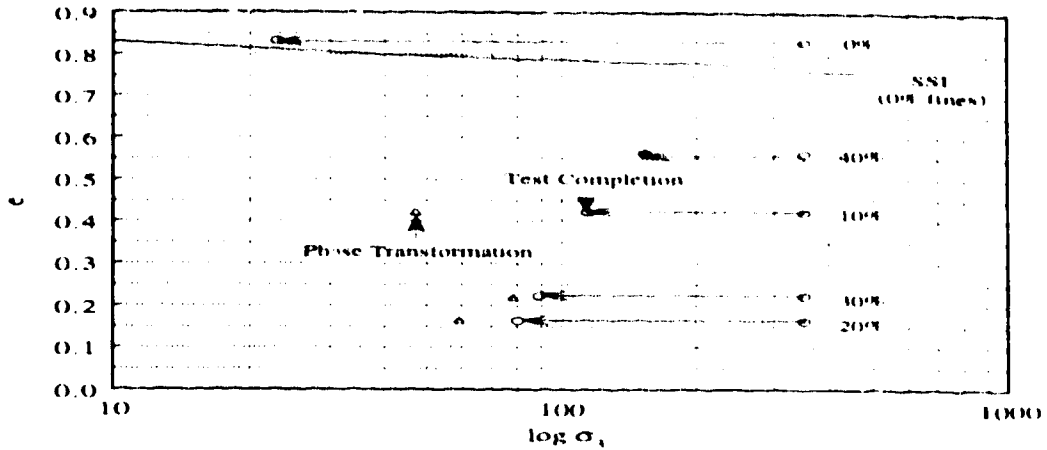


Figure 4.2.1a Steady-State Results for Kaolinite

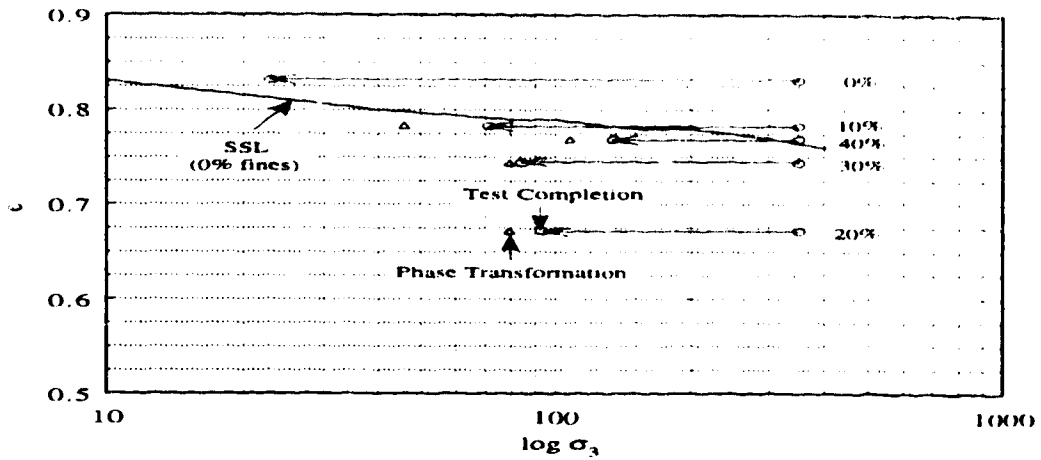


Figure 4.2.1b Steady-State Results for Crushed Silica Fines

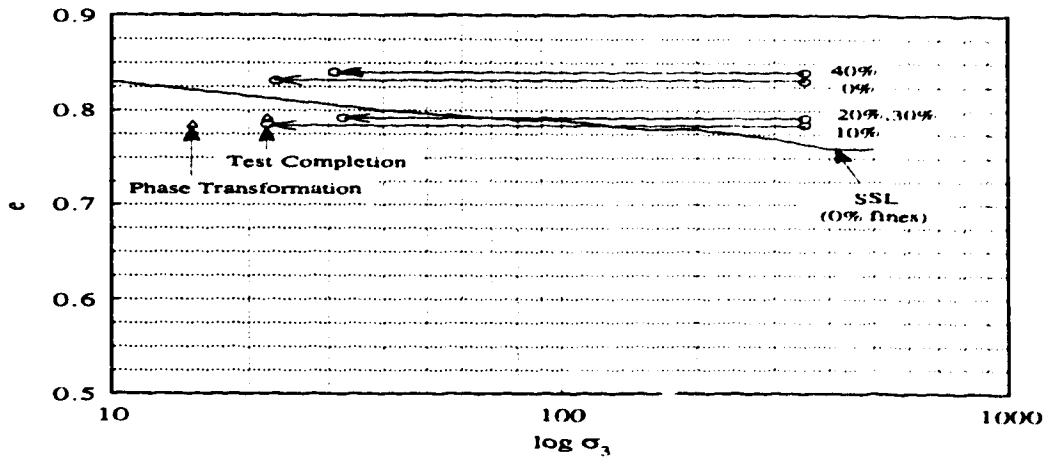


Figure 4.2.1c Steady-State Results for 70-140 Silica Sand

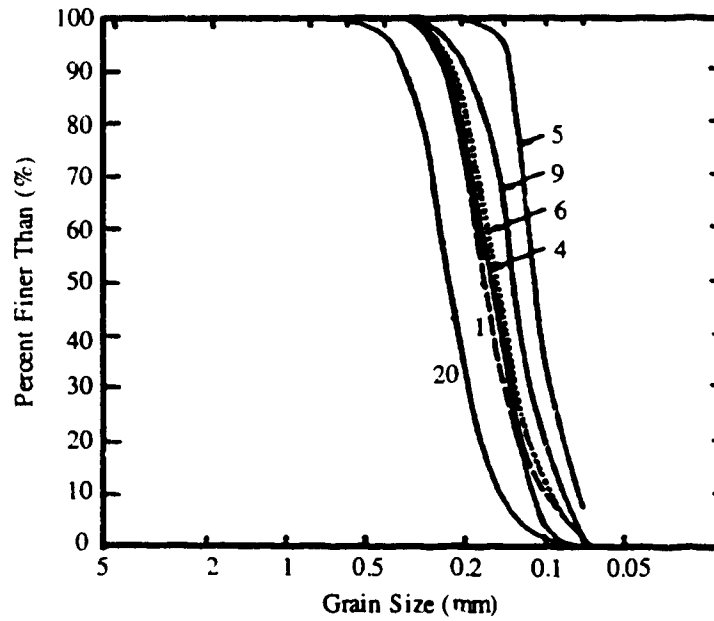
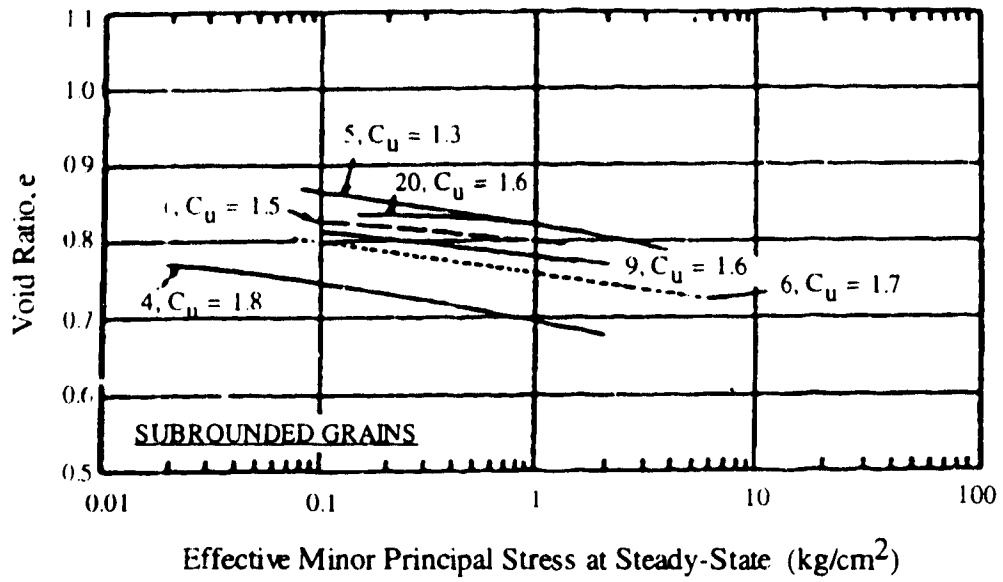


Figure 4.2.1.1 Steady-State Lines for Sands with Subrounded Grains
(after Poulos et al., 1985)

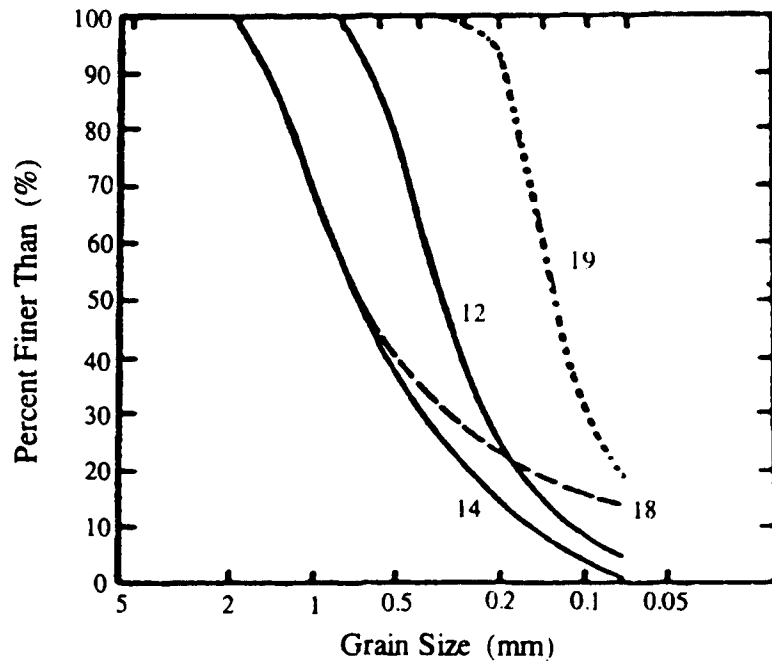
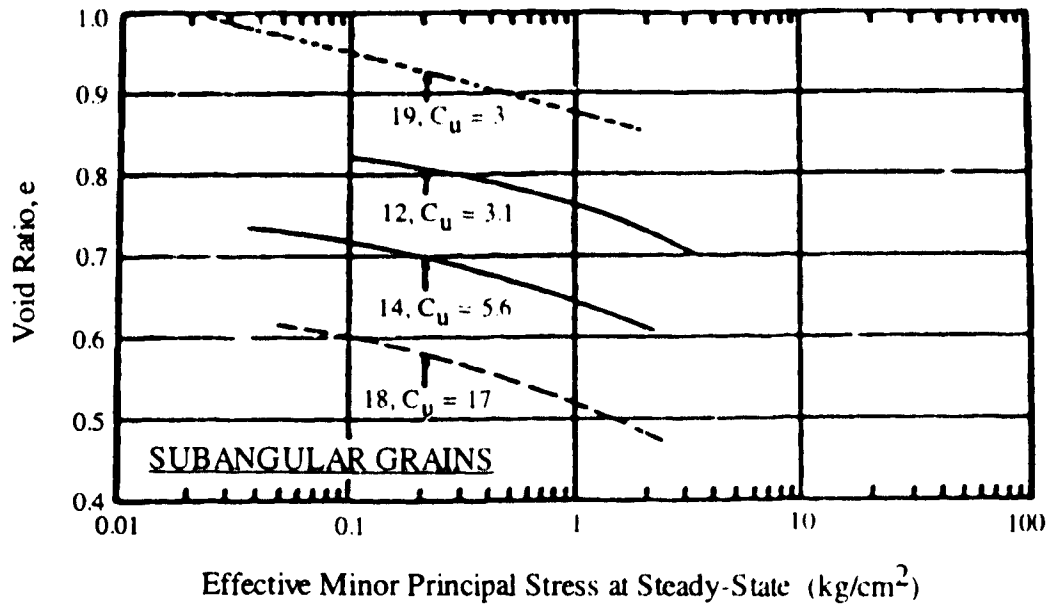


Figure 4.2.1.2 Steady-State Lines for Sands with Subangular Grains
(after Poulos et al., 1985)

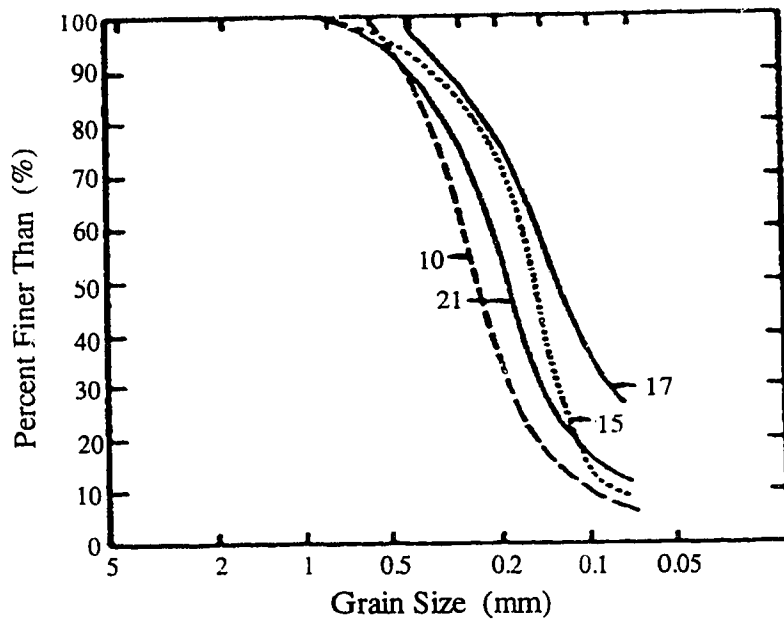
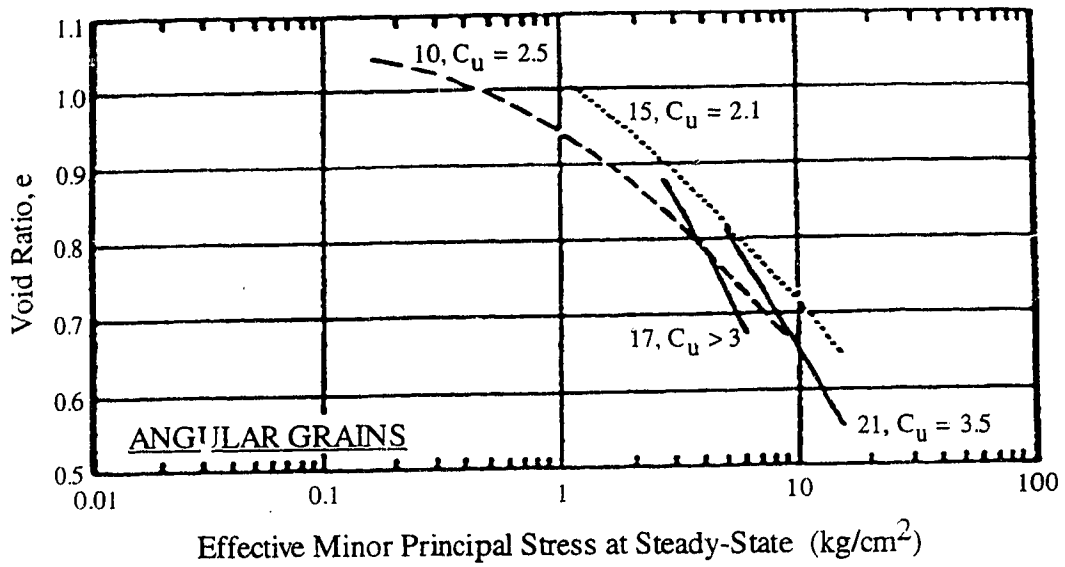


Figure 4.2.1.3 Steady-State Lines for Sands with Angular Grains
(after Poulos et al., 1985)

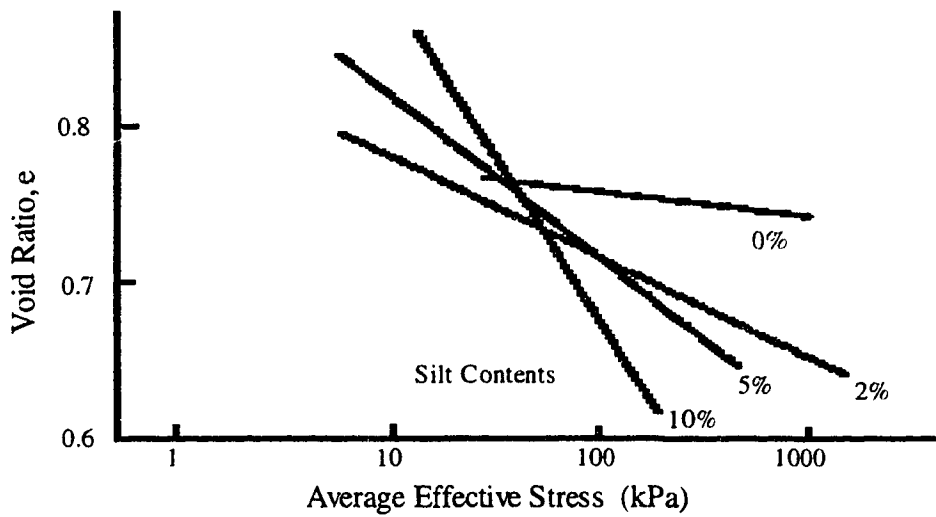
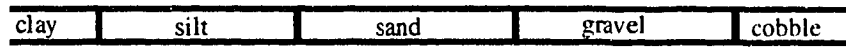
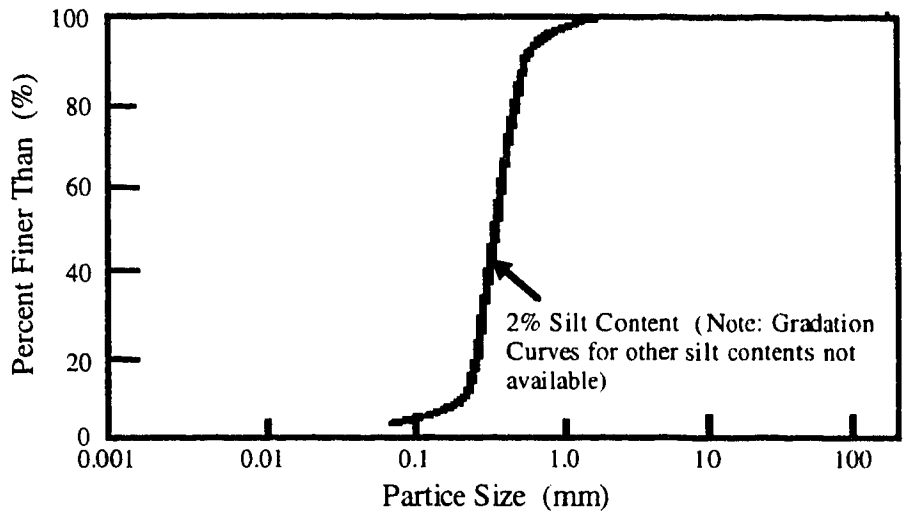


Figure 4.2.1.4 Steady-State Lines for Kogyuk Sand at Various Silt Percentages (after Been and Jefferies, 1985)

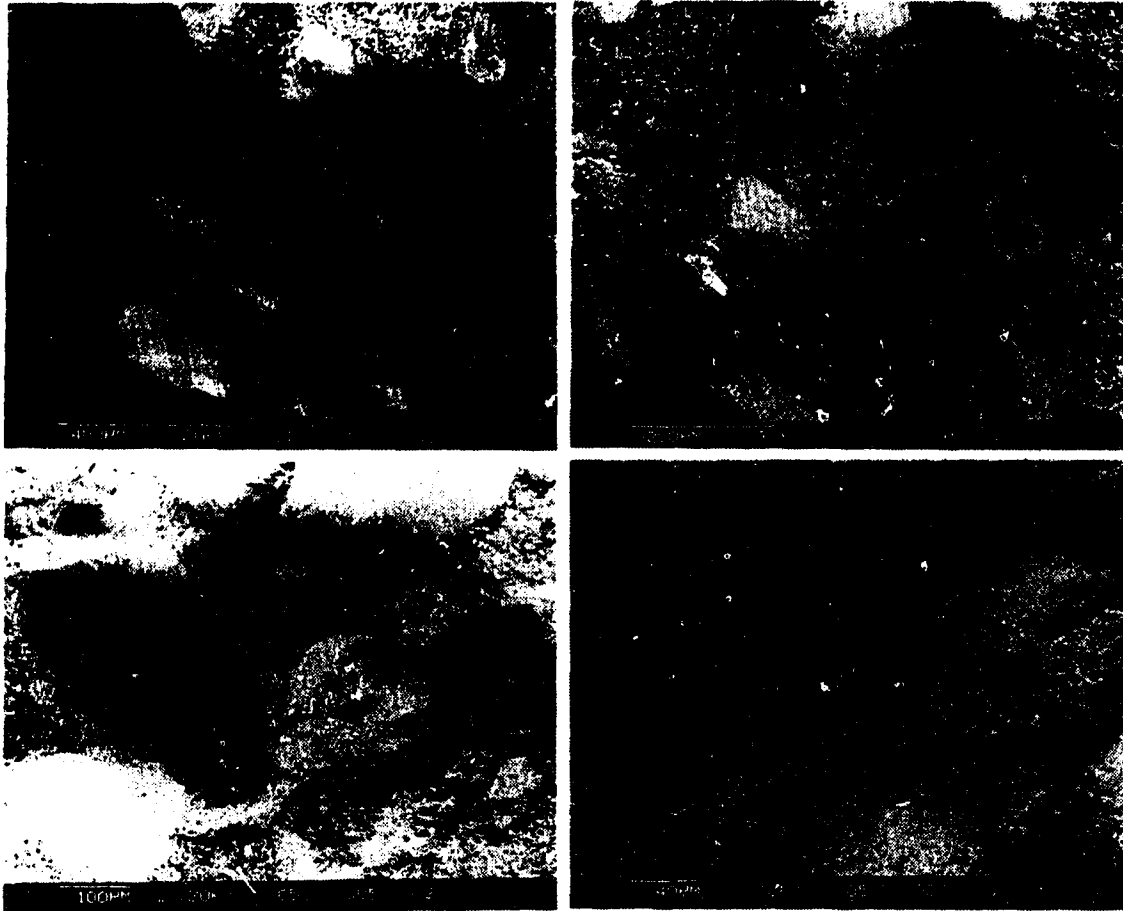


Figure 4.3.1 SEM Photographs of 20% Kaolinite Samples

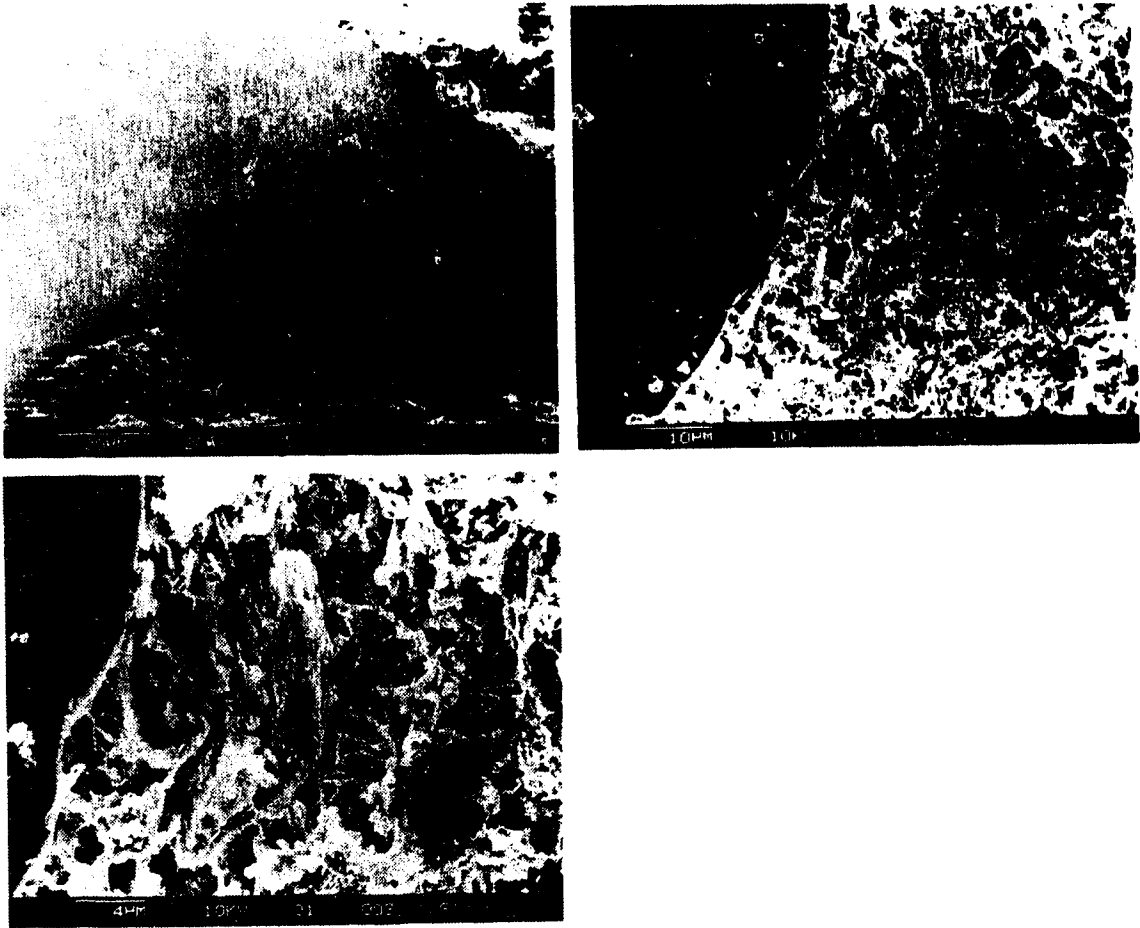


Figure 4.3.1 (cont'd)

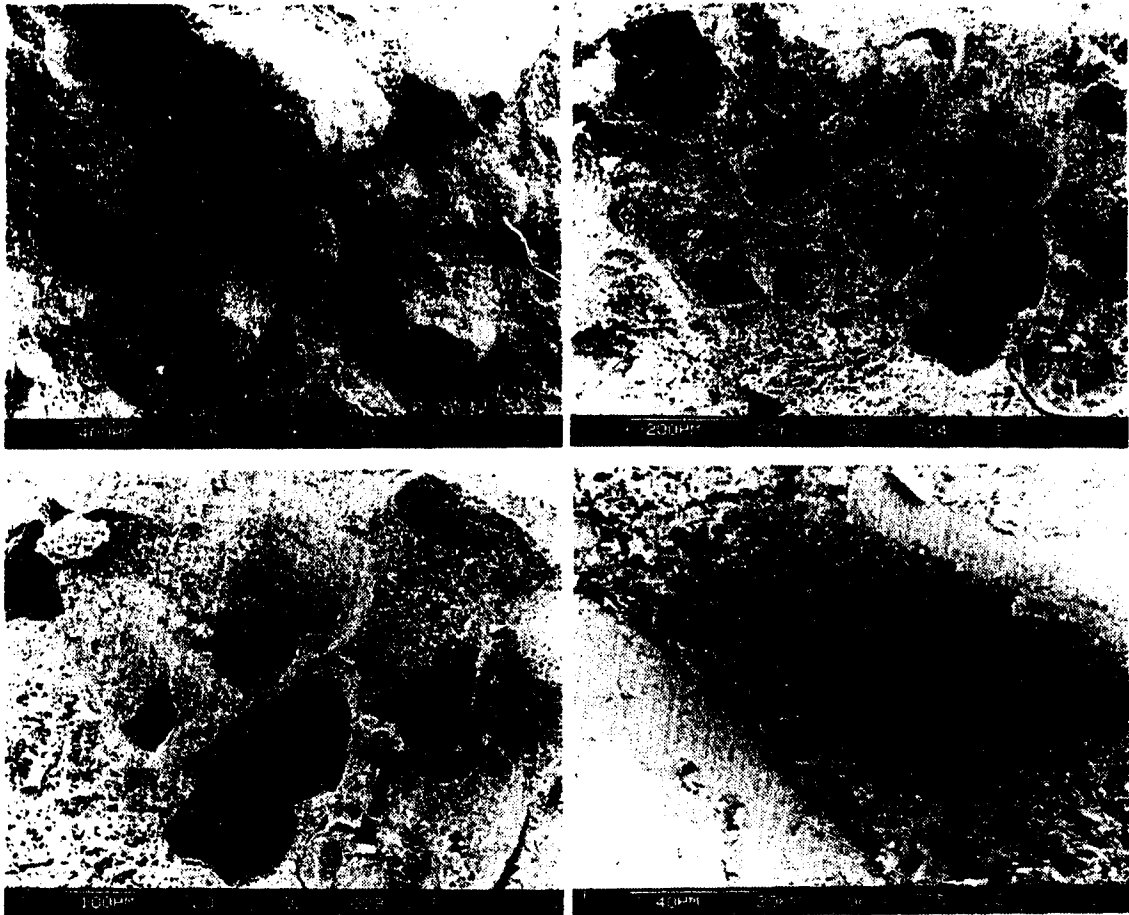


Figure 4.3.2 SEM Photographs of 40% Kaolinite Samples

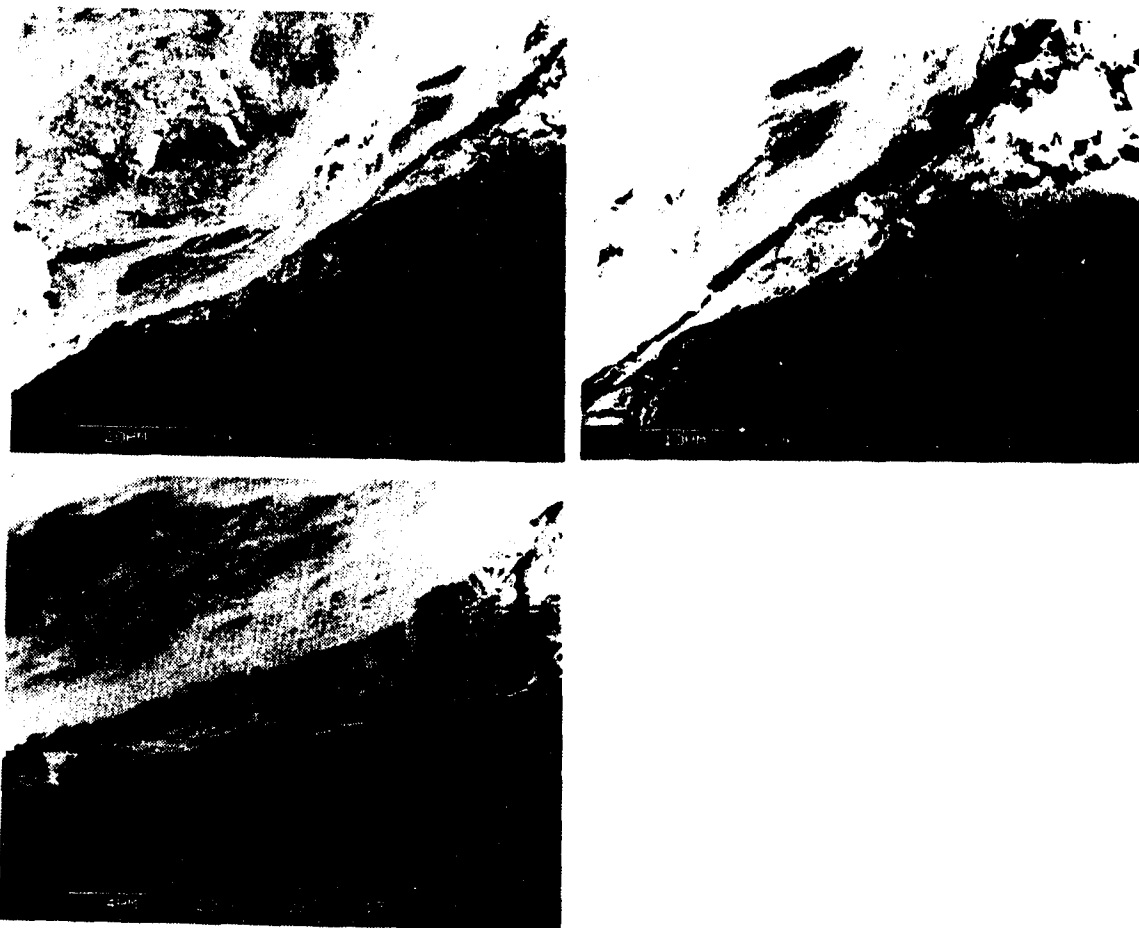


Figure 4.3.2 (cont'd)

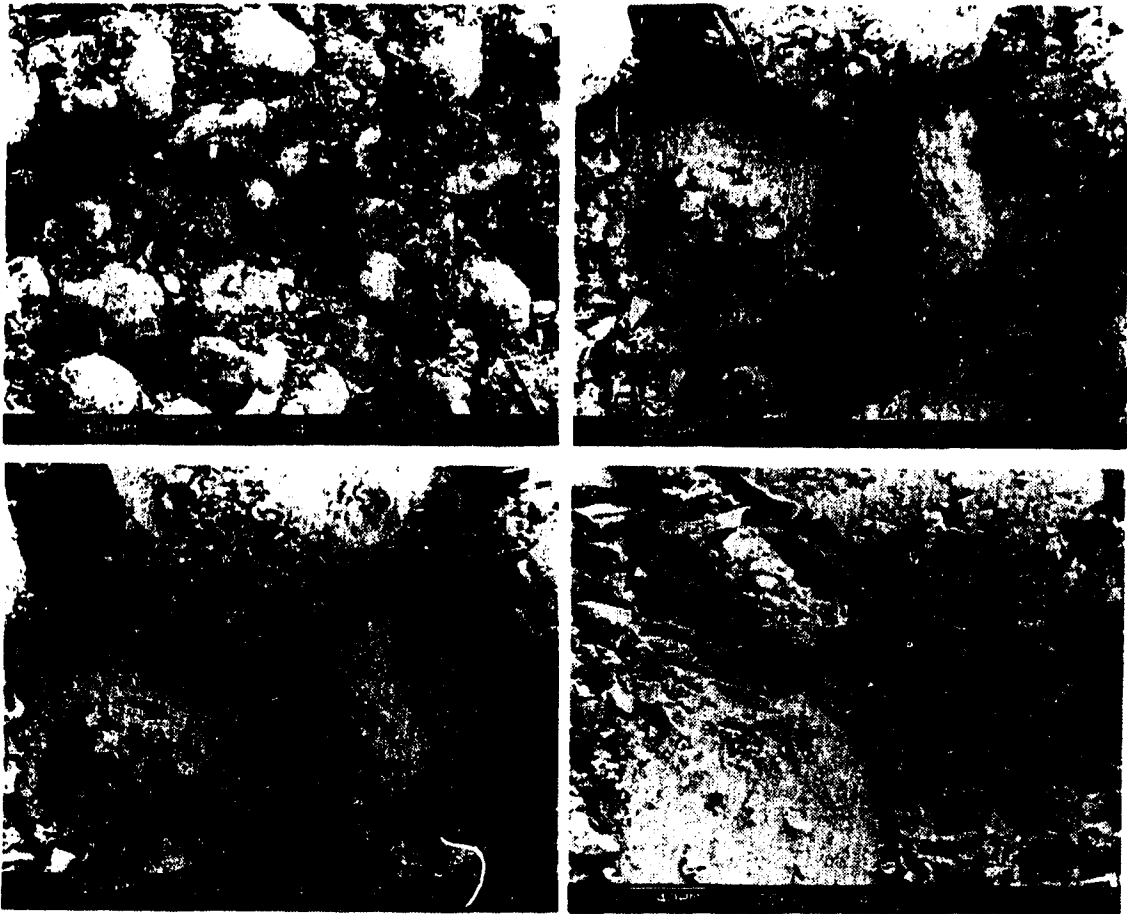


Figure 4.3.3 SEM Photographs of 20% Crushed Silica Fines Samples

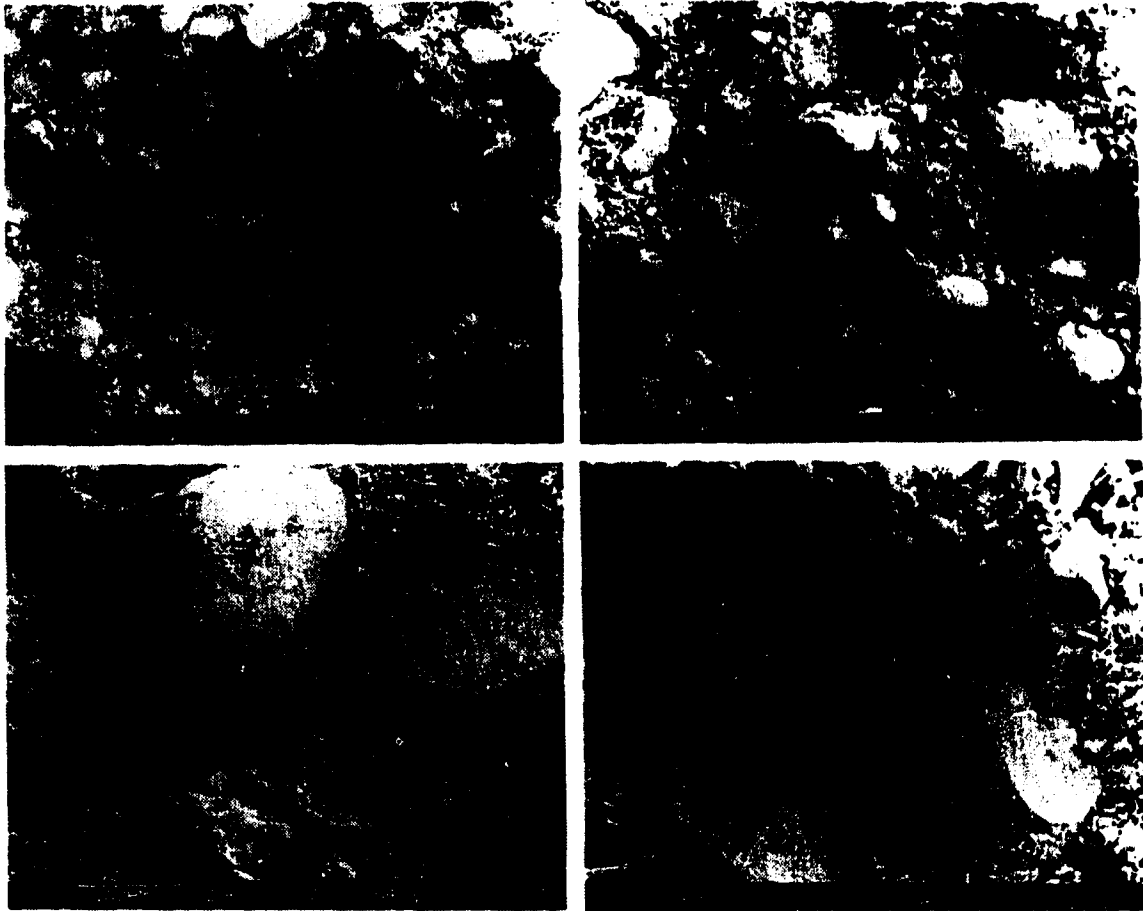


Figure 4.3.4 SEM Photographs of 40% Crushed Silica Fines Samples

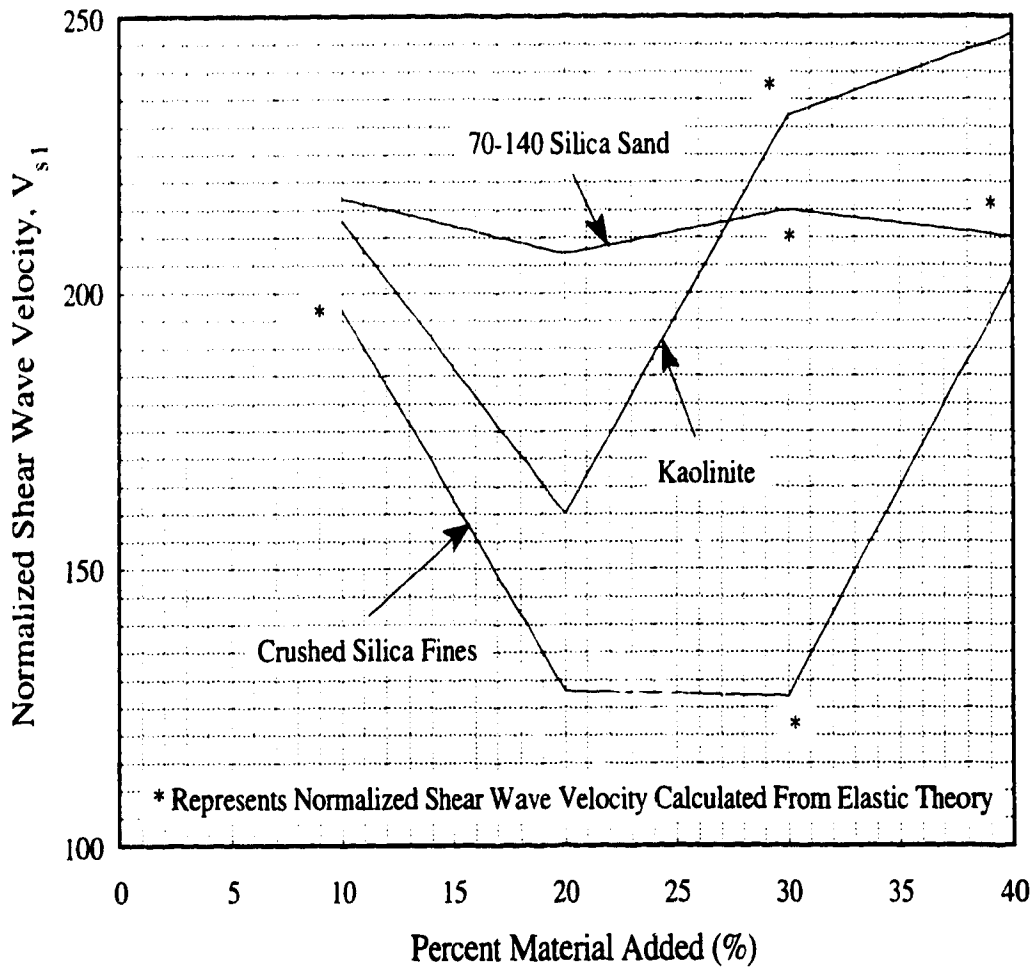


Figure 4.4.1 Normalized Shear Wave Velocity vs. Percent Material Added for Kaolinite, Crushed Silica Fines and 70-140 Silica Sand

5. DISCUSSION

5.1 Monotonic Undrained Behaviour

The observed monotonic undrained behaviour indicated that as fines ($<74\mu\text{m}$) are added, the sand becomes less collapsible. It was found at 40% fines content, the fines matrix completely governed the behaviour of the material. Similar behaviour was observed by Hird and Hassona (1990), where compressible fines (mica) were added to a uniform quartz subrounded sand. They found that the undrained brittleness decreased progressively with increasing mica content and at 30% mica content the behaviour was governed by the fines. The above results can be interpreted by understanding the particle movements during consolidation, prior to the undrained loading. The increased amount of fines promotes a higher degree of particle movement and re-orientation during consolidation so that a more stable structure is produced.

To the contrary, for reasons which will be stated, the results of Sladen et al. (1985) are not in agreement with the current results. Their results were based on interpretation of Cone Penetration Testing (CPT) data. The CPT data were converted to densities via correlations and are presented in detail in their paper. They found that the fines had a deleterious effect on the behaviour of a hydraulically placed sand based on the CPT results. At higher fines contents the density achievable was found to decrease and the drainage was impeded, resulting in a more collapsible structure. The impeded drainage led to the development of excess pore pressures. It was for these reasons they stated that "...the potential for liquefaction is much lower for a clean sand than for a dirty sand, all else being equal." (Sladen et al. 1985), where clean refers to a sand with 0% fines below $74\mu\text{m}$.

Researchers and designers have been dealing with interpretation difficulties of CPT and Standard Penetration Testing (SPT) data for years. Seed's (1984) method of liquefaction evaluation has been the method of choice for many years. His correction graph for varying fines contents can be seen in Figure 5.1.1. Two separate paths are indicated on Figure 5.1.1. Path (a) indicates that when compared at a common cyclic resistance ratio (τ/σ') the penetration resistance $(N_1)_{60}$ decreases with increasing fines.

The decrease in penetration resistance is probably due to the combined effects of increased soil compressibility and decreased drainage during penetration (Robertson et al., 1992). The penetration resistance is a large strain measurement which is effected by soil compressibility. Varying fines contents effects the soil compressibility and therefore effects the penetration resistance. As well, the fines decrease the permeability of the soil which in turn moves the penetration process from drained to undrained. The fact that the penetration resistance goes down, does not reflect that density has decreased, and hence, the material is more susceptible to liquefaction. If the results of Sladen et al. (1985) are viewed in this context, similar trends will be found which agree with this research. In the opinion of this researcher path (b) provides a better understanding of how the material is behaving. Path (b) indicates that when compared at a common tip resistance, the resistance ratio increases with increasing fines, hence the material is less susceptible to liquefaction.

5.1.1 Behaviour of Critical Stress Ratio (CSR) Line

It is of interest to point out that the slopes of the CSR lines for the three sets of tests were approximately the same (Table 4.1.6.1). It was found that the mobilized friction angle at CSR is very close to the interparticle friction angle for quartz, ϕ_{μ} . It would seem reasonable that the preferred sliding at the majority of interparticle contacts occurs when the effective stress ratio during undrained loading corresponds to the value at ϕ_{μ} . Once this occurs plastic deformation can take place.

5.2 Steady-State Line Behaviour

The inclination of the steady-state line in Figure 4.2.1a,b,c was shown to be highly dependent on the nature (degree of angularity) of the soil grains (section 4.2.1). A more well-rounded sand, as in this study, yields a flat steady-state line, where angular sands are characterized by steeper steady-state lines. As well, the quantity of the fines added not only effects the inclination but effects the void ratio achievable and hence, the degree of shift of the steady-state line (section 4.2.1).

It was pointed out by DeMatos (1988) that sands with the same type of grains, but differing only in grain size distribution, hence different coefficient of uniformities, exhibit parallel steady-state lines. In this research, combinations of sands and fines resulted in different type of grain combinations. It is hypothesized that as the percentage of angular fines added to a sub-rounded sand is increased that steady-state line steepens at a faster rate than if a rounded or plate-like fine is added. This behaviour was noted in tests performed by Hird and Hassona (1990) on mixtures of quartz sand and particles of mica.

5.2.1 Coefficient of Uniformity as a Measure of Liquefaction Potential

As was mentioned in section 4.2.1 the coefficient of uniformity, C_u was suggested (DeMatos, 1988) as a measure of the liquefaction potential. It had been suggested that as the coefficient of uniformity increases (increased fines content) so did the liquefaction potential. Based on limited tests, DeMatos (1988) indicated that the steady-state line shifted down with increased C_u . However the current research indicates that this is true to the point where possible sand grain separation occurs ($\approx 20\%$ fines), after which point the steady-state line shifts upwards. It is important to note that it is difficult to maintain a constant void ratio throughout testing. The prepared void ratios can be quite consistent, but upon saturating and consolidating a sample, the percentage of fines will effect the void ratio the sample will go to (Figures 4.1.7.1a,b,c). The variation of void ratio effects the amount the steady-state line shifts. Due to the shifting of the steady-state line, C_u alone does not provide a parameter by which the character of the soil particles or whether a soil will liquefy or not can be determined. Many attempts by various authors have been made to quantify a single parameter which can be easily obtained to determine the liquefaction potential of a soil. The state parameter (section 4.1.4.1) was used in this study to help explain why two samples at different void ratios behave in the same undrained manner. Therefore the state parameter does merit consideration as a index of liquefaction potential.

5.3 Discussion of Strain Similarities

In the present study and in previous studies (Castro et al., 1982; Chen, 1984; Kramer and Seed, 1988) of undrained triaxial tests on samples of loose saturated sands, an interesting stress-strain relationship was exhibited. The strain at which liquefaction, or in this study, limited liquefaction, is initiated is of interest. The initiation, which takes place at maximum shear stress, was found to occur at very low axial strains - typically on the order of 0.5%. After this point the degree of undrained brittleness is effected by the percentage of fines. The higher the fines content, the lower is the undrained brittleness. In this study, when 40% fines were added no strain softening response was observed.

The steady-state condition, which is represented by constant shear stress, is usually only reached after very large strains, usually on the order of 20 or 30%. This can create problems for laboratory experiments due to the strain limitations of most equipment used in the lab. Castro et al. (1982) attributes the scattering of steady-state results by different sources to this strain limitation, especially for very coarse-grained samples which can require strains greater than 30%.

Studies by Castro et al. (1982) and DeMatos (1988) and the present study, show that the steady-state is obtained at strains which depend on the nature of the sand (type of grains) and on the initial state of the soil. They found that the looser the sample, the lower was the strain at steady-state. Another qualitative finding was that a coarse-grained soil required more strain to reach steady-state than a fine grained soil, at similar conditions of density and consolidation pressure. These studies also indicate there is a relationship between the strain at steady state and the liquefaction potential of the material. The higher the undrained brittleness of the material, the lower is the strain required to reach the steady-state condition.

5.4 Fabric Effects

The results of the SEM testing were presented in section 4.3. The observations that were made were based on a macro- ($\geq 200\mu\text{m}$) and micro- ($< 200\mu\text{m}$) scale basis. On a macro-scale there were more sand grain-to-grain contacts at 20% than at 40%, where the

sand essentially floated in the fines matrix. On a micro-scale, the kaolinite samples tended to have lower void ratios than the crushed silica fines because the kaolinite fines have a higher compressibility (ability to deform around sand asperities) and are elongated in shape. Based on these observations one can only conclude that on a macro-scale the undrained response is highly dependent on fabric. Fabric, as was discussed in section 2.3.1, encompasses all parameters which effect the way the soil skeleton is constructed.

Kaolinite, in the presence of moisture, is particularly prone to aggregation (gathering of particles together) under the influence of surface tension. The aggregations tend to be quite resistant to dispersal during saturation and consolidation. Kaolinite tends to be concentrated at the sand grain contacts and at irregularities on the sand grain surfaces. As the percentage of kaolinite is increased, more kaolinite will be found around the rim of the voids and eventually begin to fill in the void spaces.

The behaviour of a material is dependent on the number and orientation of the contacts, displacement of the individual particles and the distribution of the forces. All particles, irrespective of their shape, will tend to a stable position relative to the forces acting upon them (Georgiannou, 1988). As the percentage of fines ($<74\mu\text{m}$) increases there is less sand grain contacts and a greater displacement of sand grains. The percentage of fines ($<74\mu\text{m}$) governs the manner to which the shear plane (from the monotonic undrained test) passes through the samples. At higher fines contents, the shear plane will pass through more fine particles, and hence, the undrained behaviour of the material will be governed more by the fines fraction than by the sand fraction. At the highest fines content (40%) used in this study, the fines governed the undrained behaviour, which was represented by the strain hardening of the kaolinite and crushed silica fines samples. This type of behaviour is commonly found in samples which are composed entirely of fines, such as a clay.

Fabric also played an important role in the shear wave velocity study (section 4.4). When fines ($<74\mu\text{m}$) were added, the normalized shear wave velocity decreased with increasing confining pressure to phase transformation, then increased and leveled off at steady-state. Even though at each percentage of fines the shear wave velocity leveled off at steady-state, the particular values were not the same for each test. Trends

indicated higher shear wave velocities at 10 and 40% fines than at 20 and 30% fines, suggesting that as the soil matrix was altered from a sand to a fines dominated structure, the shear wave velocity will vary.

When the gradation was altered (sand gradation changes from uniform to well-graded), the shear wave velocity increased with increasing confining pressure and again leveled off at steady-state. Since the undrained behaviour was not greatly affected by gradation, the shear wave velocities were expected to be relatively similar, which was the case. Even though the shear wave velocity results were on a limited number of tests, the trends indicated that fabric again played an important role.

Many of the observational differences which are made in steady-state studies, shear wave studies and others can be ascribed to fabric changes in the sand matrix. Studies by Been and Jefferies (1985) have indicated that cohesionless soils may have different fabrics at the same void ratio. It can then be postulated that to properly characterize the behaviour of a sand one must consider two variables: one which combines the influence of void ratio and effective stress, such as the State parameter (section 2.5.2); and a fabric parameter which characterizes the arrangement of the sand grains.

5.4.1 Loose Sands in Nature

Loose sands prepared by moist tamping for this research resulted in samples, prior to saturation, at high initial void ratios. After saturation and consolidation the samples were at void ratios which resulted in a limited liquefaction behaviour. This implies that even if a sample can be prepared at a high initial void ratio, after saturation and consolidation, the samples will be at low enough void ratio that only limited liquefaction or purely dilatant behaviour will occur. Therefore, one can argue that sands in nature, which have certainly been subject to some degree of saturation and consolidation, will not exhibit purely contractant behaviour, but instead exhibit limited liquefaction or at high enough fines contents, purely dilatant behaviour. Because of the inherent structure which is developed when fines are present, very loose sand samples can not exist in nature. Only where clean (0% fines) sands are located, which are few and far between in nature, will purely contractant behaviour occur and result in collapse liquefaction flow failures.

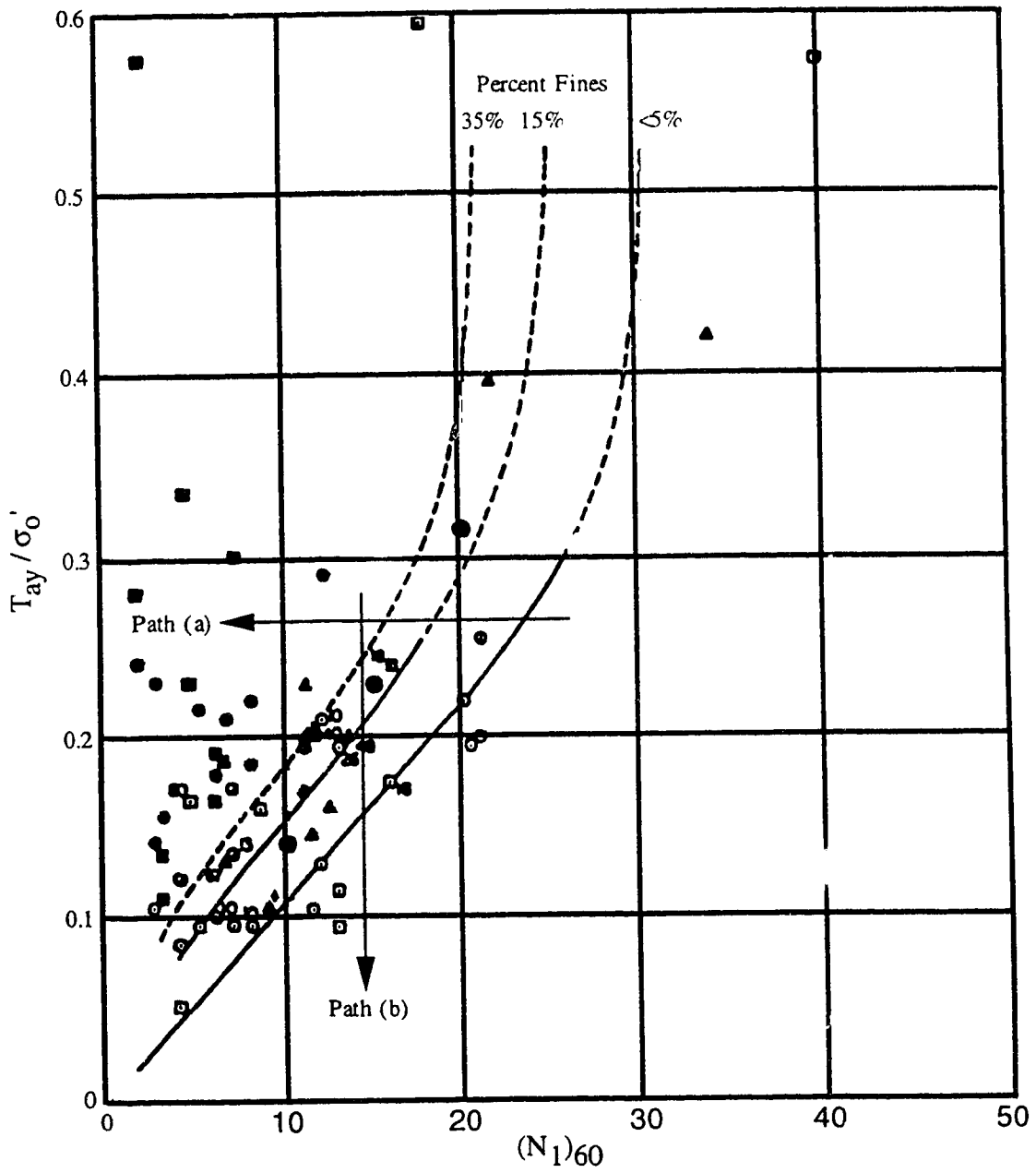


Figure 5.1.1 Resistance Ratio vs. Tip Resistance for Silty Sands
(after Seed et al., 1984)

6. SUMMARY AND CONCLUSIONS

For most of the tests that were performed in this study, the stress path reached a peak point, began to strain soften (representing undrained brittleness), then curled back (at the “elbow”) and strain hardened towards the steady-state envelope. The percentage of fines in the sample governs the amount of undrained brittleness. The higher the fines content the lower was the undrained brittleness. For samples at the highest percentage of fines (40%), the stress path indicated only strain hardening towards the steady-state envelope, ie. no brittleness.

If all the points of peak shear stress were connected in the stress space (s' - t), a line would be defined called the critical stress ratio (CSR) line. This line determines where the initiation of strain softening will occur (the “trigger” which was defined by Sladen et al., 1985). This line is unique for a particular sand and type of fines and was used to normalize the results for each series of tests. The line is unique because up to peak shear stress, small strain (<0.5%) behaviour governs and all tests exhibit similar stress paths. The normalization procedure worked not only very well when comparing with one type of fines, but also when comparing among all types of fines (Figures 4.1.4.2a,b). Using this procedure it was possible to get a clear picture of the effect of fines (74 μ m) versus gradation on the collapse of loosely prepared sand samples. It was found that the percentage of fines below 74 μ m and not their plasticity is what influenced the undrained response of a sand. Both plastic- and non-plastic-type fines behaved essentially similarly. The comparison plots also indicated that the undrained response is not significantly effected when the gradation was varied from uniform to well-graded, provided there was no increase in fines. Therefore, using the CSR line as oppose to the steady-state line, which is difficult to establish accurately, provides an alternative method of normalizing and a viable way of rationalizing the undrained response of a sand samples.

One of the trends that was found during the research was that undrained brittleness decreased as the percentage of fines (<74 μ m), for both plastic- and non-plastic-type, increased. At a fines fraction of 40% the response of the material dominated by the fines. It is important to emphasize that the undrained brittleness is not controlled by the plasticity of the fines but by the amount of the fines (ie. percentage less than 74 μ m).

The second trend observed during this research is related to the change in gradation of the host sand. The monotonic undrained behaviour was virtually unchanged as the gradation varied from uniform to well-graded. Although gradation was altered, the fines ($<74\mu\text{m}$) remained unchanged. It can therefore be concluded that it is the percentage of fines below $74\mu\text{m}$ which governs the fabric and hence the monotonic behaviour of a particular sandy soil.

The amount of structural instability was shown to decrease with increasing fines content. The percentage and plasticity of the fines effected the degree to which the initial void ratio (e_i) changed during saturation and consolidation. The consolidated void ratio (e_c) would therefore be different depending on the percentage and plasticity of the fines added. The difference in consolidated void ratio influences the position of the steady-state line. The inclination of the steady-state line was not determined in this research. This would require identical tests to be performed at a different effective stress level. The shifting of the steady-state line presents practical problems for liquefaction stability analyses. Many of the parameters which are required are difficult to obtain with any sufficient accuracy, considering how sensitive undrained behaviour is to parameter variability.

The state parameter (section 4.1.4.1) was used to explain why two samples at different void ratios behave in the same undrained manner. Samples which behave in the same undrained manner were found to have similar state parameters. This helps to explain why a 20% kaolinite sample at a void ratio of 0.16 behaved in the same undrained manner as a 20% crushed silica fines sample at a void ratio of 0.67. Both samples had essentially the same state parameter. This was found to be the case for all percentages of fines ($<74\mu\text{m}$). Although the state parameter was found not to be a universal index, it does merit consideration as a means of comparing materials which behave in the same undrained manner.

The use of the Scanning Electron Microscope (SEM), although expensive and elaborate for most engineering applications, does merit some consideration in large liquefaction studies. Studying SEM photographs helps the engineer to understand how the soil is behaving on a granular level. SEM photographs reveal the grain-to-grain contacts and the interaction between the coarse and fines fractions. SEM photography takes out much of the guess work in soils analyses. Another major benefit of using SEM

photography as a tool in geotechnical engineering is that only small “undisturbed” samples are required for the analysis. Although this seems high-tech, when multi-million dollar remediation work is being considered, attention to particle contact behaviour is important.

The SEM work which was carried out for this research confirmed the behaviour obtained during monotonic undrained testing. The SEM photographs (Figures 4.3.1 to 4.3.4) confirmed the dominance of the fines at the highest percentage of fines tested (40%). From the photographs no sand grain contact could be observed at 40% fines content, indicating a fines dominated behaviour.

A subsidiary study involving shear wave measurement was also undertaken. The results, although based only on the trends of a limited number of tests, did present some interesting results. These results were again fabric dependent. When fines ($<74\mu\text{m}$) were varied reverse trends of shear wave velocity with increasing mean effective confining pressure was witnessed as compared to when gradation was varied. When fines ($<74\mu\text{m}$) were added the shear wave velocity decreased with increasing mean effective stress until phase transformation and then increased as the stress path approached maximum obliquity, a trend which is opposite to what is expected. As well, the shear wave velocity tended to be lower at 20 to 30% fines contents and higher at 10 and 40% fines contents. When gradation (adding 70-140 silica sand) was varied (uniform to well-graded) the shear wave velocity increased with increasing mean effective stress and peaked as the stress path approached maximum obliquity, representing a normal trend. The shear wave velocities for the various percentages of 70-140 silica sand, at the same effective stress level, were similar. It was not clear from this research why there was reverse trends of shear wave velocity when fines ($<74\mu\text{m}$) was altered. It can be hypothesized that the fabric imparted by the fines on the sand could influence the shear wave velocity behaviour and/or how some of the shear wave velocities were determined using the theory of elasticity. Additional testing would have to be completed to verify these results.

A very important problem involved with in situ liquefaction studies is related to the small strains at which collapse liquefaction can be triggered. For sands which can be triggered by collapse liquefaction more sensitive instrumentation is required, This is because of the low strains ($<0.5\%$) involved, for which many types of conventional

slope instrumentations, based on periodic measurements, will not provide adequate warning of impending instabilities.

It is very important to distinguish between a stability problem and a deformation problem. A stability problem is one in which the soil fails; a deformation problem is one in which the deformations of the soil cause undesirable behaviour of the structure. If collapse liquefaction - a stability problem - is found to be possible, then questions of deformations become secondary, assuming that the collapse liquefaction can be triggered. If a soil mass is not susceptible to collapse liquefaction then it is necessary to estimate the deformation that may occur due to any postulated loading, since the deformations may control the design. If the material is strain hardening, hence non-collapsible, then a collapse liquefaction study is not required.

In short, very loose clean (0% fines) sands that can exhibit collapse liquefaction should not be left in place, because in most cases only small strains are needed to trigger a flow slide. Most in situ dirty sands will be subject to limited liquefaction. The degree of limited liquefaction is related to the percentage of fines and not their plasticity. The percentage of fines will govern whether a stability or a deformation problem should be looked at.

Concerning engineering practice for liquefaction potential, Peck (1979) noted that sometimes the latest scientific discovery is not always in the right direction. Peck pointed out that science has a way of correcting itself and making progress, which may temporarily lead the unwary astray, but should not intimidate the experienced engineer. Although there is a high level of research regarding liquefaction phenomena that is presently underway, more research coupled with improved engineering practice is required.

REFERENCES

- Alarcon-Guzman, A. Leonards, G.A. and Chameau, J.L. 1988. Undrained Monotonic and Cyclic Strength of Sands. ASCE Journal of Geotechnical Engineering Division, **114**(10): 1089-1109.
- Arthur, J.R.F. and Menzies, B. 1972. Inherent Anisotropy in a Sand. Géotechnique, **22**(1): 115-128.
- Atkinson, J.H. and Bransby, P.L. 1978. **The Mechanics of Soils, an Introduction to Critical State Soil Mechanics**. McGraw-Hill, London, England.
- Rates, C.R. 1989. Dynamic Soil Property Measurements During Triaxial Testing. Géotechnique. Liquefaction and Cyclic Mobility of Saturated Sands. ASCE Journal of Geotechnical Engineering Division, **101**: 551-569.
- Been, K. and Jefferies, M.G. 1985. A State Parameter for Sand. Géotechnique, **35**(2): 99-112.
- Been, K., Jefferies, M.G. and Hachey, J. 1991. The Critical State of Sands. Géotechnique, **41**(3): 365-381.
- Bishop, A.W. and Wesley, L.D. 1975. A Hydraulic Triaxial Apparatus for Controlled Stress Path Testing. Géotechnique, **25**(4): 657-670.
- Bishop, A.W. 1967 Progressive failure - with special reference to mechanism causing it. Proceedings of the Geotechnical Conference, Oslo, Norway, **2**: 142-150.
- Castro, G. 1969. Liquefaction of Sands. Ph. D. Thesis, Harvard University, Cambridge, MA, Harvard Soil Mechanics Series, No. 81.
- Castro, G. 1975. Liquefaction and Cyclic Mobility of Saturated Sands. ASCE Journal of Geotechnical Engineering Division, **101**: 551-569.
- Castro, G. and Poulos, S.J. 1977. Factors affecting Liquefaction and Cyclic Mobility. ASCE Journal of Geotechnical Engineering Division, **103**: 501-516.
- Castro, G., Enos, J.L., France, J.W., Poulos, S.J. 1982. Liquefaction Induced by Cyclic Loadings. Geotechnical Engineers Inc., Winchester, MA, Prepared for the NSF, Washington, DC.
- Chern, J.C. 1985. Undrained Response of Saturated Sands with Emphasis on Liquefaction and Cyclic Mobility. Ph.D. Thesis. University of British Columbia, Vancouver, BC.
- Craig, R.F. 1987. **Soil Mechanics**. 4th ed., Van Nostrand Reinhold Company, New York.

- Dávila, R.S. 1992. The Influence of Fines Content and Specific Surface Area on Freezing of Sandy Soils. M.Sc. Thesis. Dept. of Civil Eng., University of Alberta, Edmonton, AB.
- De Matos, M. 1988. Mobility of Soil and Rock Avalanches. Ph.D. Thesis. Dept. of Civil Eng., University of Alberta, Edmonton, AB.
- Dyvik, R. and Madshus, C. 1985. Laboratory Measurement of G_{max} using Bender Elements, Advances in the art of Soil Testing under Cyclic Loads. ASCE, New York.
- Finn, W.D.L., Bransby, P.L. and Pickering D.J. 1970. Effect of Strain History on Liquefaction of Sands. ASCE Journal of the Soil Mechanics and Foundations Division, **96**(SM6): 1917-1934.
- Frydman, S., Zeitlen, J.G. and Alpan, I. 1973. The membrane effect in Triaxial Testing of Granular Soils. Journal of Testing and Evaluation, **1**(1): 37-41.
- Georgiannou, V.N. 1988. Behaviour of Clayey Sands under Monotonic and Cyclic Loading. Ph.D. Thesis, Dept. of Civil Eng., Imperial College of Science, Technology and Medicine, London, England.
- Georgiannou, V.N., Burland, J.B. and Hight, D.W. 1990. The Undrained Behaviour of Clayey Sands in Triaxial Compression and Extension. Géotechnique, **40**(3): 431-449.
- Georgiannou, V.N., Hight, D.W. and Burland, J.B. 1991. Undrained Behaviour of Natural and Model Clayey Sands. Japanese Society of Soil Mechanics and Foundation Engineering, **31**(3): 17-29.
- Gohl, W.B. and Finn, W.D.L. 1991. Use of Piezoceramic Bender Elements in Soil Dynamics Testing. Recent Advance in Instrumentation Data Acquisition and Testing in Soil Dynamics. ASCE convention, Orlando, Florida. Geotechnical special publication No. 29.
- Gu, W.H. 1992. Liquefaction and Post-Earthquake Deformation Analysis. Ph.D. Thesis. Dept. of Civil Eng., University of Alberta, Edmonton, AB.
- Hardin, B.O. and Richart Jr., F.E. 1963. Elastic Wave Velocities in Granular Soils. ASCE Journal of the Soil Mechanics and Foundations Division, **89**(SM1): 33-64.
- Hardin, B.O. and Drnevich, V.P. 1972. Shear Modulus and Damping of Soils: Measurements and Parameter Effects. ASCE Journal of the Soil Mechanics and Foundations Division, **98**(6): 603-624.
- Hird, C.C. and Hassona, F.A.K. 1986. Discussion on "A State Parameter for Sand". Géotechnique, **36**: 124-127.

- Hird, C.C. and Hassona, F.A.K. 1990. Some Factors Affecting the Liquefaction and Flow of Saturated Sands in Laboratory Tests. *Engineering Geology*, **28**: 149-170.
- Ishihara, K., Tatsuoka, F. and Yasuda, S. 1975. Undrained Deformation and Liquefaction of Sand under Cyclic Stresses. *Japanese Society of Soil Mechanics and Foundation Engineering*, **15**(1): 29-44.
- Ishihara, K., Troncoso, J., Kawase, Y. and Takahashi, Y. 1980. Cyclic Strength Characteristics of Tailings Materials. *ASCE Journal of Geotechnical Engineering Division*, **20**(4): 127-142.
- Konrad, J.M. 1990. Minimum Undrained Strength of Two Sands. *ASCE Journal of Geotechnical Engineering Division*, **116**(6): 932-947.
- Konrad, J.M. 1990. Minimum Undrained Strength Versus Steady-State Strength of Sands. *ASCE Journal of Geotechnical Engineering Division*, **116**(6): 948-963
- Kramer, S.L. and Seed, H.B. 1988. Initiation of Soil Liquefaction Under Static Loading Conditions. *ASCE Journal of Geotechnical Engineering Division*, **114**(4): 412-430.
- Kuerbis, R.H. 1989. The Effect of Gradation and Fines Content on the Undrained Loading Response of Sand. M.Sc. Thesis. Dept. of Civil Eng., University of British Columbia, Vancouver, BC.
- Kuerbis, R.H. and Vaid, Y.P. 1989. Undrained Behaviour of Clean and Silty Sands. Proc. of discussion session on Influence of Local Conditions on Seismic Response. XII International Conf. on Soil Mech. and Found. Eng. Rio de Janeiro: 91-100.
- McRoberts, E.C. and Sladen, J.A. 1992. Observations on Static and Cyclic Sand-Liquefaction Methodologies. *Canadian Geotechnical Journal*, **29**: 650-665.
- Mitchell, J.K. 1976. **Fundamentals of Soil Behaviour**. Edition John Wiley and Sons, New York.
- Miura, S. and Toki, S. 1982. A Sample Preparation Method and its Effect on Static and Cyclic Deformation. Strength Properties of Sands. *ASCE Journal of Geotechnical Engineering Division*, **22**(1): 61-77.
- Mulilis, J.P., Seed, H.B., Chan, C.K., Mitchell, J.K. and Arulanandan, K. 1977. Effect of Sample Preparation on Sand Liquefaction. *ASCE Journal of the Soil Mechanics and Foundations Division*, **103**: 91-108.
- Nishio, S. and Tamaoki, K. 1990. Stress Dependency of Shear Wave Velocities in Diluvial Gravel Samples During Triaxial Compression Tests. *Japanese Society of Soil Mechanics and Foundation Engineering*, **30**(4): 42-52.
- Oda, M. 1981. Anisotropic Strength of Cohesionless Sand. *ASCE Journal of the Soil Mechanics and Foundations Division*, **108**: 1219-1231.

- Parry, R.H.G. and Nadarajah, V. 1973. Observations on Laboratory Prepared, Lightly Overconsolidated Specimens of Kaolin. *Géotechnique*, **24**(3): 345-358.
- Peck, R.B. 1979. Liquefaction potential: Science versus Practice. *ASCE Journal of Geotechnical Engineering Division*, **105**: 393-398.
- Poulos, S.J. 1981. The Steady State of Deformation. *ASCE Journal Of Geotechnical Engineering Division*, **107**: 553-562.
- Poulos, S.J., Castro, G. and France, J.W. 1985. Liquefaction Evaluation Procedure. *ASCE Journal of Geotechnical Engineering Division*, **111**: 772-791.
- Poulos, S.J., Castro, G. and France, J.W. 1988. Liquefaction Evaluation Procedure: Reply. *ASCE Journal of Soil Mechanics and Foundation Division*, **114**: 232-256.
- Raju, V.S. and Sadasivan, S.K. 1974. Membrane Penetration in Triaxial Tests on Sands. *ASCE Journal of Geotechnical Engineering Division*, **100**(GT4): 482-489.
- Robertson, P.K., Woeller, D.J. and Finn, W.D.L. 1992. Seismic Cone Penetration Test for evaluating Liquefaction Potential under Cyclic Loading. *Canadian Geotechnical Journal*, **29**: 686-695.
- Roscoe, D.H. 1970. The Influence of Strains in Soil Mechanics. Tenth Rankine Lecture. The Institution of Civil Engineers, London, England.
- Roscoe, K.H., Schofield, A.N. and Thurairajah, A. 1963. An Evaluation of Test Data for Selecting a Yield Criteria for Soils. *Laboratory Shear Testing of Soils*. STP 361. ASTM, Philadelphia: 111-128.
- Rowe, P.W. 1962. The Stress-Dilatancy Relation for Static Equilibrium of an Assembly of Particles in Contact. *Proc. Royal Society A.*, **269**: 500-527.
- Sasitharan, S. Robertson, P.K. and Sego, D.C. 1992. Sample Disturbance from Shear Wave Velocity Measurements. *Conference Proceedings, 45th Geotechnical Conference*, Toronto, Ontario.
- Sasitharan, S. (unpublished) Ph.D. Thesis. Dept. of Civil Eng., University of Alberta, Edmonton, AB.
- Schofield, A.N. and Wroth, C.P. 1968. **Critical State Soil Mechanics**. McGraw-Hill, London, England.
- Schultheiss, P.J. 1981. Simultaneous Measurements of P and S Wave Velocities During Conventional Laboratory Soil Testing Procedures. *Marine Geotechnical*, **4**(4): 343-367.

- Seed, H.B., Tokimatsu, K., Harder, L.F. and Chung, R.M. 1985. Influence of SPT Procedures in Soil Liquefaction Resistance Evaluations. *ASCE Journal of Geotechnical Engineering Division*, **111**(12): 1425-1445.
- Seed, H.B., Seed, R.B., Harder, L.F. and Jany, H.-L. 1988. Re-Evaluation of the slide in the Lower San Fernando Dam in the Earthquake of February 9, 1971. Report UCB/EERC -88/04, University of California, Berkeley.
- Shirley, D.J. 1978. An Improved Shear Wave Transducer. *Journal of the Acoustical Society of America*, (63): 1643-1645.
- Sladen, J.A., D'Hallander, R.D. and Krahn, J. 1985. The Liquefaction of Sands, a Collapse Surface Approach. *Canadian Geotechnical Journal*, **22**: 564-578.
- Sladen, J.A., D'Hallander, R.D., Krahn, J. and Mitchell, D.E. 1985. Back Analysis of the Nerleck Berm Liquefaction Slides. *Canadian Geotechnical Journal*, **22**: 579-588.
- Sladen, J.A. and Handford, G. 1987. A Potential Systematic Error in Laboratory Testing of Loose Sands. *Canadian Geotechnical Journal*, **24**: 462-466.
- Thomann, T.G. and Hryciw, R.D. 1990. Laboratory Measurement of Small Strain Modulus Under K_0 Conditions. *Geotechnical Testing Journal*, **13**(2): 97-105.
- Trollope, D.H. and Zafar, S.M. 1952. A Study of the Shear Strength of Saturated Sand, and Sand:Clay Mixtures, in Triaxial Compression. 2nd International Conference on Soil Mechanics and Foundation Engineering, Australia-New Zealand.
- Troncoso, J.H. and Verdugo, R. 1985. Silt Content and Dynamic Behaviour of Tailings Sands. *Proceedings of the Eleventh International Conference on Soil Mechanics and Foundation Engineering*, **3**, San Francisco.
- Vaid, Y.P. and Negussey, D. 1982. A Critical Assessment of Membrane Penetration in the Triaxial Test. University of British Columbia, Vancouver, BC, Soil Mechanics Series No. 61.
- Vaid, Y.P. and Negussey, D. 1984. A Critical Assessment of Membrane Penetration in the Triaxial Test. *Geotechnical Testing Journal*, **7**(2): 70-76.
- Vaid, Y.P. and Chern, J.C. 1985. **Cyclic and Monotonic Undrained Response of Saturated Sands**. *Advances in the art of Testing Soils Under Cyclic Conditions*. V. Khosla, ed. ASCE, New York, N.Y.: 120-147.
- Vaid, Y.P. and Chung, E.F.K. 1989. Preshearing and Undrained Response of Sand. University of British Columbia, Vancouver, BC, Soil Mechanics Series No. 128.
- Vaid, Y.P., Fisher, J.M., Kuerbis, R.H. and Negussey, D. 1990. Particle Gradation and Liquefaction. *Geotechnical Testing Journal*, **116**(4): 698-703.

- Verdugo, R., Ishihara, K. and Towhata, I. 1992. Steady-State Line as a Reference State. IX Panamerican Conference: 1171-1184.
- Wood, D.M. 1990. **Soil Behaviour and Critical State Soil Mechanics**. Cambridge University Press, New York, N.Y.
- Youd, T.L. 1973. **Factors Controlling Maximum and Minimum Densities of Soils**. ASTM, STP 523: 98-112.
- Yudhbir and Abedinzadeh, R. 1991. Quantification of Particle Shape and Angularity Using the Image Analyzer. *Geotechnical Testing Journal*, **14**(3): 296-308.